Biotechnology Advances 82 (2025) 108589

Contents lists available at ScienceDirect

Biotechnology Advances

journal homepage: www.elsevier.com/locate/biotechadv

Polyester-derived monomers as microbial feedstocks: Navigating the landscape of polyester upcycling

Katerina Foka [1], Christina Ferousi [1], Evangelos Topakas [*]

Industrial Biotechnology & Biocatalysis Group, Biotechnology Laboratory, School of Chemical Engineering, National Technical University of Athens, 15772 Athens, Greece

ARTICLE INFO

Keywords:
Plastics
Polyesters
Microbial upcycling
Synthetic biology
Metabolic engineering
Added value products

ABSTRACT

Since their large-scale adoption in the early 20th century, plastics have become indispensable to modern life. However, inadequate disposal and recycling methods have led to severe environmental consequences. While traditional end-of-life plastics management had predominantly relied on landfilling, a paradigm shift towards recycling and valorization emerged in the 1970s, leading to the development of various, mostly mechano-chemical, recycling strategies, together with the more recent approach of biological depolymerization and upcycling. Plastic upcycling, which converts plastic waste into higher-value products, is gaining attention as a sustainable strategy to reduce environmental impact and reliance on virgin materials. Microbial plastic upcycling relies on efficient depolymerization methods to generate monomeric substrates, which are subsequently metabolized by native or engineered microbial systems yielding valuable bioproducts. This review focuses on the second phase of microbial polyester upcycling, examining the intracellular metabolic pathways that enable the assimilation and bioconversion of polyester-derived monomers into industrially relevant compounds. Both biodegradable and non-biodegradable polyesters with commercial significance are considered, with emphasis on pure monomeric feedstocks to elucidate intracellular carbon assimilation pathways. Understanding these metabolic processes provides a foundation for future metabolic engineering efforts, aiming to optimize microbial systems for efficient bioconversion of mixed plastic hydrolysates into valuable bioproducts.

1. Introduction

Since their inception in the early 20th century, plastics have become integral to daily life, with global production soaring from 1.5 Mt. in 1950 to 400 Mt. in 2023 (Statista, 2024). By 2020, the total mass of plastics on Earth reached 8 Gt, twice that of all terrestrial and marine animals combined (Elhacham et al., 2020). This surge, coupled with inadequate disposal and/or recycling methods, has led to significant plastic waste accumulation, leading to greenhouse gas emissions, microplastic soil contamination, and overall severe land and sea

Abbreviations: 4HB, 4-hydroxybutyric acid; AA, adipic acid; ACP, acyl-carrier protein; ALE, adaptive laboratory evolution; Ara5P, D-arabinose 5-phosphate; BDO, 1,4-butanediol; BHAC, β-hydroxyaspartate cycle; BHET, bis(2-hydroxyethyl) terephthalate; BNC, bacterial nanocellulose; CA, Caproic acid; CDW, cell dry weight; CHMS, 4-carboxy-2-hydroxymuconate-6-semialdehyde; DAH, 1,6-diaminohexane; DAHP, 3-deoxy-D-arabino-heptulosonate 7-phosphate; DCD, 1,2-dihydroxy-3,5-cyclohexadiene-1,4-dicarboxylate; DHB, 2–4-dihydroxybutyric acid; DHBA, hydroxybenzaldehyde; DMAPP, dimethylallyl pyrophosphate; dTDP-L-rhamnose, deoxythymidine-diphospho-L-rhamnose; DXP, 1-deoxy-d-xylulose-5-phosphate; EG, ethylene glycol; FPP, farnesyl pyrophosphate; G3P, glyceraldehyde 3-P; GA, gallic acid; Gcl, glyoxylate carboligase; Glu-1-P, glucose-1-phosphate; Glu-6-P, glucose-6-phosphate; GPP, geranyl diphosphate; HHA, 6-hydroxyhexanoic acid; HMBPP, 4-hydroxy-3-methyl-2-(*E*)-butenyl-4-diphosphate; IPP, isopentenyl pyrophosphate; LA, lactic acid; lcl-PHAs, long-chain-length PHAs; MA, muconic acid; mcl-PHAs, medium-chain-length PHAs; MEP, 2-*C*-methyl-D-erythritol-4-phosphate; MHET, mono(2-hydroxyethyl) terephthalate; MLA, malic acid; P3HB, poly(3-hydroxybutyrate); P4HB, poly(4-hydroxybutyrate); PBAT, Poly(butylene adipate-co-terephthalate); PBS, Polybutylene succinate; PBSA, Poly(butylene succinate-co-adipate); PCA, protocatechuic acid; PCL, polycaprolactone; PDC, 2-pyrone-4,6-dicarboxylic acid; PEP, phosphoenolpyruvate; PET, poly(ethylene terephthalate); PG, pyrogallol; PHAs, polyhydroxyalkanoates; PLA, poly(lactic acid); RPET, *R. jostii* strain PET; SA, succinic acid; scl-PHAs, short-chain-length PHAs; TaCo, tartonyl-CoA; TCA, tricarboxylic acid; TPA, terephthalic acid; UDP-Glu, uridine diphosphate glucose; VA, vanillic acid; WT, wild type; Xylu5P, D-xylulose 5-phosphate; βKA, β-ketoadipate.

* Corresponding author.
E-mail addresses: aikfoka@chemeng.ntua.gr (K. Foka), cferousi@chemeng.ntua.gr (C. Ferousi), vtopakas@chemeng.ntua.gr (E. Topakas).
[1] Equal contribution.

https://doi.org/10.1016/j.biotechadv.2025.108589
Received 1 January 2025; Received in revised form 10 April 2025; Accepted 25 April 2025
Available online 10 May 2025

pollution (Pratiwi et al., 2024; Zhang et al., 2021). Substantial risks are posed to wildlife and ecosystems, from marine animals ingesting or becoming entangled in plastic debris (Morunga, 2024), to microplastics being found in various water bodies and food sources, eventually accumulating in cells and tissues (Al Mamun et al., 2023). Analyses on human liver and brain samples suggested an increasing trend of micro- and nanoplastics accumulation, with the total mass concentration of plastics in the brains having increased by about 50 % in the past 8 years (Nihart et al., 2025). Although the extent to which microplastics and nanoplastics could cause human harm and/or toxicity is yet unclear, several studies have established correlations between their presence and chronic biological effects and health hazards (Al Mamun et al., 2023).

1.1. Traditional end-of-life plastics management

Linear economy models for plastics that are based on a "take-make-dispose" approach, where fossil-based raw materials are extracted, transformed into products, and ultimately discarded as waste in landfills, are not sustainable due to both significant environmental deterioration and resource depletion. Conversely, the circular economy model focusing on "reduce-reuse-recycle-recover," aims to create a sustainable system by designing long-lasting products while minimizing waste. End-of-life plastics management that has been solely focused on landfilling, started experiencing a paradigm shift in the early 1970s, when the first worldwide plastic waste recycling mill was established in Pennsylvania, USA (Lancen, 2023). Since then, four main types of plastics recycling processes have been developed, extensively studied, and optimized at industrial scale.

Primary recycling, also known as closed-loop recycling, involves reprocessing plastic waste into the same or similar products without significantly altering its chemical structure, while secondary recycling, or mechanical recycling, requires sorting, cleaning, shredding, and reprocessing plastics into pellets, flakes, or powders. These materials are then used to manufacture new plastic parts and products, often undergoing multiple cycles without significant performance loss (Schyns and Shaver, 2021). Although mechanical recycling is widely used for reprocessing plastic packaging, contributing significantly to Europe's average packaging recycling rate of 65 % in 2022 (European Commission Eurostat, 2025), it is severely constrained by material downcycling due to thermomechanical degradation from harsh remelting conditions.

Tertiary recycling, widely known as chemical recycling, has been extensively studied and widely adopted, as complete plastic depolymerization into oligomeric intermediates and/or their constituent monomeric feedstocks offers the potential for limitless recyclability (Liu et al., 2023). Pyrolysis, photocatalysis, and supercritical fluids are the main chemical methods for plastics processing. Pyrolysis, a well-established technique, uses heat to convert plastics into gases, liquid oils, and chars. Photocatalysis employs light and catalysts to break polymers into smaller molecules (Liu et al., 2023). Emerging approaches like solvolysis enable monomer recovery from polyesters at lower temperatures than pyrolysis, while supercritical fluids offer exceptional solubility and mass transfer properties for efficient plastic decomposition into gas, liquid, and solid product (Liu et al., 2023; Vollmer et al., 2020).

Mechanochemical plastic degradation is a form of chemical recycling that uses mechanical forces, such as grinding, milling, and shearing, to induce chemical transformations and recover valuable monomers or building blocks for material reuse (Zhou et al., 2023b). These processes lower the activation energy and increase the reaction rates by altering crystal structures and generating reactive species (Jicsinszky et al., 2023). Ultrasonication, the most common solution-phase method, creates elongational flow fields that stretch and break polymer chains, while ball milling induces transformations through collision and shear forces (Zhou et al., 2023b). Extrusion, a scalable and solvent-free process, applies heat and shear via rotating screws, leading to polymer softening, degradation, or crosslinking, depending on material properties and processing conditions (Schyns and Shaver, 2021). While chemical and mechanochemical recycling hold promise as transformative plastic waste management solutions to counter plastic waste and resource depletion, process inefficiencies and high energy and cost requirements are still hindering their scalability (Pagola, 2023; Singh and Walker, 2024).

Quaternary recycling, more accurately referred to as waste-to-energy route, relies on incineration for the generation of heat and electricity. In several European countries, waste-to-energy incineration is part of district heating systems, offering renewable energy. Copenhagen's Amager Bakke facility, for instance, provides both electricity and district heating, supporting the city's carbon-neutral goals (State of Green, 2024). Sweden, often cited as a global leader in sustainability, has embraced waste-to-energy incineration to the extent that nearly half of its household waste is converted into energy, helping to keep landfill use at just 1 %, with 34 plants supplying heat and electricity to millions of homes (Welch et al., 2022). The carbon intensity of incineration is higher than renewable energy but lower than coal and, thus, its role in reducing carbon footprints depends on factors like waste composition and efficiency. As such, waste-to-energy should be part of a comprehensive strategy that includes waste reduction, recycling, and renewable energy adoption, rather than relied upon too heavily.

1.2. Biological plastics depolymerization

Biological depolymerization of plastics helps mitigate plastic waste accumulation by breaking down polymers into biodegradable components and offers an alternative to conventional mechanochemical recycling methods with low by-product generation. Microbial degradation involves the action of microorganisms such as bacteria and fungi, that break down polymers into simpler compounds or convert them into carbon dioxide, water, and new biomass, alongside the production of valuable biocompounds. In natural environments, this biodegradation process involves the secretion of extracellular enzymes that attach to the plastic surface, depolymerize it into oligomeric or monomeric compounds and, ultimately, allow microbial cells to assimilate them as carbon source. Enzyme-mediated biocatalytic depolymerization utilizes these specific enzymes to catalyze the breakdown of polymer chains in vitro, making the process highly selective and efficient (Mohanan et al., 2020).

The biodegradability of plastics is primarily determined by their chemical structure, with factors such as molecular composition, crystallinity, and the presence of hydrolysable bonds influencing the efficiency of biodegradation. Plastics with more chemically accessible and amorphous structures generally degrade more readily than those with highly crystalline or chemically resistant components. The efficiency of biodegradation is also highly dependent on specific environmental conditions. Although the latter might often be suboptimal in natural ecosystems, resulting in incomplete degradation (Wang et al., 2024b), proper waste management, such as industrial composting or controlled biodegradation, can ensure reintegration into biological cycles. All things considered, the incentivized growing demand for biodegradable plastics aligns with circular economy models, offering a more sustainable alternative to conventional plastics, which persist in the environment for centuries. This shift is reflected in market trends that highlight the increasing demand for sustainable and biodegradable materials across various industries. The global production volume of the non-biodegradable but widely used poly(ethylene terephthalate) (PET) was approximately 25 Mt. in 2023 but is projected to grow at a compound annual growth rate of only 4 % by 2030 (Statista, 2023). In contrast, the biodegradable poly(lactic acid) (PLA)—albeit only reaching 0.68 Mt. in 2023—is expected to grow significantly, with a compound annual growth rate exceeding 20 % between 2025 and 2030, according to a report published by Mordor Intelligence on the PLA market size and share analysis.

Biodegradation of plastics was first reported in the late 1960s, with a

mixed fungal culture degrading polyester polyurethane (Darby and Kaplan, 1968). The first pure microbial degrader, *Aureobasidium pullulans*, was identified in 1974 for its ability to degrade polycaprolactone (PCL), facilitated by PCL's hydrolysable ester bonds and low crystallinity (Fields et al., 1974). Subsequent studies in the 1970s and 1980s documented microbial degradation of PCL and polyvinyl alcohol by *Penicillium* and *Pseudomonas* species (Benedict et al., 1983; Shimao et al., 1983; Tokiwa and Suzuki, 1977). Research accelerated in the 1990s, with over 400 studies published by 2020, alongside a growing catalogue of plastic-degrading microorganisms and enzymes (Gambarini et al., 2022). Several databases, including PMBD (Gan and Zhang, 2019), PlasticDB (Gambarini et al., 2022), and PAZy (Buchholz et al., 2022), compile biodegradation data, with over 200 plastic-degrading enzymes and 800 microbial species being identified thus far (Gambarini et al., 2021). The field of enzyme-mediated plastic depolymerization is rapidly advancing, driven by innovations in protein engineering to enhance enzyme stability, specificity, and efficiency. Significant progress in rational design, directed evolution, and semi-rational approaches has led to notable improvements in enzymatic performance, while the integration of machine learning and artificial intelligence-based tools is further accelerating the discovery and optimization of plastic-degrading biocatalysts (Grigorakis et al., 2025).

1.3. Plastic waste upcycling

Plastic waste upcycling is the process of transforming plastic waste into new, higher-value products, that is rapidly gaining attention as an effective strategy to reduce environmental impact and decrease reliance on virgin materials. Microbial plastics upcycling heavily relies on efficient and chemically distinct depolymerization approaches to obtain plastic-derived monomers. The latter serve as carbon sources for microbial cultures that metabolize and transform them into valuable products. The first step, i.e., plastic depolymerization, can be achieved via different routes as outlined earlier, while the second step, i.e., production of added-value products, is based either on native or, more frequently, engineered microbial systems. Microbial metabolic engineering facilitates the development of modified microbial chassis capable of transforming plastic-derived monomers into industrially significant products. Undoubtedly, comprehensive approaches that integrate plastic degradation and the production of value-added compounds by a single system represent the ultimate goal for creating efficient and specialized microbial factories. These systems advance industrial biotechnology by upcycling waste materials into commercially valuable products while simultaneously reducing reliance on finite natural resources.

Polyesters are a class of plastics synthesized through polycondensation reactions between dicarboxylic acids and diols, characterized by the presence of ester functional groups in their main chain. Owing to their relatively labile chemical structure, polyesters are more readily depolymerized than other, more recalcitrant plastics. This inherent susceptibility to breakdown has made polyesters the primary focus of microbial upcycling research thus far, as they offer a more feasible route for bioconversion into value-added products.

This review focuses on the second phase of the microbial upcycling process of selected polyesters: the assimilation of polyester-derived monomers and their subsequent conversion into valuable bioproducts (Table 3). We selected both biodegradable and non-biodegradable polyesters that can be fully degraded into defined monomers and have commercial relevance, either with a significant market presence or projected growth. Most studies discussed here focus on pure monomeric feedstocks rather than mixed plastic hydrolysates—where literature remains limited—enabling precise elucidation of carbon assimilation pathways and demonstrating the upcycling potential of each microbial system. This knowledge lays the groundwork for the ultimate design of systems that efficiently convert mixed hydrolysates into valuable biocompounds. Our objective is to systematically identify and present the intracellular metabolic pathways that have been demonstrated—or hypothesized—to be operable during microbial upcycling of their corresponding monomers. By elucidating these pathways, we aim to enhance the understanding of intracellular metabolism underlying the biosynthesis of value-added compounds, thereby providing a foundation for future metabolic engineering efforts to refine and optimize microbial upcycling strategies.

2. Selected polyesters and depolymerization monomers

Based on the criteria mentioned above, the biodegradable polyesters poly(butylene adipate-*co*-terephthalate) (PBAT), poly(butylene succinate) (PBS), poly(butylene succinate-*co*-butylene adipate) (PBSA), PCL, and PLA were included in the current discussion, along with the non-biodegradable PET (Fig. 1). Although PET is recyclable and amenable to controlled enzymatic degradation, it is not classified as biodegradable due to its high durability and resistance to natural degradation, as the process is inherently slow and environmentally insignificant.

2.1. Poly(ethylene terephthalate)

PET is a semi-aromatic, thermoplastic polyester synthesized through the polymerization of terephthalic acid (TPA) and ethylene glycol (EG). Known for its high mechanical strength, excellent barrier properties, and optical clarity, it is widely used in textiles and packaging. With over 55 Mt. produced globally in 2021, PET accounts for about 6 % of global polymer production, ranking among the "big five" polymers (Plastics Europe, 2023). Its physical properties vary based on processing, with crystallization degree significantly affecting its characteristics.

TPA (IUPAC: benzene-1,4-dicarboxylic acid) is an organic compound characterized by two carboxyl groups located at positions one and four of a benzene ring. TPA is a crucial precursor in the production of PET and serves as a fundamental building block for other polyesters, such as PBAT. Research has increasingly focused on the potential of TPA, derived from various polymers, for the synthesis of value-added compounds. Notably, several microorganisms have demonstrated the ability to assimilate TPA and produce a diverse array of valuable products. These include protocatechuic acid (PCA), various downstream aromatic and dicarboxylic acids, β-ketoadipate, lycopene, bacterial nanocellulose (BNC), and polyhydroxyalkanoates (PHAs) (Fig. 2, Table 1).

EG (IUPAC: ethane-1,2-diol) is a vicinal diol that emerges as the degradation product of the non-biodegradable polyester PET. Microbial assimilation of EG generates crucial intermediates like glycolate and glyoxylate, that can tap into the central carbon metabolism and enable the synthesis of various products, such as small aromatics, 2–4-dihydroxybutyric acid (DHB), BNC and PHAs (Fig. 3, Table 2).

2.2. Poly(lactic acid)

PLA is an aliphatic biodegradable polyester made from lactic acid (LA) units, with structural diversity based on the enantiomeric ratio. Poly(L-lactic acid) and poly(D-lactic acid) are semi-crystalline, while poly(D,L-lactic acid) is amorphous and degrades faster (de França et al., 2022). PLA's thermal, mechanical, optical, and barrier properties are comparable to PET, and it can be molded into various forms such as nanoparticles, films, and scaffolds. Initially limited to medical use due to high cost and low availability, advancements in production have expanded its applications to consumer goods, drug delivery, and tissue engineering (Khouri et al., 2024).

LA (IUPAC: 2-hydroxypropanoic acid) is a prominent chiral alpha-hydroxy acid, that exists in two enantiomeric forms. The growing commercial interest in LA is largely due to its role as a precursor for PLA, although studies have demonstrated that it can also be converted into valuable bioproducts such as BNC, butyric and caproic fatty acids, and PHAs, highlighting its versatility and importance in sustainable bioprocesses (Fig. 3, Table 2).

Table 3
Summary of (engineered) upcycling microbial systems discussed in Chapter 3.

Added-value Product	Substrate	Microorganism	Outcome*	Reference
Protocatechuic acid	PET hydrolysate (3 mM TPA)	*E. coli* PCA-1	81 % MY after 3 h	(Kim et al., 2019)
	PET feedstock (65 mM)	*E. coli* M1B_M2F	0.9 % MYd after 120 h	(Zheng et al., 2024)
Gallic acid	TPA (3 mM)	GA-2b system (*E. coli* PCA-1 & *E. coli* HBH-2)	93 % MY after 24 h	(Kim et al., 2019)
Catechol	TPA (3 mM)	*E. coli* CTL-1	90 % MY after 4 h	(Kim et al., 2019)
	TPA (3 mM)	*E. coli* MA-1	85 % MY after 6 h	(Kim et al., 2019)
Muconic acid	PET hydrolysate (32 mM TPA)	*P. putida* KT2440-tacRDL	68 % MY after 60 h	(Liu et al., 2022a, 2022b)
	PET hydrolysate (50 mM TPA & 50 mM EG)	TC-EM consortium (Pp-TC + Pp-EM)	33 % MY after 96 h *(calculated on both)*	(Bao et al., 2023)
	HHA (136 mM)	*E. coli* [pKK-AcChnDE]	86 % MYd after 82 h	(Y.-R. Oh et al., 2023)
	HHA from PCL (20 mM)	*E. coli* [pDSK-AcChnDE]	100 % MY after 16 h	(Y. R. Oh et al., 2022)
Adipic acid	TPA (1 mM)	alg-*E. coli*_pPCA1_-pAA4	79 % MY after 24 h	(Valenzuela-Ortega et al., 2023)
	TPA from bottles (1 mM)		45 % MY after 24 h	
	TPA from hot stamping foils (1 mM)		66 % MY after 24 h	
Pyrogallol	TPA (3 mM)	*E. coli* PG-1a strain	33 % MY after 6 h	(Kim et al., 2019)
Vanillic acid	TPA (3 mM)	VA-2a system (*E. coli* PCA-1 & *E. coli* OMT-2^{His})	42 % MY after 48 h	(Kim et al., 2019)
Vanillin	TPA (3 mM)	*E. coli* RAR-pVanX	74 % MY after 24 h	(Sadler and Wallace, 2021)
2-Pyrone-4,6-dicarboxylic acid	TPA (3 mM)	*E. coli* PCA & *E. coli* PDC_{TPA}	99 % MY after 6 h	(M. J. Kang et al., 2020)
	BHET (124 mM)	*P. putida* AW165	76 % MY after 96 h	(Werner et al., 2021)
	PET hydrolysate (3 mM BHET)	*P. putida* AW165	45 % MY after 24 h	(Werner et al., 2021)
β-Ketoadipic acid	TPA (3 mM)	*E. coli* βKA	98 % MY after 72 h	(You et al., 2023)
	TPA (14 mM) *(two-stage bioconversion)*	*E. coli* βKA (Δ*poxB*)	96 % MY after 24 h	(You et al., 2023)
	mixed HDPE+PS + PET feedstock (350 mg)	*P. putida* AW307	24 % CY after 9 h	(Sullivan et al., 2022)
Lycopene	TPA & EG (20 mM each)	*R. jostii* strain PET S6	0.004 % MY after 96 h *(calculated on both)*	(Diao et al., 2023)
	PET hydrolysate (429 mM TPA & 434 mM EG)	*R. jostii* strain PET S6	0.003 % MY after 60 h *(calculated on both)*	(Diao et al., 2023)
Polyhydroxyalkanoates	PET pyrolysate (20 mM TPA)	*P. putida* GO16	6 % MYd after 48 h	(Kenny et al., 2008)
	PET pyrolysate (20 mM TPA)	*P. putida* GO19	6 % MYd after 48 h	(Kenny et al., 2008)
	PET pyrolysate (20 mM TPA)	*P. frederiksbergensis* GO23	6 % MYd after 48 h	(Kenny et al., 2008)
	TPA (90 mM)	*P. putida* GO16	17 % MYd after 48 h	(Kenny et al., 2012)
	TPA (109 mM) & waste glycerol (201 mM)	*P. putida* GO16	16 % MYd after 48 h *(calculated on both)*	(Kenny et al., 2012)
	PET hydrolysate (30 mM TPA & 30 mM EG)	*P. umsongensis* GO16 KS3	1 % MYd after 28 h *(calculated on both)*	(Tiso et al., 2021)
	EG (100 mM)	*P. putida* MFL185	6 % MYd after 72 h	(Franden et al., 2018)
	AA (27 mM)	*P. putida* KT2440ge ΔPpaaF-paaYX:: P14g ΔpsrA	9 % CY after 48 h	(Ackermann et al., 2021)
	SA (42 mM)	*P. putida* mt-2	15 % CDW	(Shahid et al., 2013)
	SA (42 mM)	*R. palustris* SP5212	0.1 % MYd after 8 d	(Mukhopadhyay et al., 2005)
	PET hydrolysate (50 mM TPA & 50 mM EG) *(fed-batch fermentation, one feeding)*	T-E consortium (Pp-T + Pp-E)	2 % MYd after 108 h *(calculated on both)*	(Bao et al., 2023)
3-(3-hydroxyalkanoyloxy) alkanoic acid	TPA (17 mM)	*P. umsongensis* GO16 KS3 pSB01	1 % MYd after 28 h	(Tiso et al., 2021)
Poly(3-hydroxybutyrate)	TPA (60 mM)	*P. stutzeri* TPA3P	12 % CDW	(Liu et al., 2021)
	PET granules (2 M)	*I. sakaiensis* 201-F6	9 % CY after 6 d	(Fujiwara et al., 2021)
	SA (42 mM)	*C. glutamicum* DSM 20137	8 % CDW	(Shahid et al., 2013)
	SA (42 mM)	*B. megaterium* DSM 509	40 % CDW	(Shahid et al., 2013)
	LA (222 mM)	*R. eutropha NRRL* B14690	0.4 % MYd after 60 h	(Khanna and Srivastava, 2005)
	LA & acetic acid *(pH-stat substrate titration; two-stage fed-batch culture)*	*R. eutropha*	50 g/L	(Tsuge et al., 2001)
Poly(4-hydroxybutyrate)	BDO (60 mM)	*P. putida* NB10	8 % CDW	(Qian et al., 2023)
	BDO (80 mM) & octanoic acid (20 mM)	*P. putida* B10.2	5 % MY after 48 h	(Li et al., 2020)
Bacterial nanocellulose	TPA (120 mM)	*K. xylinus* DSM2004	4 % MYd after 18 d	(Esmail et al., 2022)
	TPA (120 mM)	*K. xylinus* DSM46604	0.8 % MYd after 18 d	(Esmail et al., 2022)
	TPA (*n/a*) & EG (47 mM)	*K. xylinus* DSM2004	0.6 g/L	(Esmail et al., 2022)
	TPA (*n/a*) & EG (7 mM)	*K. xylinus* DSM46604	0.2 g/L	(Esmail et al., 2022)
	EG (322 mM)	*K. xylinus* DSM2004	3.2 % MYd after 18 d	(Esmail et al., 2022)
	PLA hydrolysate (*n/a*)	*K. medellinensis* ID13488	4 g/L	(Sourkouni et al., 2023)
Glycolic acid	EG (0.5 M)	*Y. lipolytica* IMUFRJ 50682	86 % MY after 72 h	(Carniel et al., 2023)
	EG (2 mM)	*P. naganishii* AKU4267	88 % MY after 120 h	(Kataoka et al., 2001)
	EG (1 M)	*G. oxydans* DSM 2003	87 % MY after 48 h	(Wei et al., 2009)
	EG (2 mM)	*Rhodotorula* sp. 3Pr-126	92 % MY after 120 h	(Kataoka et al., 2001)
	EG (200 mM)	*Burkholderia* sp. EG13	99 % MY after 24 h	(Gao et al., 2014)
	EG (161 mM)	*E. coli* MG1655	80 % MYd after 140 h	(Pandit et al., 2021)

(*continued on next page*)

Table 3 (*continued*)

Added-value Product	Substrate	Microorganism	Outcome*	Reference
	EG from PET hydrolysate (11 mM)	*G. oxydans* KCCM 40109	99 % MY after 12 h	(Kim et al., 2019)
2,4-Dihydroxybutyric acid	EG (45 mM)	*E. coli* TW354	2 % MY after 48 h	(Frazão et al., 2023)
L-tyrosine	EG (270 mM)	*E. coli* EGT01	6 % MY after 96 h	(Panda et al., 2023)
Phenylalanine	EG (160 mM)	*E. coli* EGP01	6 % MY after 96 h	(Panda et al., 2023)
p-Coumaric acid	EG (160 mM)	*E. coli* EGC02	4 % MY after 96 h	(Panda et al., 2023)
Butyric acid	LA (32 mM)	*E. hallii* L2–7	70 % MY after 24 h	(Duncan et al., 2004)
	LA (29 mM)	*A. caccae* L1–92	82 % MY after 24 h	(Duncan et al., 2004)
	LA (112 mM)	*M. hexanoica*	89 % MYd after 30 h	(S. Kang et al., 2022)
Caproic acid	LA (279 mM)	*R. bacterium* CPB6	33 % MYd after 6 d	(Zhu et al., 2017)
	LA (20 mM)	*M. elsdenii* J1	10 % MY after 40 h	(Marounek et al., 1989)
	BDO (20 mM)	*P. putida* KT2440	84 % MY after 49 h	(Li et al., 2020)
4-Hydroxybutyrate	BDO (111 mM)	*G. oxydans DSM 50049*	88 % MY after 24 h	(Ismail et al., 2024)
	PBAT hydrolysate (44 mM BDO & 9 mM AA)	*G. oxydans DSM 50049*	50 % MY after 10 h *(calculated on BDO)*	(Ismail et al., 2024)
Succinic acid	BDO (111 mM)	*G. oxydans DSM 50049*	50 % MY after 24 h	(Ismail et al., 2024)
Malic acid	BDO (444 mM)	*U. trichophora* AP037	33 % MYd after 15 d	(Phan et al., 2023)
Rhamnolipids	BDO (15 mM)	*P. putida* KT2440 B10.1 pPS05	9 % MYd after 4 d	(Utomo et al., 2020)
1,4-Butanediol	SA (*n/a*)	*E. coli ECKh-422*	*n/a*	(Yim et al., 2011)
1,6-Diaminohexane	AA (34 mM)	*E. coli ΔsthA-DAH86*	4 % MYd after 72 h	(Wang et al., 2023)

* *MY: molar yield, calculated as (mol of product / mol of substrate) x 100 %; MYd: mass yield, calculated as (g of product / g of substrate) x 100 %; CY: carbon yield, calculated as (mol of C in product / mol of C in substrate) x 100 %; CDW: cell dry weight; n/a: not available.*

2.3. Poly(ε-caprolactone)

PCL is a synthetic, exclusively fossil-based polymer composed of 6-hydroxyhexanoic acid (HHA) units, chemically synthesized via the ring-opening polymerization of ε-caprolactone (Suzuki et al., 2020). Known for its biocompatibility, biodegradability, and mechanical strength, PCL is often blended with hydrophilic or cationic polymers to form amphiphilic block copolymers used in drug delivery systems, such as nanocarriers for co-delivery of drugs and genes (Gaspar et al., 2016), as well as in biodegradable packaging (Mclauchlin and Thomas, 2012). PCL's flexibility, low melting point, and blend compatibility make it highly processable for biomedical applications, including bone tissue engineering (Zaroog et al., 2019), catheters, blood bags, and implantable contraceptives (Mateos-Timoneda, 2009; Singh et al., 2021).

HHA (IUPAC: 6-hydroxyhexanoic acid) is a straight-chain omega-hydroxy fatty acid that is the only resulting monomer from the complete hydrolysis of PCL. Next to its repolymerization, it is also involved in the chemical production of adipic acid (AA), a precursor of nylon-6,6; AA production from HHA has also been microbially engineered (Fig. 2, Table 1).

2.4. Poly(butylene succinate)

PBS is a biodegradable, aliphatic thermoplastic polyester, synthesized from 1,4-butanediol (BDO) and succinic acid (SA) by condensation polymerization, and is of broad scientific and industrial interest due to its compostability according to ISO EN13432 standard (Barletta et al., 2022). PBS can be produced from both renewable and non-renewable monomers, though most commercial products are derived from fossil resources. It offers excellent melt processability, chemical resistance, and biodegradability, but its biodegradation is slow due to high crystallinity (Fredi and Dorigato, 2021). Due to its low Young's modulus, PBS is often blended with other polymers and additives to improve mechanical strength and expand its applications (Barletta et al., 2022). PBS is primarily used in food packaging, shopping bags, agriculture films, plant pots, and hygiene products, with limited use in biomedical applications due to insufficient biocompatibility (Fredi and Dorigato, 2021). The global PBS market is projected to grow at a compound annual growth rate of 20 % from 2022 to 2030, responding to the increasing demand from end-use industries (Grant View Reearch, 2025).

SA (IUPAC: butanedioic acid) is a dicarboxylic acid that can be derived from the degradation of PBS and PBSA, and, apart from its industrial applications, shows potential as a substrate for microbial upcycling. SA serves as a key intermediate in the tricarboxylic acid (TCA) cycle and, as such, can serve as the carbon and energy source for the microbial production of valuable compounds, namely BDO and various types of PHAs (Fig. 3, Table 2).

BDO (IUPAC: butane-1,4-diol) is a primary alcohol and a key depolymerization monomer for PBS, PBSA, and PBAT. Numerous microorganisms, both native and engineered, can utilize BDO as a sole carbon source, either for biomass assimilation or towards the production of value-added products. The high-value products derived from the upcycling of BDO include 4-hydroxybutyric acid (4HB), poly(4-hydroxybutyrate) (P4HB), SA, malic acid (MLA), and rhamnolipids (Fig. 3, Table 2).

2.5. Poly(butylene succinate-co-butylene adipate)

PBSA is a biodegradable, fossil fuel-based aliphatic polyester synthesized from BDO, SA, and AA. It can be produced via polycondensation or transesterification of BDO with the dimethyl esters of SA and AA (Debuissy et al., 2017). This unique monomer combination gives PBSA excellent mechanical strength, flexibility, and thermal stability, making it suitable for various applications. While traditionally derived from fossil fuels, PBSA monomers can also come from bio-based feedstocks (Niaounakis, 2015). PBSA offers superior processability, lower melting temperature, lower crystallinity, and higher biodegradability than PBS (Debuissy et al., 2017). Its low crystallinity makes it ideal for film applications, particularly in the food industry, as well as in biomedical, life, and agricultural packaging (Aliotta et al., 2022; Wu, 2012).

AA (IUPAC: hexanedioic acid) is a dicarboxylic acid and one of the resulting monomers after hydrolysis of the heteropolymers PBAT and PBSA. Apart from its use for repolymerization, either for PBSA and PBAT (Debuissy et al., 2017; Jian et al., 2020), or for nylon-6,6 (Van Duuren et al., 2014), it can also be microbially upcycled to PHAs and 1,6-diaminohexane (DAH) (Fig. 2, Table 1).

2.6. Poly(butylene adipate-co-terephthalate)

PBAT is a biodegradable aromatic copolyester synthesized from BDO, AA, and TPA via random polycondensation. The inclusion of aliphatic components enhances its hydrolytic biodegradability, allowing it to degrade under composting conditions. With moderate crystallinity, good thermal stability, and strong processing stability, PBAT is ideal for extrusion and film blowing. It is promoted as a biodegradable alternative to low-density polyethylene, offering similar flexibility and resilience. PBAT is widely used in packaging and agricultural applications,

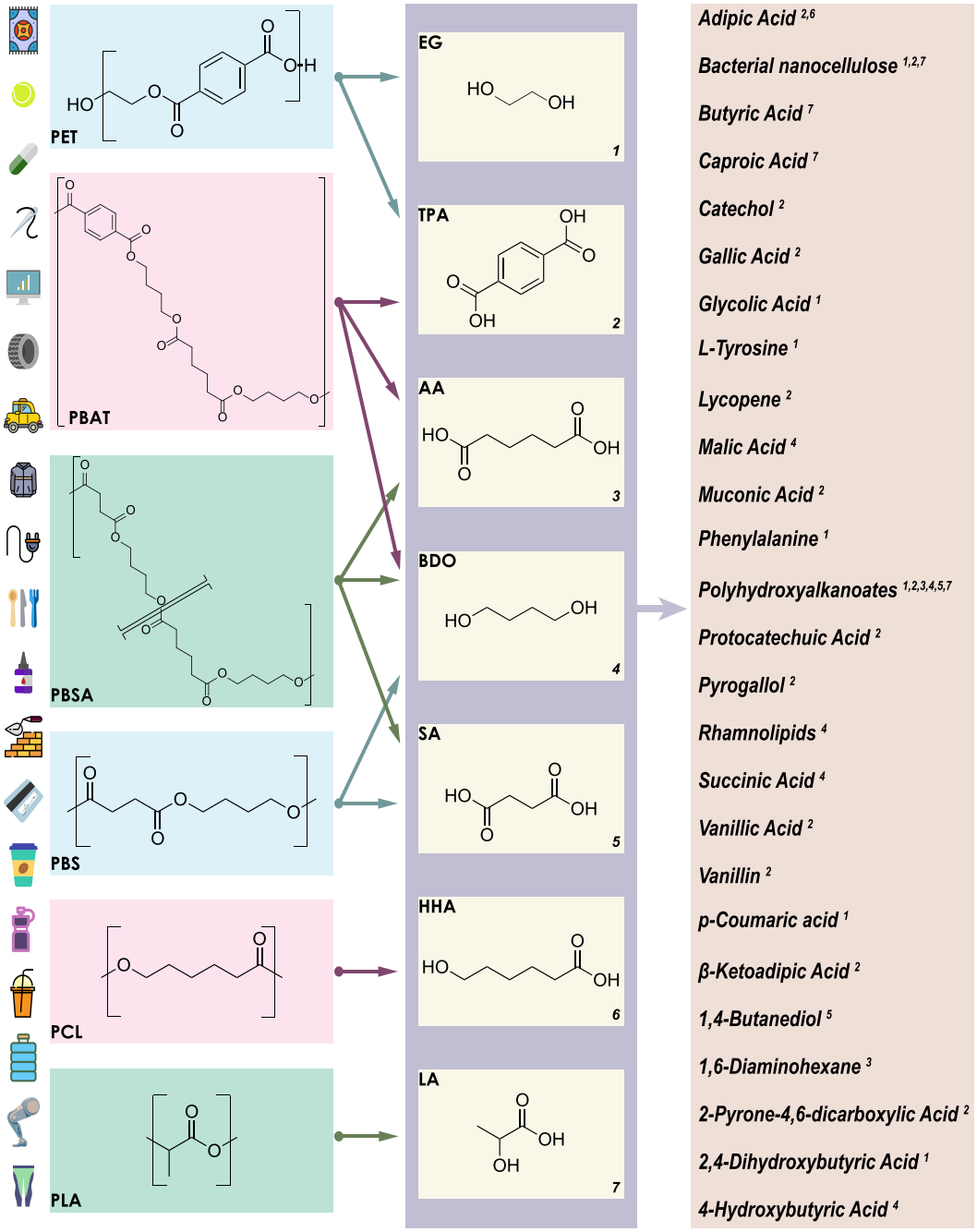

Fig. 1. Chemical composition of polyesters, their corresponding monomers, and the monomer-derived added-value products of microbial upcycling. The colored icons illustrate the commercial applications of polyesters. The superscript numbers in product names correspond to the monomers from where they were derived. The colored icons have been supplied as vector files and modified under a free license from the Vectreezy website (https://www.vecteezy.com/). PET, poly (ethylene terephthalate); PBAT, poly(butylene adipate terephthalate); PBSA, poly(butylene succinate-*co*-adipate); PBS, poly(butylene succinate); PCL, poly(ε-caprolactone); PLA, poly(lactic acid); EG, ethylene glycol; TPA, terephthalic acid; AA, adipic acid; BDO; 1,6-butanediol; SA, succinic acid; HHA, 6-hydroxycaproic acid; LA, lactic acid.

particularly for compostable bags and mulch films (Jian et al., 2020).

3. Microbial upcycling systems

Complete depolymerization of these polyesters yields seven distinct monomers, some of which are shared degradation products with broad biotechnological potential. Notably, multiple monomers can be converted into the same high-value compounds with diverse applications, from commodity and specialty chemicals to bioactive pharmaceuticals, food additives, and biopolymers (Section 4). TPA is extensively studied for its role in producing short aromatic compounds, the carotenoid lycopene, BNC, and PHAs. EG can serve as a primary carbon source for anaerobic acetogenic bacteria, while it can also be assimilated aerobically via various natural and synthetic pathways. Currently, these have been coupled with the biosynthesis of glycolic acid, small aromatic compounds and PHAs. LA enters metabolism at the pyruvate level, supporting microbial production of BNC, PHAs, butyric acid, and caproic acid. BDO is a versatile substrate feeding into the TCA cycle, yielding MLA, SA, 4HB, P4HB, and rhamnolipids. AA can be microbially converted into PHAs and DAH, while HHA serves as a precursor for AA

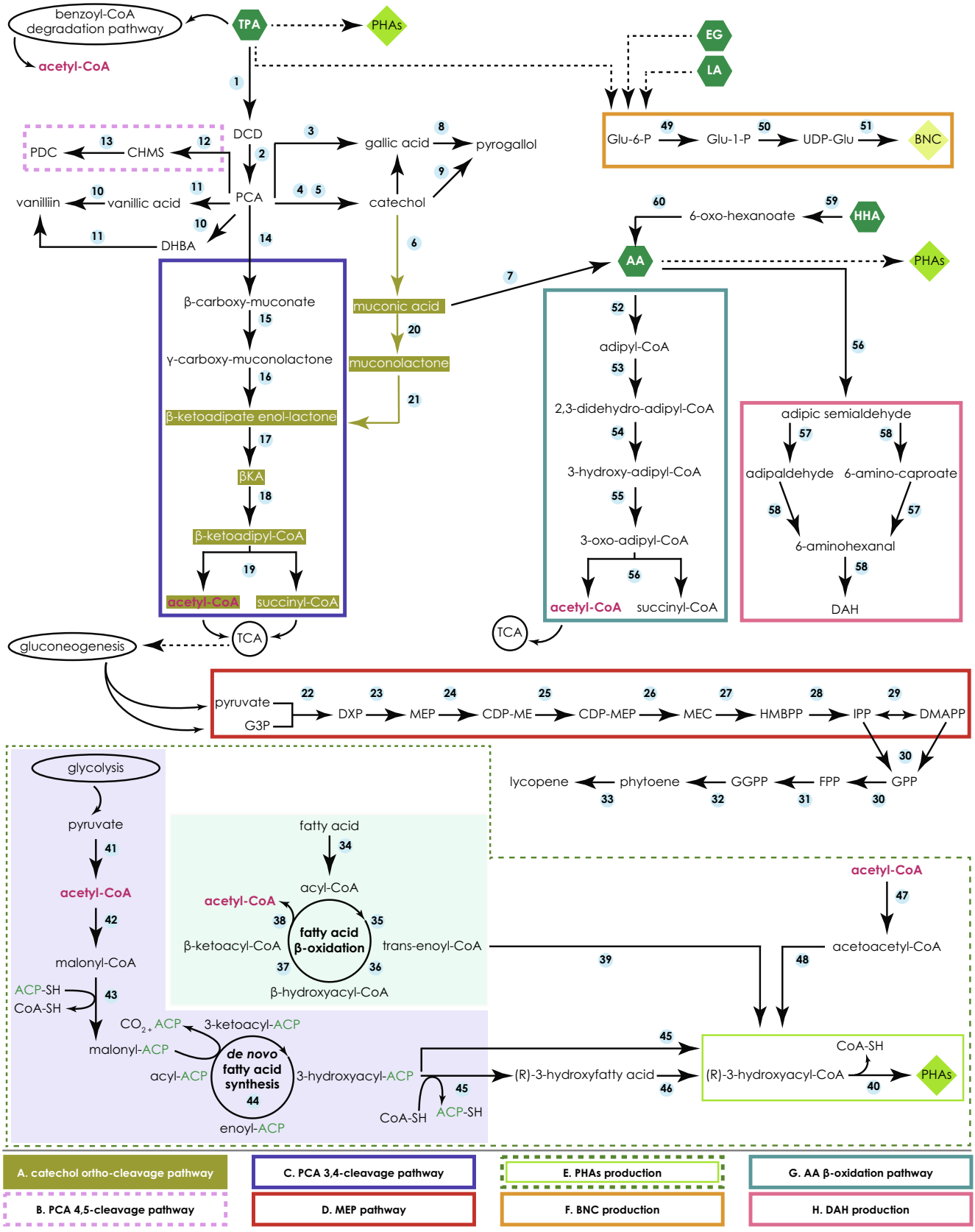

(caption on next page)

Fig. 2. Native and engineered intracellular metabolic pathways for assimilation and upcycling of polyester-derived monomers (part A). Polyester-derived monomers are depicted in green hexagons. Dashed arrows indicate multistep processes. Numbers in grey octadecagons refer to enzymes catalyzing each reaction. Long and short names of enzymes can be found collectively in Table 1. AA, adipic acid; ACP, acyl carrier protein; CDP-ME, 4-diphosphocytidyl-2C-methyl-d-erythritol; CDP-MEP, 4-diphosphocytidyl-2C-methyl-d-erythritol-2-phosphate; CHMS, 4-carboxy-2-hydroxymuconate-6-semialdehyde; DAH, 1,6-diaminohexane; DCD, 1,2-dihydroxy-3,5-cyclohexadiene-1,4-dicarboxylate; DHBA, hydroxybenzaldehyde; DMAPP, dimethylallyl pyrophosphate; DXP, 1-deoxy-d-xylulose-5-phosphate; FPP, farnesyl pyrophosphate; G3P, glyceraldehyde 3-P; GGPP, geranylgeranyl diphosphate; GPP, geranyl diphosphate; HHA, 6-hydroxycaproic acid; HMBPP, 4-hydroxy-3-methyl-2-(*E*)-butenyl-4-diphosphate; IPP, isopentenyl pyrophosphate; MEC, 2C-methyl-d-erythritol-2,4-cyclodiphosphate; MEP, 2-C-methyl-D-erythritol-4-phosphate; BNC, bacterial nanocellulose; PCA, protocatechuic acid; PDC, 2-Pyrone-4,6-dicarboxylic acid; PHAs, polyhydroxyalkanoates; TCA, tricarboxylic acid cycle; TPA, terephthalic acid; βKA, β-ketoadipic acid. (For interpretation of the references to colour in this figure legend, the reader is referred to the web version of this article.)

biosynthesis.

3.1. PHAs biosynthesis

Evidently, numerous upcycling studies have focused on the production of PHAs, that constitute a diverse class of biodegradable and biocompatible polyesters and offer promising applications as sustainable bioplastics. PHAs accumulate as intracellular granules in microbial cells, primarily as energy reserves and in response to environmental stress, such as nutrient limitation or exposure to high temperatures, osmotic changes, and UV radiation. These granules serve a dual role, providing both a storage source and a protective mechanism for microbes under unbalanced growth conditions (Zhou et al., 2023a). The PHA diversity includes monomer structures, polymer chain structures, molecular weights, functionalization and all the combinations. To date, over 150 unique PHAs have been identified, which are generally categorized based on the carbon length of their monomeric units into short-chain-length PHAs (scl-PHAs; C_3-C_5), medium-chain-length PHAs (mcl-PHAs; C_6-C_{14}) and long-chain length PHAs (lcl-PHAs; $>C_{15}$) (Ladhari et al., 2023). Scl-PHAs are known for their rigidity and strength, with polyhydroxybutyrates being among the most common species, while mcl-PHAs exhibit greater elasticity and flexibility, broadening the applicability of these biopolymers across various sectors (Pandey et al., 2022). Lcl-PHAs are less studied and much more rarely encountered, since only a few bacterial species have been shown to produce them, e.g., *Aureispira marina* and *Shewanella oneidensis* (Sehgal and Gupta, 2020).

PHAs can be synthesized as homopolymers, composed of a single type of monomer, or as copolymers, incorporating multiple different monomeric units. Mcl-PHAs are predominantly synthesized as copolymers and usually consist of C_8-C_{12} monomers, while scl-PHAs can be either homopolymers or copolymers, with the most common and the first industrially produced homopolymer being poly(3-hydroxybutyrate) (P3HB). This structural variability of PHAs allows for customization of physical and mechanical properties, enabling tailored applications (Zhou et al., 2023a). In the context of upcycling, PHAs represent a valuable microbial product from waste-derived carbon sources, providing a sustainable route to converting plastic waste into environmentally friendly materials with extensive commercial potential. Although the exact details of the molecular mechanisms governing microbial synthesis of PHAs, as well as the intricate interplay among different intracellular metabolic pathways, are not fully deciphered, it is established that this biosynthesis process has high energy demands, and can be separated into two stages, namely the generation of 3-hydroxyacyl-CoA and its subsequent polymerization into PHAs.

For the initial stage, microorganisms utilize three primary metabolic pathways, i.e., acetoacetyl-CoA synthesis, de novo fatty acid synthesis, and fatty acid β-oxidation (Fig. 2**, Pathway E**). All three pathways provide 3-hydroxyacyl precursors via different routes and then converge to the polymerization reaction catalyzed by PHA synthase (PhaC or PhbC), regardless of the length of the acyl group, to produce either homopolymers or copolymers (Mozejko-Ciesielska et al., 2019; Sathya et al., 2018).

Bacteria can produce PHAs from various carbon sources, including sugars and fatty acids, and adjust their metabolic pathways accordingly. When using aliphatic carbon sources like fatty acids, bacteria utilize the β-oxidation pathway. In the β-oxidation cycle, fatty acids are first CoA-activated and then oxidized by acyl-CoA dehydrogenase to form trans-enoyl-CoA. Trans-enoyl-CoA is then hydrated by enoyl-CoA hydratase, producing (*S*)-3-hydroxyacyl-CoA, which undergoes a second oxidation step catalyzed by 3-hydroxyacyl-CoA dehydrogenase to yield 3-ketoacyl-CoA. In the final step of the cycle catalyzed by 3-ketoacyl-CoA thiolase, acetyl-CoA is released, and a shortened fatty acyl-CoA re-enters the cycle (Wang et al., 2024a). Notably, 3-ketoacyl-CoA thiolase and 3-hydroxyacyl-CoA dehydrogenase have been implicated in the monomer composition of produced PHAs (Możejko-Ciesielska and Mostek, 2019; Ouyang et al., 2007). For PHA synthesis, a side reaction, facilitated by R-β-hydroxyacyl-CoA hydratase (PhaJ), converts trans-enoyl-CoA to (*R*)-3-hydroxyacyl-CoA that is, subsequently, polymerized by PhaC.

For carbon sources unrelated to growth, the de novo fatty acid synthesis pathway is employed for PHA synthesis. Unlike the β-oxidation pathway, which degrades fatty acids to produce 3-hydroxyacyl-CoA intermediates, the de novo pathway synthesizes fatty acids directly, generating intermediates used to form monomers for PHA polymerization. In this pathway, carbon substrates are first converted to acetyl-CoA through glycolysis or other metabolic processes and then carboxylated to malonyl-CoA through the action of acetyl-CoA carboxylase. Fatty acid synthase, a multi-enzyme complex made of six enzymes and an acyl carrier protein, subsequently catalyzes successive cycles of condensation, reduction, dehydration, and a second reduction step, leading to the formation of long-chain acyl-carrier protein (ACP) fatty acid intermediates (Mashima et al., 2009). Among these intermediates, (*S*)-3-hydroxyacyl-ACP is either converted to the enantiomer (*R*)-3-hydroxyacyl-CoA by acyl-ACP:CoA transacylase (PhaG) (Hoffmann et al., 2000; Mozejko-Ciesielska et al., 2019), or first converted to (*S*)-3-hydroxy fatty acid by PhaG and then CoA-activated to (*R*)-3-hydroxyacyl-CoA by acyl-CoA synthase (alkK) (Chacón et al., 2024).

Another PHA biosynthesis pathway, initially identified and studied in *Zoogloea ramigera* and *Alcaligenes eutrophus* (Davis et al., 1987; Ploux et al., 1988; Schubert et al., 1988), begins with the condensation of two acetyl-CoA molecules, a reaction catalyzed by 3-ketothiolase (PhbA; PhaA). Acetoacetyl-CoA is then reduced to (*R*)-3-hydroxy-butyryl-CoA by the enzyme acetoacetyl-CoA reductase (PhbB; PhaB). In the final step, the polymerization of (*R*)-3-hydroxybutyryl-CoA to P3HB is catalyzed by PHA synthase (PhbC; PhaC) through a condensation reaction. Although this pathway is usually used to produce P3HB, other scl-PHAs like P4HB can be synthesized via this route by forming the relevant intermediates (Sathya et al., 2018).

Based on the pathways described above, any microorganism capable of assimilating available carbon sources and converting them to acetyl-CoA can synthesize PHAs through any of these pathways, provided it possesses the genetic information for the necessary enzymatic machinery and the latter is operable under the given conditions.

3.2. Terephthalic acid

3.2.1. PCA, downstream aromatics and dicarboxylic acids

The conversion of TPA to PCA is a key step of the TPA biodegradation pathway utilized by several aerobic bacterial species capable of

Table 1
Enzyme names as discussed in the text sections and presented in figure pathways with numerical codes corresponding to octadecagons in Fig. 2.

Section	Pathway	No	Long Name	Short Name(s)
3.2.1	**Gallic acid production**	**1**	TPA 1,2-dioxygenase	TPADO; TphAabc
		2	DCD dehydrogenase	DCDDH; TphB
		3	*p*-hydroxybenzoate hydroxylase	PobA
	Catechol production	**4**	PCA decarboxylase	AroY
		5	4-hydroxybenzoate decarboxylase	KpdB
	Muconic acid production	**6**	catechol dioxygenase	CatA
	Adipic acid production	**7**	enoate reductase	BcER
	Pyrogallol production	**8**	pyrogallol decarboxylase	LpdC
		9	phenol hydroxylase	PhKLMNOPQ
	Vanillic acid & vanillin production	**10**	carboxylic acid reductase	CAR
		11	catechol *O*-methyltransferase	COMT
3.2.2	**B. PCA 4,5-cleavage pathway**	**12**	PCA 4,5-dioxygenase	PCD4,5; LigAB
		13	CHMS dehydrogenase	LigC
		14	PCA 3,4-dioxygenase	PCD3,4; PcaHG
		15	3-carboxy-*cis*,*cis*-muconate cycloisomerase	PcaB
3.2.3	**C. PCA 3,4-cleavage pathway**	**16**	4-carboxymuconolactone decarboxylase	PcaC
		17	β-ketoadipate enol-lactone hydrolase	PcaD; CAtD
		18	β-ketoadipate succinyl CoA transferase	PcaIJ; CatIJ
		19	β-ketoadipyl CoA thiolase	PcaF; CatF
		20	muconate cycloisomerase	CatB
		21	muconolactone D isomerase	CatC
3.2.4	**D. MEP pathway**	**22**	DXP synthase	DXS
		23	DXP reductoisomerase	DXR; IspC
		24	CDP-ME cytidylyltransferase	IspD
		25	CDP-ME kinase	IspE
		26	MEC synthase	IspF
		27	HMBPP synthase	IspG
		28	HMBPP reductase	IspH
		29	isopentenyl-diphosphate isomerase	IDI
		30	FPP synthase	IspA
		31	GGPP synthase	CrtE
		32	phytoene synthase	CrtB
		33	phytoene desaturase	CrtI
3.2.5	**E. PHAs production**	**34**	thiokinase	*n/a*
		35	acyl-CoA dehydrogenase	*n/a*
		36	enoyl-CoA hydratase	*n/a*
		37	β-hydroxyacyl-CoA dehydrogenase	*n/a*
		38	β-ketoacyl-CoA thiolase	*n/a*
		39	R-β-hydroxyacyl-CoA hydratase	PhaJ
		40	PHA synthase	PhaC; PhbC
		41	pyruvate dehydrogenase	*n/a*
		42	acetyl-CoA carboxylase	ACC
		43	malonyl acetyl transacylase	*n/a*
		44	fatty acid synthase	FASN
		45	acyl-ACP:CoA transacylase/ acyltransferase	phaG
		46	acyl-CoA synthase	alkK
		47	3-ketothiolase	PhbA; PhaA
		48	acetoacetyl-CoA reductase	PhbB; PhaB
		49	phosphoglucomutase	PGM
	F. BNC production	**50**	UDP-Glu pyrophosphorylase	*n/a*
		51	cellulose synthase	Bcs
		52	CoA transferase	DcaIJ
		53	acyl-CoA dehydrogenase	DcaA
3.7	**G. Adipic acid β-oxidation pathway**	**54**	enoyl-CoA hydratase	DcaE; PaaF; FaaB
		55	hydroxyacyl-CoA dehydrogenase	DcaH; PaaH
		56	acyl-CoA thiolase	DcaF; PaaJ; PcaF-1
3.7.2	**H. DAH production**	**57**	carboxylic acid reductase	CAR
		58	transaminase	TA
3.8.1	**Adipic acid production**	**59**	HAA dehydrogenase	ChnD
		60	6-oxohexanoate dehydrogenase	ChnE

n/a: not available.

metabolizing TPA as their sole carbon source, including *Comamonas* sp. E6, *Delftia tsyryhatensis* T7, and *Rhodococcus* sp. (Choi et al., 2005; Sasoh et al., 2006; Shigematsu et al., 2003). This pathway involves two critical enzymes, a TPA 1,2-dioxygenase (TPADO) which catalyzes the conversion of TPA to 1,2-dihydroxy-3,5-cyclohexadiene-1,4-dicarboxylate (DCD) and a DCD dehydrogenase, that further converts DCD to PCA (Fig. 2) (Salvador et al., 2019; Sasoh et al., 2006). The latter serves as a precursor for the subsequent production of various high-added value compounds and is also metabolized intracellularly via three distinct catabolic pathways: the 2,3-cleavage, the 3,4-cleavage, and the 4,5-cleavage pathway; all these funneling PCA to the TCA cycle (Nojiri et al., 2014). TPA could also be metabolized through anaerobic methanogenic processes, bypassing the PCA intermediate, with methane and/or carbon dioxide as end products (Kleerebezem and Lettinga, 2000). In this case, TPA catabolism proceeds via the benzoyl-CoA degradation pathway, as showcased in *Syntrophorhabdus aromaticivorans* UI, involving a series of sequential transformations leading to acetyl-CoA (Gao et al., 2022). However, neither anaerobic methanogens nor any microbial syntrophies of the oxic-anoxic interface with TPA-degrading potential have been the focus of any engineered studies towards plastic waste valorization, presumably due to the inherent difficulty of anaerobicity.

The biosynthetic route for PCA from TPA was engineered in *Escherichia coli* PCA-1 strain, incorporating the genes for the heterotrimeric O_2-dependent TPA dioxygenase (TphAabc) and the NAD^+-dependent DCD dehydrogenase (TphB) from *Comamonas* sp. E6. This engineered strain achieved conversion of TPA to PCA at a molar yield of 81 % within 3 h of incubation (Kim et al., 2019). Taking it a step further, an engineered *E. coli* strain was developed to combine both extracellular degradation of PET and intracellular conversion of TPA to PCA, allowing for efficient PET degradation and PCA production directly from PET feedstock. This was achieved by constructing a two-module biocatalytic system. Module 1 consisted of the membrane protein OmpA fused with a genetically optimized PETase (FAST-PETase: functional, active, stable and tolerant PETase) (Lu et al., 2022) to anchor the enzyme on the cell surface, facilitating both PET hydrolysis and intracellular incorporation of the resulting TPA. Module 2 involved the cytoplasmic pathway of TPADO and DCD dehydrogenase from *Comamonas* sp. E6. Optimization of enzyme expression, linker length between proteins, and reaction conditions achieved a maximum mass yield of about 1 % PCA after 120 h, illustrating the feasibility of PET upcycling despite the modest yield (Zheng et al., 2024).

3.2.1.1. Gallic acid. PCA can be converted to gallic acid (GA) by a PCA hydroxylase with meta-hydroxylation activity. An enzyme with this activity, *p*-hydroxybenzoate hydroxylase (PobA) from *Pseudomonas putida* KT2440, was expressed in *E. coli*, resulting in GA production from PCA with a molar yield of 40 % after 12 h. Further optimization was achieved by expressing a double-mutant version of the enzyme, $PobA^{Mut}$ (T294A/Y385F), in *E. coli* strain HBH-2, which led to an 84 % increase in

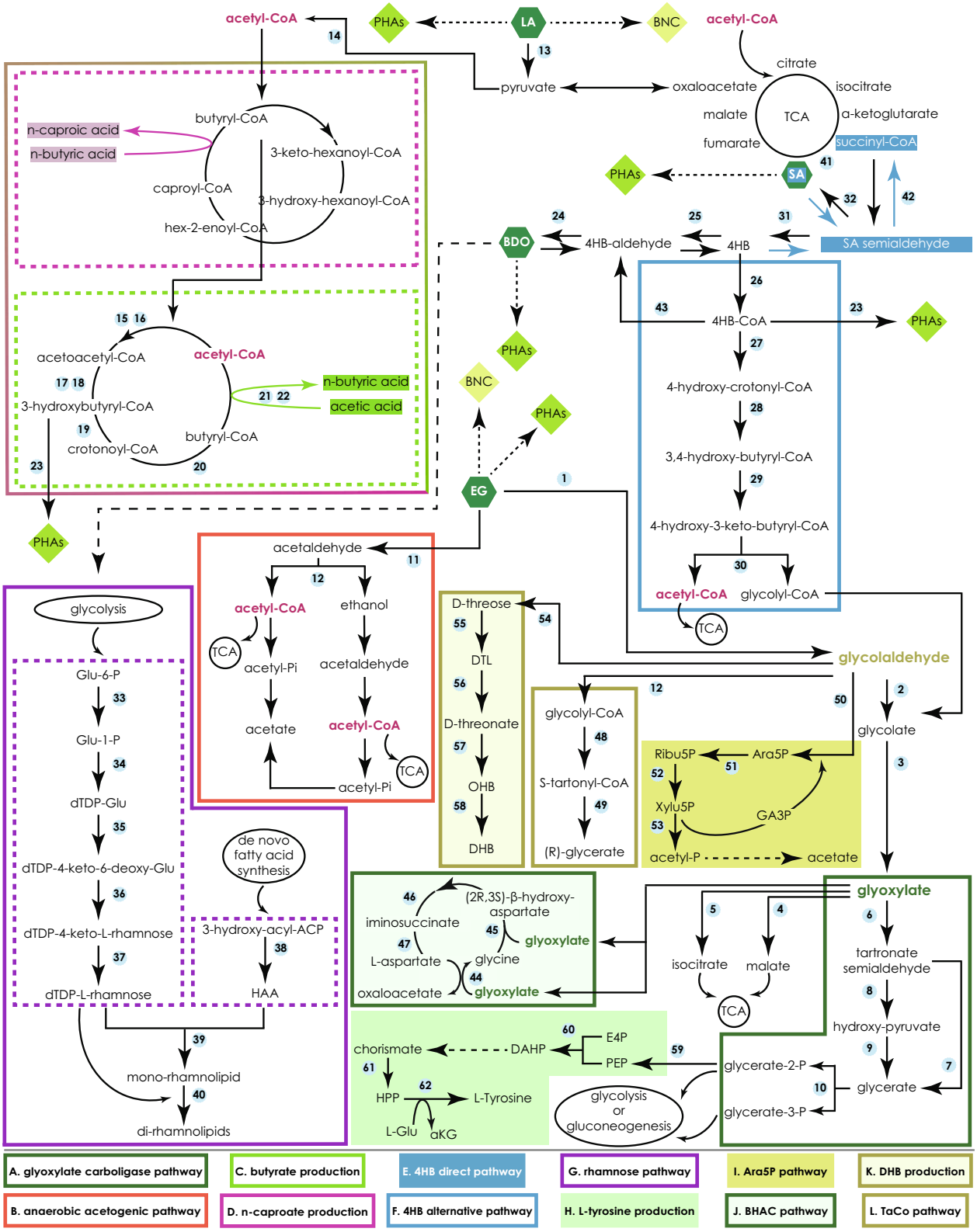

Fig. 3. Native and engineered intracellular metabolic pathways for assimilation and upcycling of polyester-derived monomers (part B). Polyester-derived monomers are depicted in green hexagons. Dashed arrows indicate multistep processes. Numbers in grey octadecagons refer to enzymes catalyzing each reaction. Long and short names of enzymes can be found collectively in Table 2. 4HB, 4-hydroxy-butyrate; αKG, α-ketoglutarate; ACP, acyl carrier protein; acetyl-P, acetyl phosphate; Ara5P, D-arabinose 5-phosphate; BDO, 1,4-butanediol; BHAC, β-hydroxyaspartate cycle; BNC, bacterial nanocellulose; DAHP, 3-deoxy-D-arabino-heptulosonate 7-phosphate; DHB, 2,4-dihydroxybutyric acid; dTDP-Glu, deoxythymidine diphosphate glucose; DTL, D-threono-1,4-lactone; EG, ethylene glycol; E4P, erythrose-4-phosphate; GA3P, glyceraldehyde 3-phosphate; Glu-1-P, glucose-1-phosphate; Glu-6-P, glucose-6-phosphate; HAA, 3-(3-hydroxy alkanoyl oxy) alkanoic acid; HPP, 4-hydroxyphenylpyruvate; LA, lactic acid; L-Glu, L-glutamate; OHB, 2-oxo-4-hydroxybutyrate; PEP, phosphoenolpyruvate; PHAs, polyhydroxyalkanoates; Ribu5P, D-ribulose 5-phosphate; SA, succinic acid; TaCo, tartronyl-CoA pathway; TCA, tricarboxylic acid; Xylu5P, D-xylulose 5-phosphate. (For interpretation of the references to colour in this figure legend, the reader is referred to the web version of this article.)

Table 2
Enzyme names as discussed in the text sections and presented in figure pathways with numerical codes corresponding to octadecagons in Fig. 3.

Section	Pathway	No	Long Name	Short Name(s)
			PQQ quinone-dependent alcohol dehydrogenase	PedE; PedH
		1	1,2-propanediol oxidoreductase	FucO
			glycolaldehyde reductase	YqhD
	Glycolate and glyoxylate production		Zinc-dependent alcohol dehydrogenase	Gox0313
		2	glycolaldehyde dehydrogenase	PP_0545; PedI; AldA
		3	glycolate oxidase	GlcDEF
		4	malate synthase	GlcB
		5	isocitrate lyase	AceA
		6	glyoxylate carboligase	Gcl
		7	tartronate semialdehyde reductase	GlxR
	A. Glyoxylate carboligase pathway	8	hydroxypyruvate isomerase	Hyi
3.3.1		9	hydroxypyruvate reductase	TtuD
		10	glycerate kinase	*n/a*
		44	aspartate-glyoxylate aminotransferase	BhcA
	J. β-Hydroxyaspartate cycle	45	β-hydroxyaspartate aldolase	BhcC
		46	β-hydroxyaspartate dehydratase	BhcB
		47	iminosuccinate reductase	BhcD
		12	aldehyde dehydrogenase	PduP
	L. Tartronyl-CoA pathway	48	glycolyl-CoA carboxylase	
		49	tartronyl-CoA reductase	
		50	fructose 6-phosphate aldolase	FsaA
	I. D-arabinose 5-phosphate-dependent glycolaldehyde assimilation pathway	51	D-arabinose 5-phosphate isomerase	KdsD
		52	D-ribulose 5-phosphate 3-epimerase	Rpe
		53	phosphoketolase	CaPkt
		54	D-threose aldolase	Ec. FsaATA
		55	D-threose dehydrogenase	Pc.TadH
3.3.2	**K. DHB production**	56	D-threono-1,4-lactonase	Tt.Lac11
		57	D-threonate dehydratase	Hh.AraD
		58	2-oxo-4-hydroxybutyrate reductase	Ec. Mdh5Q
		59	Enolase	Eno
		60	DAHP synthase	AroG
3.3.3	**H. L-tyrosine production**	61	chorismate mutase/ prephenate dehydrogenase	TyrA
		62	transaminase	
3.3.4	**B. Anaerobic acetogenic pathway**	11	propane diol dehydratase	PduCDE
		12	CoA-dependent propionaldehyde dehydrogenase	PduP
3.3.5	**PHAs**	13	lactate dehydrogenase	LDH
		14	pyruvate dehydrogenase	PDH
3.4.2	**C. Butyrate production**	15	acetyl-CoA acetyltransferase	AtoB
		16	3-ketothiolase	PhbA; PhaA
		17	3-hydroxybutate dehydrogenase	Hbd
		18	acetoacetyl-CoA reductase	PhbB; PhaB
		19	enoyl-CoA hydratase	Crt
		20	butyryl-CoA dehydrogenase	Bcd
		21	butyryl-CoA:(acceptor) oxidoreductase	But; CoAT
		22	butyrate kinase	buk
		23	PHA synthase	PhbC; PhaC
		24	aldehyde dehydrogenase	ALD; adhE2
		25	alcohol dehydrogenase	ADH
		26	4HB-CoA transferase	Cat2
	F. 4HB alternative oxidation pathway	27	acyl-CoA dehydrogenase	*n/a*
3.5.1		28	enoyl-CoA hydratase	*n/a*
		29	3-hydroxyacyl-CoA dehydrogenase	*n/a*
		30	acetyl-CoA acetyltransferase	*n/a*
		31	4HB dehydrogenase	4HBd
	E. 4HB direct oxidation pathway	32	succinate semialdehyde dehydrogenase	*n/a*
		33	phosphoglucomutase	PGM
		34	G1P thymidylyltransferase	RmlA
		35	dTDP-D-glucose 4,6-dehydratase	RmlB
3.5.3	**G. Rhamnose pathway**	36	dTDP-6-deoxy-D-xylo-4-hexulose 3,5-epimerase	RmlC
		37	dTDP-6-deoxy-L-lyxo-4-hexulose reductase	RmlD
		38	3-hydroxyacyl-ACP-O -3 hydroxyacyltransferase	RhlA
		39	rhamnosyltransferase I	RhlB
		40	rhamnosyltransferase II	RhlC
		41	succinyl-CoA synthetase	SucCD
3.6.1	**BDO formation**	42	CoA-dependent succinate semialdehyde dehydrogenase	SucD
		43	4HB-CoA reductase	*n/a*

n/a: not available; PQQ: pyrroloquinoline quinone; dTDP: deoxythymidine diphosphate.

GA production compared to the wild type (WT) PobA. For GA production directly from TPA, the strains PCA-1 and HBH-2 were co-cultured to facilitate the sequential conversion of TPA to PCA and, subsequently, PCA to GA. Under the optimized co-culturing conditions, the GA-2b system achieved a molar yield of 93 % for the conversion of TPA to GA after 24 h, without the accumulation of PCA (Kim et al., 2019).

3.2.1.2. Catechol. Catechol is another valuable aromatic compound that can be produced from PCA via decarboxylation. This conversion was demonstrated using the enzyme AroY, a highly conserved PCA decarboxylase, expressed in *E. coli* strain CTL-1, which achieved a 98 % molar yield of catechol from PCA after 5 h. Strain CTL-1, co-expressing TphAabc, TphB, and AroY, converted TPA to catechol with a molar yield of 90 % without PCA accumulation after 4 h (Kim et al., 2019).

3.2.1.3. Muconic acid. Catechol can serve as a precursor for the biosynthesis of muconic acid (MA) through ring cleavage (Fig. 2, **Pathway A**). This conversion was successfully achieved by *E. coli* strain CDO-1 via expression of CatA—a non-heme Fe(III)-dependent catechol 1,2-dioxygenase from *P. putida* KT2440. To establish the biosynthetic pathway for MA production starting from TPA, the MA biosynthesis pathway was combined with the catechol biosynthetic route of *E. coli* strain CTL-1. The resulting engineered strain, i.e., MA-1, effectively converted TPA to MA with a molar yield of 85 % after 6 h of incubation,

without the accumulation of intermediate compounds (Kim et al., 2019). Another study focused on valorization of PET hydrolysates towards MA production via engineering *P. putida* KT2440; the inherent conversion of PCA to MA via catechol by this strain had already been established (Johnson et al., 2016). The strain was modified to integrate both a TPA degradation pathway and a pathway for MA production via its intermediates. To serve the first purpose, genes encoding a protocatechuate 3,4-dioxygenase (*pcaHG*) were replaced by the *tph* cluster from *Pseudomonas stutzeri*, which included a transcriptional regulator (TphR), a TPA transporter (TpaK), the TphAabc TPADO, and the TphB DCD dehydrogenase. Additionally, codon-optimized genes for a protocatechuate decarboxylase (*aroY*) and a flavin prenyltransferase (*ecdB*) from *Enterobacter cloacae* were introduced to enhance catechol production. Overexpression of CatA, together with deletions of the downstream metabolic genes i.e., muconate lactonase (*catB*) and muconolactone isomerase (*catC*), were performed to set up the MA biosynthetic pathway. The resulting engineered strain, *P. putida* KT2440-tacRDL, achieved efficient conversion of TPA to MA with a molar yield of 100 % under optimized conditions. This multifunctional strain successfully produced 0.5 g MA/g PET, reaching 68 % of the theoretical conversion rate, demonstrating its potential for sustainable PET upcycling (Liu et al., 2022b).

3.2.1.4. Adipic acid. AA is another commercially important platform chemical that can be produced via the PCA branch, through a shortcut of the catechol ortho-cleavage catabolic pathway. Eight genes, essential for the complete conversion of TPA down to AA, were engineered in *E. coli*, organized in two separate vectors (Valenzuela-Ortega et al., 2023). TPA conversion to PCA was achieved by the *Comamonas* sp. E6 $TphA_{abc}$ and TphB enzymes, while PCA conversion to AA involved the sequential action of the PCA decarboxylase AroY from *Klebsiella pneumoniae*, a subunit of the 4-hydroxybenzoate decarboxylase KpdB from *K. pneumoniae*, responsible for AroY activation by generation of prenylated flavin mononucleotide, the CatA catechol dioxygenase from *P. putida*, and finally the [4Fe—4S]-dependent enoate reductase BcER from *Bacillus coagulans* (Joo et al., 2017), responsible for muconic acid reduction to AA. When grown on TPA, the double-vector transformed *E. coli* strain could not perform MA hydrogenation to AA, therefore, only reaching MA production, albeit at a yield of 92 %. The use of polycistronic mRNA for tighter translation control and alginate hydrogels for cell immobilization, led to the alg-*E. coli*_pPCA1_-pAA4 strain that produced AA with a yield of 79 %, corresponding to 115 mg/L. As proof of concept, the valorization of post-consumer PET bottles and hot stamping foils was investigated, via alkaline depolymerization of PET and subsequent conversion of the resulting TPA to AA by the above-mentioned *E. coli* engineered strain. These processes yielded 65 mg/L and 96 mg/L AA (66 % yield), from PET bottles and hot stamping foils, respectively (Valenzuela-Ortega et al., 2023).

3.2.1.5. Pyrogallol. Pyrogallol (PG) can also be biosynthesized via the PCA branch, either through decarboxylation of GA derived from PCA hydroxylation, or hydroxylation of catechol produced via PCA decarboxylation. To achieve PG synthesis via GA, the GA decarboxylase LpdC from *Lactobacillus plantarum* (Jiménez et al., 2013) was integrated into the engineered *E. coli* strain HBH-2 capable of GA biosynthesis, resulting in the construction of *E. coli* strain PG-1a, expressing TphAabc, TphB, $PobA^{Mut}$, and LpdC. This strain produced PG from TPA at a molar yield of 33 % after 6 h; however, it also generated catechol as a byproduct due to the promiscuous activity of LpdC towards PCA. To address catechol accumulation, a secondary pathway was developed that utilized the *PhKLMNOPQ* operon from *P. stutzeri* OX1 coding for the complete protein machinery of a phenol hydroxylase that has been shown to promiscuously hydroxylate catechol to PG (Wang et al., 2018). The engineered *E. coli* strain CH-1 expressing a functional PH converted catechol to PG with a yield of 67 %, although when combined with the original GA biosynthesis pathway from strain PG-1b, the accumulation of catechol persisted, and PG production was lower than in PG-1a. An alternative strategy for PG biosynthesis was constructed by integrating PCA conversion to catechol using AroY, followed by catechol hydroxylation to PG using the enzymatic machinery produced by *phKLMNOPQ* from *P. stutzeri* OX1. The optimized PG-2b system, combining *E. coli* strains CTL-1 and CH-1 in a co-culture, achieved a molar yield of 19 % for PG production, although a substantial amount of catechol remained unconverted (Kim et al., 2019).

3.2.1.6. Vanillic acid. PCA can also be converted to vanillic acid (VA) by the action of a catechol *O*-methyltransferase (COMT) when S-adenosyl methionine serves as a co-substrate. Various OMTs were heterologously expressed in *E. coli* BL21 and, among them, OMT from *Homo sapiens* (*Hs*COMT) demonstrated the highest molar yield of VA from PCA at 29 % (Kim et al., 2019). To facilitate production of VA from TPA, a biosynthetic pathway comprising TphAabc and TphB for PCA production, along with *Hs*OMT, was constructed in the engineered strain *E. coli* VA-1. Nonetheless, complete consumption of 3 mM TPA within 72 h yielded just 0.6 % VA, while accumulation of PCA was observed. To enhance the low conversion rate of PCA to VA, the modified strain OMT-2^{His} was developed, where a hexameric histidine was attached to the N-terminus of *Hs*OMT for increased protein solubility. *E. coli* OMT-2^{His} growth in a medium supplemented with methionine in equimolar concentrations to PCA, resulted in an increased molar yield of VA up to 45 %. Further improvement of PCA conversion to VA was achieved using a double-catalyst system, VA-2a, with the strains PCA-1 and OMT-2^{His} added in the co-culture at a 1:3 cell density ratio. The VA produced from TPA increased to a yield of 9 % after 48 h, although the molar yield from PCA remained at 6 %. Enhancing oxygen supply through improved aeration in the VA-2b system increased ATP generation, raising the molar yield of VA from TPA by 4.7-fold, albeit with about 40 % of TPA remaining unconverted. Optimizing the initial cell ratio of the two strains, as well as the fluxes of TPA to PCA and PCA to VA, was deemed essential for further improvement of the overall conversion efficiency (Kim et al., 2019).

3.2.1.7. Vanillin. Vanillin is another aromatic compound that can be produced via the PCA branch, through two similar enzymatic pathways guided by the action of a carboxylic acid reductase (CAR) and a COMT. CAR can catalyze both the reduction of PCA to hydroxybenzaldehyde (DHBA) and the conversion of VA to vanillin, while COMT catalyzes both PCA or DHBA methylation to VA and vanillin, respectively. *E. coli* MG1655 RARE strain, known for its reduced aromatic aldehyde reduction properties, was engineered to convert TPA all the way to vanillin (Sadler and Wallace, 2021). The necessary enzymes were assembled into two vectors: pVan1, coding for the TPA 1,2-dioxygenase and the DCD dehydrogenase from *Comamonas* sp. E6, and pVan2, coding for a *Nocardia iowensis* carboxylic acid reductase (*Ni*CAR), and a point mutant of the soluble form of catechol *O*-methyltransferase (S-COMT Y200L) from *Rattus norvegicus*. Additionally, a third plasmid, pSfp, encoding a phosphopantetheinyl transferase from *Bacillus subtilis*, was introduced to facilitate post-translational modification of *Ni*CAR. The resulting strain, *E. coli* RARE-pVanX, produced detectable amounts of vanillin from TPA, although the conversion was initially less than 1 %, with significant accumulation of the intermediates PCA, DHBA and VA. Following optimization of culture conditions, including pH, temperature, incubation time, and the addition of L-methionine, n-butanol, and oleyl alcohol to improve membrane permeability and in situ product removal, the biotransformation was significantly improved, resulting in a maximum molar yield of 74 %. The engineered pathway was further employed to demonstrate the upcycling potential of post-consumer PET waste into vanillin, by coupling enzymatic PET hydrolysis by the thermostable LCC^{WCCG} (Tournier et al., 2020) with vanillin production from the released TPA by *E. coli* RARE_pVanX (Sadler and Wallace, 2021).

3.2.2. PCA 4,5-cleavage pathway

In the PCA 4,5-cleavage pathway (Fig. 2, **Pathway B**), PCA is transformed into 4-carboxy-2-hydroxymuconate-6-semialdehyde (CHMS) by PCA 4,5-dioxygenase (PCD4,5 and LigAB). CHMS is then non-enzymatically converted to an intramolecular hemiacetal form and, eventually, oxidized to 2-pyrone-4,6-dicarboxylic acid (PDC) by CHMS dehydrogenase (LigC) (Harwood and Parales, 1996). To enable TPA conversion to PDC, *E. coli* XL1-Blue strain was transformed with two separate vectors, encoding the necessary genes for TPA conversion to PCA (TphAabc and TphB) and PCA conversion to PDC (*ligAB* and *ligC*), respectively (Kang et al., 2020). The resulting engineered *E. coli* PDC_{TPA} achieved a molar yield of 91 % PDC from TPA. To further optimize this process, a double-catalyst system was developed by combining *E. coli* PCA strain for TPA degradation and *E. coli* PDC_{PCA} strain for PDC synthesis, in a co-culture with a 3:5 cell density ratio. The system achieved a 99 % molar yield conversion of TPA to PDC, without accumulating PCA after 6 h of incubation.

3.2.3. PCA 3,4-cleavage pathway

During the PCA 3,4-cleavage pathway (Fig. 2, **Pathway C**), also known as ortho-cleavage or β-ketoadipate (βKA) pathway, PCA is converted to 3-carboxy-*cis*,*cis*-muconate by a PCA 3,4-dioxygenase (PCD3,4), which is eventually converted to βKA by the sequential activities of 3-carboxy-*cis*,*cis*-muconate cycloisomerase, 4-carboxymuconolactone decarboxylase, and β-ketoadipate enol-lactone hydrolase (Harwood and Parales, 1996).

P. putida, that naturally employs the PCA 3,4-cleavage pathway, the most ubiquitous among bacteria, was engineered for the complete conversion of bis(2-hydroxyethyl) terephthalate (BHET) to βKA (Werner et al., 2021). The first step of this conversion involved BHET hydrolysis to mono(2-hydroxyethyl) terephthalate (MHET) and subsequent hydrolysis of the latter to TPA and EG. This was achieved by the incorporation of the *Ideonella sakaiensis* genes coding for PETase and MHETase, respectively. The second step of the overall conversion involved the genetic modification of the strain to facilitate TPA conversion to PCA, which was achieved by utilizing the $TphA_{abc}$ TPADO and the TphB DCD dehydrogenase from *Comamonas*, together with the TpaK transporter from *Rhodococcus jostii* for active membrane transport of TPA. Interestingly, the supplementation of BHET cultures with an additional 3.6 g/L glucose every 24 h— initially containing BHET and glucose in a 7:10 ratio—led to complete hydrolysis of BHET and substantially reduced MHET accumulation. Subsequently, to enable BHET conversion to βKA, *pcaIJ* encoding the 3-oxoadipate CoA-transferase was deleted, generating the final strain *P. putida* AW165. When this engineered strain was cultivated in a pH-controlled bioreactor supplied with BHET for 96 h, 32 g/L BHET were converted to about 15 g/L βKA, with a molar yield of 76 % and a productivity of 0.16 g βKA/L/h. Interestingly, in the proof-of-concept phase where chemocatalytic glycolysis of PET resulted in BHET and MHET, the conversion of the latter to βKA reached only 45 % molar yield. This reduced βKA production was associated with a pH decrease and was, thus, attributed to levulinic acid catabolism— a product of βKA decarboxylation below pH 7.0 (Werner et al., 2021).

In another study, *E. coli* was genetically engineered to enable both TPA degradation and βKA synthesis, with the latter proceeding via catechol and its ortho-cleavage pathway that merges with the PCA 3,4-cleavage pathway at the level of β-ketoadipate enol-lactone. The TPA degradation module, comprising *tphAabc* and *tphB* from *Comamonas* sp. E6, was incorporated in one vector, while another vector was coding for the AroY PCA decarboxylase from *K. pneumoniae*, leading to catechol formation. The third vector included the *P. putida* KT2440 cat operon genes (*catabc*) together with *pcaD* from *P. putida*, responsible for enol-lactone hydrolysis to β-KA (Harwood and Parales, 1996). Utilizing glycerol as the primary carbon source, this engineered *E. coli* βKA strain exhibited efficient TPA conversion to βKA achieving 98 % molar yield, albeit slow metabolism of glycerol and accumulation of acetic acid— a deleterious factor for TPA conversion— were observed. Higher oxygen supply and regulation of acetic acid formation by *poxB* gene deletion— PoxB catalyzes the irreversible conversion of pyruvate into acetic acid— led to improved growth rates. Eventually, a two-stage bioconversion process was established for *E. coli* βKA ΔpoxB strain, consisting of the growth phase at pH 7.0, followed by the βKA production phase at pH 5.5. A total of 13.6 mM βKA was successfully produced with 96 % conversion efficiency (You et al., 2023).

3.2.4. Lycopene synthesis

Lycopene biosynthesis proceeds either via the 2-*C*-methyl-D-erythritol-4-phosphate (MEP) pathway found in prokaryotes (Fig. 2, **Pathway D**), or the mevalonate pathway operative in eukaryotes, such as yeasts and filamentous fungi. Both pathways converge to produce the precursors of lycopene, i.e., isopentenyl pyrophosphate (IPP) and dimethylallyl pyrophosphate (DMAPP) (Xu et al., 2021). In the MEP pathway, lycopene synthesis begins with the condensation of the key glycolytic intermediates, glyceraldehyde 3-P (G3P) and pyruvate, and continues in a nearly linear pathway. G3P and pyruvate are condensed to form 1-deoxy-d-xylulose-5-phosphate (DXP)—a reaction catalyzed by DXP synthase (DXS)— which is then converted to MEP by DXP reductoisomerase (DXR or IspC). A series of enzymes, namely 4-diphosphocytidyl-2C-methyl-d-erythritol cytidylyltransferase (IspD) and kinase (IspE), 2C-methyl-d-erythritol-2,4-cyclodiphosphate synthase (IspF), 4-hydroxy-3-methyl-2-(*E*)-butenyl-4-diphosphate (HMBPP) synthase (IspG), and HMBPP reductase (IspH), successively catalyze the conversion of MEP to IPP, along with the respective intermediates. Subsequently, isopentenyl-diphosphate isomerase (IDI) catalyzes the isomerization of IPP to DMAPP, that are eventually condensed into geranyl diphosphate (GPP). GPP is converted to farnesyl pyrophosphate (FPP) by FPP synthase (IspA), followed by successive catalysis by geranylgeranyl diphosphate synthase (CrtE), phytoene synthase (CrtB), and phytoene desaturase (CrtI) to ultimately yield lycopene (Wang et al., 2020b).

The TCA cycle plays both catabolic and anabolic roles by oxidizing acetyl-CoA to CO_2 for ATP production and supplying precursor metabolites and NADPH for biosynthesis. In the absence of glucose, sugar biosynthesis from TCA intermediates is essential for growth, requiring phosphoenolpyruvate (PEP) carboxykinase to convert oxaloacetate to phosphoenolpyruvate. The metabolic link between glycolysis, gluconeogenesis, and the TCA cycle is centered on the PEP–pyruvate–oxaloacetate node, also known as the anaplerotic node (Alteri et al., 2009; Basu et al., 2018; Marrero et al., 2010; Sauer and Eikmanns, 2005). Therefore, assimilated carbon, upon entering the TCA cycle, can be redirected towards gluconeogenesis under specific metabolic conditions.

Several *Rhodococcus* sp. strains possess the complete enzymatic machinery for lycopene biosynthesis, with *R. jostii* strain PET (RPET) is also capable of growing using PET hydrolysates as the sole carbon source. WT RPET cultures, fed with equimolar concentrations of TPA and EG, produced three unknown carotenoids and lycopene at low concentrations. Informed by the case of *Corynebacterium glutamicum*, where overexpression of CrtE, CrtB, and CrtI enhanced the flux from the precursor molecules towards lycopene, the RPET strain was metabolically engineered to incorporate the synthetic operon *crtEBI* (Henke et al., 2016). Indeed, the RPET engineered strain achieved lycopene synthesis of 630 μg/L, a 300-fold improvement over the WT, all the while the previously observed unknown carotenoids were substantially decreased, suggestive of competing mechanisms to lycopene biosynthesis. Another approach focused on the supply increase of the precursors IPP and DMAPP through the modification of their biosynthetic pathway. A synthetic *dxs-idi* operon, coding for the enzymes DXS and IDI, was expressed in RPET leading to a 390-fold augmentation of lycopene production (817 μg/L). However, the co-expression of *crtEBI* and *dxs-idi* had no cumulative effect but, instead, resulted in slightly lower yields compared to each individual approach (606 μg/L). The feasibility of upcycling PET into value-added chemicals was validated by exploring

lycopene production by the engineered RPET strain with 10 % *v*/v PET hydrolysates—resulting from alkaline hydrolysis— as the sole carbon source. The culture achieved a final lycopene titer of 1.2 mg/L, which improved to 1.3 mg/L in fed-batch fermentations (Diao et al., 2023).

3.2.5. Biopolymers synthesis

3.2.5.1. PHAs. The soil-isolated *Pseudomonas* strains, *P. putida* GO16, *P. putida* GO19, and *P. frederiksbergensis* GO23, were found to metabolize TPA as a sole carbon and energy source, while, simultaneously, accumulating mcl-PHAs at 23–27 % of their total cell dry weight (CDW) after 48 h. All three strains converted TPA to PHAs, but with varying efficiencies and polymer properties. Strain GO19 had the highest conversion efficiency, producing 8.4 mg/L/h of PHA. GO16 and GO19 showed higher PHA accumulation rates, though these were short-lived. Strain GO23, despite a lower initial rate, sustained its accumulation longer, making it potentially more suitable for industrial applications. GO16 and GO19 mainly produced 3-hydroxydecanoic acid polymers, while GO23 also synthesized 3-hydroxydodecanoic acid and 3-hydroxydodecenoic acid. All strains produced small amounts of 3-hydroxyhexanoic acid and 3-hydroxyoctanoic acid (Kenny et al., 2008).

Building upon the insights from shaken flask experiments, fed-batch fermentations with *P. putida* GO16 were optimized to enhance the conversion of TPA to PHAs. When TPA was the sole carbon source, *P. putida* GO16 achieved a CDW of 8.7 g/L and a PHA concentration of 2.6 g/L within 48 h, with PHA reaching 30 % of the CDW. The PHA produced was primarily composed of 3-hydroxydecanoic acid, though with a reduced proportion of 3-hydroxydodecenoic acid. Interestingly, continuous but decreasing nitrogen supply throughout the fermentation, instead of the conventional nitrogen limitation approach, led to a biomass yield of 0.6 g/g TPA, a PHA yield of 0.2 g/g TPA, and a 10-fold increase of PHA productivity (0.05 g/L/h) for *P. putida* GO16. On the other hand, when waste glycerol was supplied as the sole carbon source, *P. putida* GO16 utilized 222 g of the substrate, resulting in the accumulation of 108.9 g of biomass and 35.6 g of PHA over 48 h; the produced PHAs were primarily composed of C_8, C_{10}, and C_{12} monomers. In experiments where TPA and waste glycerol were co-supplied at the same ratio, the molecular weight of the PHAs decreased, and the monomer composition shifted to include higher proportions of C_{12} and C_{14} monomers, particularly 3-hydroxytetradecanoic acid and 3-hydroxytetradecenoic acid, which were absent when TPA was the sole carbon source. Mixed substrate fermentations with waste glycerol and TPA improved both biomass accumulation and PHA productivity compared to TPA alone, leading to a 1.2-fold increase in TPA utilization, a 1.6-fold rise in biomass productivity, and a 2-fold boost in PHA productivity, suggesting that co-feeding strategies could generally enhance productivity in similar cases (Kenny et al., 2012).

Another study evaluated the PHAs synthesis potential of *Pseudomonas umsongensis* GO16 KS3—a strain adapted through adaptive laboratory evolution (ALE) to grow on EG—when grown on enzymatically hydrolyzed amorphous PET films with a 47 % degree of depolymerization (Tiso et al., 2021). Remarkably, complete TPA consumption occurred within 23 h while EG was depleted at a 3.5-fold slower rate. After nitrogen depletion, PHA accumulation reached 7 % of CDW, with a biomass yield of 0.2 g CDW/g substrate and a PHA yield of 0.014 g /g substrate, with mcl-PHAs composed of C_8, C_{10}, and C_{12} monomers. Subsequently, *P. umsongensis* GO16 KS3 was engineered with the 3-(3-hydroxyalkanoyloxy) alkanoic acid synthesis plasmid pSB01 (Tiso et al., 2017a), enhancing the expression of RhlA, a 3-hydroxyacyl-ACP-O-3 hydroxyacyltransferase that catalyzes the formation of 3-(3-hydroxyalkanoyloxy) alkanoic acid by linking two activated β-hydroxy fatty acids. The engineered strain synthesized 3-(3-hydroxyalkanoyloxy) alkanoic acid exclusively from TPA, achieving a production rate of 5 mg/L/h and a yield of 0.01 g 3-(3-hydroxyalkanoyloxy) alkanoic acid /g TPA, while EG apparently only supported growth (Tiso et al., 2021).

Another *Pseudomonas* strain isolated from PET waste, *P. stutzeri* TPA3, was able to catabolize TPA, but didn't naturally accumulate any form of PHA. This strain was found to harbor the necessary genes for TPA conversion to PCA, which is subsequently metabolized into succinyl-CoA and acetyl-CoA through the βKA pathway (Harwood and Parales, 1996). By introducing the *phbCAB* operon from *Ralstonia eutropha*, responsible for the conversion of acetoacetyl-CoA to P3HB, engineered *P. stutzeri* TPA3P produced pure P3HB from TPA; notably, PhbC from *R. eutropha* is exclusively synthesizing scl-PHAs (Li et al., 2011). This engineered strain accumulated P3HB up to 12 % of CDW, when grown on 10 g/L TPA as the sole carbon source (Liu et al., 2021).

Beyond pseudomonads, the bacterial strain *I. sakaiensis* 201-F6, renowned for its PET-degrading capability, was found to possess a *phaCAB* gene cluster, suggesting PHAs production. When *I. sakaiensis* 201-F6 was cultured with PET granules, a high growth was observed, achieving a DCW of up to 1.6 g/L, demonstrating that PET served as a carbon source. The low concentration of PET hydrolysates in the culture supernatant compared to the PET weight loss suggests a rapid uptake of these degradation products by the cells. After 6 days of incubation, *I. sakaiensis* accumulated PHAs accounting for 48 % *w*/w of the DCW. However, 9 % of the carbon from PET was converted to PHAs, with the majority being metabolized into other compounds, including CO_2. The predominant monomer detected was methyl-3HB, comprising approximately 100 mol%, along with trace amounts of methyl 3-hydroxyvalerate, indicating that the synthesized PHA was nearly a P3HB homopolymer. Cultivation of *I. sakaiensis* 201-F6 with the PET degradation monomers TPA and EG, resulted in reduced growth and P3HB production (<5 %), indicating the strain preferentially utilizes PET hydrolytic oligomers over the individual monomers for growth and PHA synthesis (Fujiwara et al., 2021).

3.2.5.2. Bacterial nanocellulose. BNC is an extracellular biopolymer that forms a three-dimensional network at the air-liquid culture medium interface, and at least one of its dimensions is less than or equal to 100 nm. BNC bacterial production is closely related to many metabolic pathways, such as the pentose-phosphate pathway, the Embden–Meyerhof–Parnas pathway, the TCA cycle, and gluconeogenesis. BNC biosynthesis requires glucose-6-phosphate (Glu-6-P) as its main precursor, which could result from various routes, such as direct glucose assimilation, fructose metabolism, or the intracellular cascade of TCA cycle-pyruvate-gluconeogenesis. Once at the level of Glu-6-P, the BNC pathway proceeds via three chemical conversions (Fig. 2**, Pathway F**). Isomerization of Glu-6-P by phosphoglucomutase (PGM) yields glucose-1-phosphate (Glu-1-P), which is then converted to uridine diphosphate glucose (UDP-Glu) by UDP-Glu pyrophosphorylase; UDP-Glu is then polymerized by cellulose synthase (Bcs) into linear 1,4 glucan chains, which are activated by cyclic diguanylate (di-GMP) (Barja, 2021). In *Komagataeibacter xylinus,* Bcs function depends on the *bcsABCD* operon, where *bcsA* codes for the catalytic subunit and *bcsB* for a regulatory subunit that binds to cyclic di-GMP, while the roles of *bcsC* and *bcsD* are not yet fully understood (Ross et al., 1991).

Two *K. xylinus* strains, i.e., DSM 2004 and DSM 46604, were screened for their ability to produce BNC upon cultivation on TPA and/or EG. Both strains were able to utilize the mixture of TPA and EG as carbon source and produce BNC, although with different yields and variations in their crystallinity and nanostructure. *K. xylinus* DSM 2004 achieved higher BNC production from TPA (0.8 g/L), EG (0.6 g/L), and TPA/EG mixtures (0.6 g/L) than strain DSM 46604. The latter was unable to utilize EG as the sole carbon source but reached BNC production of 0.2 g/L both from TPA and the mixture (Esmail et al., 2022).

3.3. Ethylene glycol

3.3.1. Glycolate and its assimilation

During aerobic metabolism, the assimilation of EG proceeds via the

intermediate glycolaldehyde, which can be assimilated through various natural and synthetic pathways. EG is oxidized to glycolaldehyde (Fig. 3) by two functionally redundant periplasmic pyrroloquinoline quinone-dependent alcohol dehydrogenases (PedE and PedH) in *Pseudomonas* or by a 1,2-propanediol oxidoreductase (FucO) in *E. coli*, followed by the conversion to glycolate by cytoplasmic aldehyde dehydrogenases (PP_0545, PedI, and AldA). Some microorganisms can further oxidize glycolate to glyoxylate by the membrane anchored glycolate oxidase GlcDEF, and the latter can shortly enter the TCA cycle via either ligation with acetyl-CoA by malate synthase (GlcB) for the formation of malate, or condensation with succinate by isocitrate lyase (AceA) for the formation of isocitrate (Franden et al., 2018).

Several WT yeasts from the genera *Saccharomyces, Pichia*, *Hansenula*, and *Yarrowia lipolytica* have demonstrated the ability to perform oxidative biotransformation of EG to glycolate. The highest yield among the yeasts was observed by *Y. lipolytica* IMUFRJ 50682, that was capable of glycolate production, uncoupled to cell growth metabolism, at a molar yield of 86 % from 0.5 M EG; interestingly, this strain appeared tolerant up to 2 M EG titers (Carniel et al., 2023). *Pichia naganishii* AKU 4267 produced 35.3 g/L from 10 % *v*/v EG, achieving a molar conversion yield of 26 %. After optimizing the culture conditions, the yield increased to 88 % after 120 h, with complete substrate consumption, no intermediate accumulation, and the production of 150 g/L glycolate. However, when 20 % v/v EG was utilized, the yield dropped to 12 % (Kataoka et al., 2001).

The ability of *Gluconobacter* to convert EG to glycolate was also evaluated in various strains of *G. oxydans*, with *G. oxydans* DSM 2003 converting 70 g/L EG to 70.2 g/L glycolate after 48 h, with a molar conversion yield of 87 % and no detection of by-products (Wei et al., 2009). *G. oxydans* KCCM 40109 outperformed the previous, utilizing EG derived from microwave-radiated depolymerized PET, and achieving a maximum molar yield of 99 % with 10.7 mM EG within 12 h (Kim et al., 2019).

Soil-isolated microorganisms *Rhodotorula* sp., *Cryptococcus* sp., and *Burkholderia* sp. EG13 were also capable of growing on EG and producing glycolate, with molar conversion yields above 10 %. *Rhodotorula* sp. 3Pr-126 initially achieved a molar yield of 19 %, which was improved to 92 % after culture optimization. As a result, 110 g/L glycolate was produced after 120 h, with complete EG consumption and no intermediate accumulation. However, when the EG supply was doubled, i.e., 20 % v/v, the molar yield was 3-fold lower (Kataoka et al., 2001). *Burkholderia* sp. EG13 produced glycolate with a yield of 99 % from 200 mM EG after 24 h. To enhance production, in-situ product removal using adsorptive biotransformation was implemented, accumulating 793 mM glycolate after the fourth feed, in a 5-L bioreactor with a 2-L working volume (Gao et al., 2014).

In addition to utilizing native systems, synthetic biology has increasingly focused on engineering model organisms to assimilate EG and convert it to glycolate. By fine-tuning factors like oxygen concentration, researchers have achieved significant yields, demonstrating the potential of using EG as a renewable substrate for producing valuable chemicals. *E. coli* MG1655 was engineered for overexpression of its own 1,2-propanediol oxidoreductase FucO—also mutated to confer oxygen-resistance— and aldehyde dehydrogenase AldA, since the WT strain is not able to efficiently metabolize EG, despite harboring the genes for the purpose. The engineered strain could, indeed, convert EG to glycolate, and while under aerobic conditions glycolate oxidation to **glyoxylate** by native **glycolate oxidase** supported growth, under oxygen-limiting conditions glycolate accumulated as a product. In bioreactor fermentations with aeration control, glycolate production began after 28 h and continued until fermentation was terminated. Over a 112-h production period, a total of 10.4 g/L glycolate was generated, with an overall yield of 0.8 g/g EG and a productivity of 0.1 g/L/h (Pandit et al., 2021).

3.3.1.1. Glyoxylate carboligase pathway. An alternative catabolic route for glycolate is the glyoxylate carboligase (gcl) pathway (Fig. 3, **Pathway A**), through which two molecules of glyoxylate are condensed by Gcl to form tartronic semialdehyde, that is further reduced to glycerate, either directly by a tartronate semialdehyde reductase (GlxR) or via the hydroxypyruvate intermediate—hydroxypyruvate isomerase (Hyi) and hydroxypyruvate reductase (TtuD) catalyze the consecutive reactions within. Eventually, glycerate is phosphorylated by glycerate kinase to give either of two glycolytic intermediates, glycerate 3-phosphate or the 2-phospho isomer, which either proceed to glycolysis or participate in gluconeogenesis, depending on the cellular needs (Pandit et al., 2021).

Mückschel and coworkers (Mückschel et al., 2012), studied EG assimilation by two *P. putida* strains. *P. putida* JM37 was able to fully convert 50 mM EG within 24 h, with no detectable intermediates. *P. putida* KT2440, however, was unable to grow on EG and required over 48 h for complete EG conversion, during which glycolate, glyoxylate, and oxalate were identified in the supernatant. Proteomics analyses revealed that both strains induced the expression of PedI that is responsible for glycolaldehyde conversion to glycolate. However, *P. putida* JM37 additionally expressed Gcl, GlcB, and AceA that leads to the incorporation of glyoxylate into the TCA cycle via the glyoxylate shunt, thus facilitating growth.

Another study utilized ALE on *P. putida* KT2440 and the resulting strains successfully grew on EG. Interestingly, they all exhibited mutations in the *gclR* gene, which encodes a putative GntR-type transcriptional regulator responsible for repressing the gcl pathway. Interestingly, a few strains also exhibited mutations in the gene with locus tag PP_2046, encoding a LysR-type transcriptional regulator likely involved in controlling the adjacent operon that encodes enzymes pertinent to β-oxidation. Additionally, mutations were identified in the PP_2262 locus tag, which encodes a putative porin located upstream of an operon associated with a two-component sensory system. To evaluate the functional significance of these mutations, reverse engineering was performed on the parental KT2440 strain. Notably, deletion of the *gclR* gene enabled growth on EG, while simultaneous deletion of both PP_2046 and PP_2262 genes resulted in the fastest growth rates and the highest final biomass production. The absence of significant growth differences upon the deletion of either PP_2046 or PP_2262 suggests a complex interplay between these secondary mutations, likely influencing the balance between substrate transport across the outer membrane and the oxidation of alcohols and aldehydes (Li et al., 2019).

Unlike conventional approaches that rely on a single microorganism for PET upcycling, emerging strategies explore the use of microbial consortia to enhance degradation and assimilation processes. To address the limitations of individual strains, a four-species microbial consortium was designed to enhance PET breakdown by alleviating the inhibitory effects of its degradation products. Two strains of *B. subtilis* 168 were modified to secrete the enzymes PETase and MHETase, enabling PET hydrolysis into TPA and EG, respectively. *R. jostii* RHA1 and *P. putida* KT2440—capable of assimilating TPA and EG, respectively— were also introduced to alleviate the inhibitory effect of the PET monomers on the depolymerizing process. Through optimization of environmental conditions and inoculation ratios, the consortium achieved a PET depolymerization rate of 23 % in seven days – an improvement of 71 % compared to the degradation achieved by *Bacillus* strains alone. Although this study does not focus on producing high-value products, it demonstrates the potential of artificial microbial consortia in both PET depolymerization and monomer assimilation, offering insights into future strategies in plastic waste valorization (Qi et al., 2021).

Another recent study explored the upcycling potential of a microbial consortium consisting of two *P. putida* strains: Pp-T, specializing in TPA assimilation, and Pp-E, in EG utilization (Bao et al., 2023). Pp-T was derived from EM42 by deleting the *pedEHI* gene cluster to prevent EG oxidation to glycolate and introducing the *tpa* gene cluster from *R. jostii* RHA1 for TPA conversion to PCA (Section 3.2.1). Pp-E was constructed from M31 by: (i) deleting the *gclR* gene, encoding a transcriptional

regulator responsible for repressing the gcl pathway, and (ii) replacing the native promoter of the glycolate oxidase (*glcDEF*), yielding glyoxylate, with a strong Ptac promoter to enhance EG assimilation. The Pp-T/Pp-E consortium depleted 75 mM each TPA and EG in 62 h, outperforming the single-engineered Pp-TE strain, and also completely processed crude PET hydrolysates containing 50 mM each TPA and EG.

To further enhance PET hydrolysate upcycling, the study implemented the "division of labor" approach for the Pp-TC/ Pp-EM consortium aiming at MA biosynthesis. Pp-TC could convert TPA to catechol, and Pp-EM could convert catechol to MA while consuming EG. Pp-TC was engineered by deleting the *catRBCA* cluster to block the main catechol catabolic pathway and introducing the codon-optimized PCA decarboxylase aroY (Section 3.2.1) and the *E. cloacae* decarboxylase enhancer ecdB for catechol conversion. Pp-EM was engineered by deleting the *catRBC* operon and enhancing the conversion of catechol to MA with a Ptac promoter for the *catA* gene. The Pp-TC/ Pp-EM consortium, with a 1:5 inoculation ratio and optimized fermentation conditions, reached a molar yield of 33 % MA from PET hydrolysates containing 50 mM each TPA and EG, outperforming previous methods and single-strain systems (Bao et al., 2023). Although optimization could further develop this process, especially in terms of PET hydrolysate toxicity effects, this study established an integrated deconstruction process from powdered plastic to microbial biomass, demonstrating the engineered consortium's high substrate conversion efficiency.

3.3.1.2. β-hydroxyaspartate cycle. The assimilation of EG in *P. putida* via the gcl pathway is constrained by the gcl reaction, which catalyzes the condensation of two glyoxylate molecules into tartronate semialdehyde, leading to CO_2 release and reduced carbon efficiency (Kaplun et al., 2008). To improve EG assimilation, an alternative glyoxylate assimilation pathway with enhanced carbon retention was explored. The β-hydroxyaspartate cycle (BHAC), originally described in the 1960s (Kornberg and Morris, 1963) and recently fully characterized in *Paracoccus denitrificans* (Schada von Borzyskowski et al., 2019), provides a more carbon-efficient alternative by converting two glyoxylate molecules into oxaloacetate without CO_2 release. The cycle begins with aspartate-glyoxylate aminotransferase (BhcA), a pyridoxal 5′-phosphate-dependent enzyme that transaminates glyoxylate into glycine, using aspartate as the preferred amino donor. The key step is then catalyzed by β-hydroxyaspartate aldolase (BhcC), which facilitates the condensation of glyoxylate and glycine to form β-hydroxyaspartate. This intermediate is subsequently dehydrated by β-hydroxyaspartate dehydratase (BhcB) to yield iminosuccinate, which is then reduced to L-aspartate by iminosuccinate reductase (BhcD), completing the cycle (Fig. 3, **Pathway J**). By implementing the BHAC into *P. putida* KT2440 and applying ALE, the resulting strain KT2440 Δgcl + BHAC exhibited enhanced growth rate and biomass yield on EG (Schada von Borzyskowski et al., 2023), outperforming previous *P. putida* strains utilizing the glycerate pathway (Franden et al., 2018; Li et al., 2019).

3.3.1.3. Tartronyl-CoA pathway. The tartronyl-CoA (TaCo) pathway was recently proposed as a synthetic route for glycolate assimilation into central metabolism, designed to incorporate CO_2 rather than releasing it. While theoretically more carbon-efficient than natural glycolate assimilation routes, the pathway remained speculative, as neither tartronyl-CoA nor its associated enzymatic reactions had been observed in nature. To realize this pathway, Scheffen et al., engineered a novel glycolyl-CoA carboxylase through rational design, high-throughput microfluidics, and microplate screening (Scheffen et al., 2021). This enzyme catalyzes the carboxylation of glycolyl-CoA to tartronyl-CoA, which is subsequently reduced to glycerate by a tartronyl-CoA reductase from *Chloroflexus aurantiacus* (Fig. 3, **Pathway L**). A TaCo-based route for EG assimilation was then constructed to enhance carbon efficiency. This pathway integrated: (i) an alcohol dehydrogenase from *G. oxydans* (Gox0313) for EG conversion to glycolaldehyde, (ii) an aldehyde dehydrogenase from *Rhodopseudomonas palustris* BisB18 (PduP) for glycolyl-CoA formation, (iii) the newly developed glycolyl-CoA carboxylase, (iv) the *C. aurantiacus* tartronyl-CoA reductase, and (v) other genetic modifications that enhanced ATP and NAD^+ regeneration. This system served as a proof of principle and produced approximately 500 μM glycerate from 119 mM EG within 2 h.

3.3.1.4. D-arabinose 5-phosphate-dependent glycolaldehyde assimilation pathway. The intracellular assimilation of EG proceeds via the intermediate glycolaldehyde. However, naturally occurring pathways for glycolaldehyde assimilation exhibit low carbon efficiency in producing acetyl-CoA. A recently designed and in vitro validated pathway enabling carbon-conserving glycolaldehyde conversion to acetyl-CoA (Yang et al., 2019) was implemented in vivo to enhance EG assimilation (Wagner et al., 2023).

This synthetic glycolaldehyde assimilation pathway comprises one heterologous enzyme and engineered endogenous *E. coli* enzymes, overexpressed in the host strain *E. coli* MG1655 ΔyqhD ΔaldA lacIq, where genes encoding the major glycolaldehyde reductase YqhD (Alkim et al., 2015) and glycolaldehyde dehydrogenase AldA (Cam et al., 2016) were deleted to promote synthetic pathway utilization. The pathway initiates with FucO, yielding glycolaldehyde (Pandit et al., 2021). Subsequently, fructose 6-phosphate aldolase (FsaA) catalyzes the aldol addition of glycolaldehyde to glyceraldehyde 3-phosphate, forming D-arabinose 5-phosphate (Ara5P). Ara5P is then converted to D-xylulose 5-phosphate (Xylu5P) via Ara5P isomerase (KdsD) and D-ribulose 5-phosphate 3-epimerase (Rpe). Finally, *Clostridium acetobutylicum* phosphoketolase (CaPkt) converts Xylu5P into acetyl phosphate, which is further metabolized into acetate (Fig. 3, **Pathway I**).

The resulting engineered *E. coli* EG4 strain, overexpressing all pathway enzymes except Rpe, facilitated EG conversion to acetyl phosphate but exhibited minimal acetate accumulation (0.096 mM from 500 mM EG), likely due to thermodynamic constraints limiting downstream flux. To support growth, glycerol was used as a co-substrate, as it leads to lower acetate production compared to glucose (Martínez-Gómez et al., 2012). Although the observed yields remain low, this study demonstrates the feasibility of the Ara5P-dependent glycolaldehyde assimilation pathway under EG-utilizing conditions, paving the way for alternative assimilation routes that integrate into central metabolism and may be coupled to value-added product biosynthesis.

3.3.2. 2,4-dihydroxybutyric acid

Based on the concept of glycolaldehyde serving as a metabolic hub, channeling carbon sources into central cellular metabolism, another synthetic modular EG-assimilating glycolaldehyde-dependent pathway has been designed, this time coupled with the production of DHB (Frazão et al., 2023). This non-natural pathway proceeds via the NAD + -dependent alcohol dehydrogenase from *G. oxydans* Gox0313 (Scheffen et al., 2021) that catalyzes EG conversion to glycolaldehyde. Two molecules of glycolaldehyde are then converted into DHB by five consecutive reaction steps. In the first step, two molecules of glycolaldehyde are fused by the action of the *E. coli* D-threose aldolase Ec.FsaATA (Szekrenyi et al., 2014), to yield a single D-threose molecule. The resulting four-carbon sugar is oxidized by the *Paraburkholderia caryophylli* D-threose dehydrogenase Pc.TadH (Sasajima and Sinskey, 1979), to D-threono-1,4-lactone, which can then be converted to the corresponding sugar acid either spontaneously or in a reaction catalyzed by the *Thermogutta terrifontis* D-threono-1,4-lactonase Tt.Lac11 (Westlake, 2019). In the last two reaction steps, D-threonate is first dehydrated to 2-oxo-4-hydroxybutyrate by the *Herbaspirillum huttiense* D-threonate dehydratase Hh.AraD (Yew et al., 2006), and then the latter is reduced to yield DHB in a reaction catalyzed by the *E. coli* 2-oxo-4-hydroxybutyrate reductase Ec.Mdh5Q (quintuple mutant) (Fig. 3, **Pathway K**) (Frazão et al., 2018).

Following enzyme screening and transport optimization, Frazão and

coworkers (Frazão et al., 2023) developed *E. coli* TW354, which produced 6.8 mM DHB from EG via glycolaldehyde, albeit with low rates and titers (2 % molar yield). While further optimization is required to enhance efficiency, this study demonstrates a promising strategy for converting EG into valuable compounds, contributing to synthetic pathway design for improved CO_2 utilization.

3.3.3. Aromatics

Subsequent studies on *E. coli* MG1655, which enabled EG conversion to glycolate (Section 3.3.1), led to the development of *E. coli* EGT01. This strain was engineered for (i) enhanced EG utilization through FucO (Pandit et al., 2021) and (ii) L-tyrosine overproduction via two gene deletions and the incorporation of pTYR01 plasmid, which overexpresses feedback-resistant *aroG* and *tyrA* under a lac promoter. Medium optimization and process engineering enabled *E. coli* EGT01 to convert 270 mM EG into L-tyrosine at a molar yield of 6 %, surpassing glucose under comparable conditions (Panda et al., 2023). Using similar strategies, the same authors engineered *E. coli* EGP01 and EGC02, achieving phenylalanine and p-coumaric acid production at molar yields of 5.7 % and 3.8 %, respectively, from 160 mM EG. Finally, EG derived from waste PET hydrolysates supported L-tyrosine biosynthesis at yields comparable to commercial EG, demonstrating the potential of these engineered strains for PET upcycling.

Comparative transcriptome analysis provided insights into the metabolic pathway enabling EG conversion to L-tyrosine in *E. coli* EGT01 (Panda et al., 2023). EG is initially oxidized to glycolaldehyde and glycolate by the 1,2-propanediol oxidoreductase FucO and the aldehyde dehydrogenase AldA, respectively. Glycolate is further oxidized to glyoxylate by glycolate oxidase (GlcDEF) and enters the gcl pathway, eventually leading to the formation of 2-phosphoglycerate. Enolase (Eno) then catalyzes its dehydration to PEP, a key precursor in the shikimate pathway. In this pathway, PEP condenses with erythrose-4-phosphate, a pentose phosphate pathway intermediate, to form 3-deoxy-D-arabino-heptulosonate 7-phosphate (DAHP), catalyzed by DAHP synthases (e.g., AroG). DAHP undergoes six enzymatic transformations to chorismate, which is decarboxylated to 4-hydroxyphenylpyruvate by the bifunctional chorismate mutase/prephenate dehydrogenase TyrA. Finally, 4-hydroxyphenylpyruvate is transaminated to L-tyrosine using L-glutamate as the amino donor (Fig. 3, **Pathway H**) (Bentley and Haslam, 1990).

3.3.4. Anaerobic acetogenic pathway

In the acetogenic bacterium *Acetobacterium woodii*, the working hypothesis for EG metabolism comprises EG dehydration to acetaldehyde (Fig. 3, **Pathway B**) by a propane diol dehydratase (PduCDE) —the only dehydratase expressed in EG-growing cells—and then dismutation to ethanol and acetyl-CoA by a CoA-dependent propionaldehyde dehydrogenase (PduP) (Trifunović et al., 2016). Acetyl-CoA is further converted to acetate with concomitant ATP formation by substrate-level phosphorylation, while ethanol is oxidized to acetate, while the reducing equivalents are recycled by reduction of CO_2 to acetate via the reductive acetyl-CoA pathway (i.e., the Wood-Ljungdahl pathway) (Trifunović et al., 2016).

3.3.5. PHAs synthesis

P. putida KT2440 has the necessary genetic inventory that would enable utilization of EG as a sole carbon source for growth via the gcl pathway (Fig. 3, **Pathway A**), but expression is, apparently, not induced under relevant conditions. One study focused on engineering *P. putida* KT2440 to efficiently metabolize EG and produce mcl-PHAs, by overexpressing the complete *gcl* operon, coding for the glycolate oxidase GlcDEF that yields glyoxylate, and the other necessary enzymes for the downstream conversion of glyoxylate to glycolytic intermediates (Section 3.3.1.1). The engineered *P. putida* MFL185 strain demonstrated the ability to grow on EG concentrations as high as 2 M and completely metabolized up to 500 mM EG within 120 h. When supplied with 100 mM EG as the sole carbon source, MFL185 produced mcl-PHAs constituting 32 % DCW, with a product yield of 0.06 g/g and most of the monomers being C_8 and C_{10} (Franden et al., 2018). ALE was also successful when performed on *P. umsongensis* GO16, resulting in the KS3 strain that could grow on EG as the sole carbon source. Additionally, when PET hydrolysates were fed to the evolved strain, PHA production associated with both EG and TPA was detected, although further detailed studies on EG utilization for PHA synthesis are deemed necessary (Tiso et al., 2021).

In a recent study, *P. putida* strains Pp-T, Pp-E and Pp-TEP were engineered for enhanced mcl-PHAs production from PET-derived substrates by overexpression of key PHA biosynthetic genes (*phaG*, *alkK*, *phaC1*, *phaC2*) under the control of a constitutive promoter (Bao et al., 2023). The resulting strains, designated Pp-TP, Pp-EP, and Pp-TEP, demonstrated significant mcl-PHA yields, with Pp-TP producing 164 mg/L, Pp-EP 31 mg/L, and Pp-TEP 128 mg/L mcl-PHAs, during TPA and EG fermentation. In fermentations using PET hydrolysate containing 50 mM each TPA and EG, the TP/EP consortium consumed all hydrolysate in 65 h and produced 296 mg/L of mcl-PHAs, while Pp-TEP left 82 % of EG unconsumed. In fed-batch fermentations, under the same hydrolysate concentration, the TP/EP consortium produced 637 mg/L of mcl-PHAs, a 92 % increase compared to Pp-TEP.

3.4. Lactic acid

3.4.1. Biopolymers synthesis

3.4.1.1. PHAs. *R. eutropha* is a model organism for PHA synthesis, as well as a major industrially important strain, as it can accumulate large amounts of intracellular PHAs under nutrient limitation. PHA production by *R. eutropha* generally occurs during the stationary phase, hence, cells are first grown to high density after which a key nutrient is limited to trigger PHA synthesis (Chakraborty et al., 2012; Huschner et al., 2015; Lee, 1996).

A strain of *R. eutropha* was investigated for its ability to grow and accumulate PHAs when provided with a medium containing acetic, butyric, lactic and propionic acids, and LA was shown to be rapidly consumed (Chakraborty et al., 2012). According to subsequent studies, the presence of both LA and acetic acid was crucial for *R. eutropha* growth and PHAs production. When these two organic acids were exclusively present in the culture medium, higher CDW and PHAs productivity were observed, reaching 75 g/L and 55 g/L, respectively (Huschner et al., 2015; Tsuge et al., 2001). *R. eutropha* NRRL B14690 was also investigated for its ability to produce P3HB when grown on LA. At concentrations of 20 g/L LA, the culture yielded 1.2 g/L biomass and 0.09 g/L P3HB. Despite yielding less than half the amount observed with fructose— the standard carbon source— LA emerged as the second most effective carbon source used for P3HB production, among the 13 different carbon sources tested (i.e., fructose, glucose, LA, xylose, sucrose, molasses, sorbose, acetic acid, starch, sodium acetate, glycerol, lactose and propionic acid) (Khanna and Srivastava, 2005).

Although P3HB has been studied for decades and is efficiently produced from renewable carbon sources, its range of applications is limited due to its brittleness, stiffness, and high melting point. However, when LA is polymerized with P3HB, forming the *co*polymer poly(3HB-*co*-LA), the mechanical properties, the flexibility, and the transparency of the biomaterial are greatly improved (Yamada et al., 2011).

E. coli XL-Blue was engineered to produce poly(3HB-co-LA) from glucose by enhancing both the biosynthesis and incorporation of lactyl-CoA into the copolymer. Key mutations in *Clostridium propionicum* propionate CoA-transferase (PctCp) produced enzymes (Pct532Cp and Pct540Cp) with improved lactyl-CoA production, increasing both polymer content and LA mole fraction in the copolymer. Moreover, site-directed mutagenesis of *Pseudomonas* PHA synthase (PhaC1 Ps6–19) enhanced lactate incorporation (Yang et al., 2010). The engineered

E. coli strain was able to synthesize pure PLA when no 3HB was supplied, while with increasing concentrations of 3HB supplied, a linear decrease of the LA fraction of the copolymer was observed.

The strain was further modified in a subsequent study, by knocking out the *ackA, ppc*, and *adhE* genes and replacing the native promoters of the *idhA* and *acs* genes. The *ackA* and *adhE* genes encode for an acetate kinase and an acetaldehyde/alcohol dehydrogenase, responsible for acetate and ethanol formation from acetyl-CoA, respectively. Consequently, their deletion led to increased levels of acetyl-CoA, a major CoA donor for the generation of both lactyl-CoA and 3HB-CoA. The *ppc* gene encodes a pyruvate carboxylase, converting pyruvate to oxaloacetate, and its deletion increased the available pyruvate for lactate synthesis. Replacement of the native promoters of the *ldhA* (D-lactate dehydrogenase) and *acs* (acetyl-CoA synthetase) genes with the trc promoter, relieved the native regulation of genes expression and allowed higher lactate and acetyl-CoA formation, respectively. Introduction of *Cupriavidus necator* (widely known as *R. eutropha*) *phaA* and *phaB* genes, encoding β-ketothiolase and acetoacetyl-CoA reductase, respectively, allowed copolymer production without 3HB feeding. The final engineered *E. coli* JLX10 strain achieved LA fractions up to 70 mol% and polymer content of 20 % *w*/w (Jung et al., 2010). Based on this study, a fermentation setup where this, or a similarly performing bacterial strain, will be feeding on LA and producing P(3HB-co-LA), could be envisaged. For this to happen, LA oxidation to pyruvate by a lactate dehydrogenase (LDH) would be followed by conversion to acetyl-CoA by a pyruvate-ferredoxin oxidoreductase. Afterwards, any of the three primary metabolic pathways providing 3-hydroxyacyl precursors (Section 3.1) would result in copolymer production.

3.4.1.2. Bacterial nanocellulose. BNC biosynthesis depends on the Glu-6-P precursor and, thus, any carbon source that can be metabolized down to the level of Glu-6-P is a valid candidate for BNC production. Indeed, LA, being converted to pyruvate by LDH, can enter gluconeogenesis and eventually yield Glu-6-P (Fig. 3) (Hanson and Owen, 2004). A recent study reported PLA hydrolysates successfully supporting growth and BNC production by *Komagataeibacter medellinensis* ID13488 (Sourkouni et al., 2023). The valorization of PLA into BNC, through enzymatic hydrolysis and microbial fermentation, yielded varying amounts of LA, 30–70 % that from glucose, depending on the pretreatment method and duration.

3.4.2. Reverse β-oxidation pathway

3.4.2.1. Butyric acid. Although there are butyrate-producing pathways where amino acids serve as major substrates, i.e., the lysine, glutarate, and 4-aminobutyrate pathways, the most prevalent bacterial pathway for butyrate production proceeds via acetyl-CoA and the reverse β-oxidation pathway (Fig. 3, **Pathway C**). According to this, the first key metabolic intermediate is acetyl-CoA, which, in this case, results from LA oxidation to pyruvate. Synthesis of bytyryl-CoA proceeds via condensation of two acetyl-CoA molecules into acetoacetyl-CoA, reduction to 3-hydroxybutyryl-CoA, and dehydration to crotonyl-CoA. All four pathways merge at a central energy-generating step where crotonyl-CoA is reduced to butyryl-CoA by a butyryl-CoA dehydrogenase electron-transferring flavoprotein complex. Subsequently, butyryl-CoA is transformed to butyrate either by butyryl-CoA:acetate CoA transferase (*but* gene) or by butyrate kinase (*buk* gene) after phosphorylation of butyryl-CoA, generating acetyl-CoA as well (Saint-Amans et al., 2001; Vital et al., 2014).

Certain bacterial strains of *Eubacterium hallii* and *Anaerostipes caccae*, known for their ability to produce butyrate, were also found to metabolize both isomers of LA. When cultivated with DL-lactate, these strains utilized the entire substrate and converted it to butyrate at concentrations exceeding 20 mM. The proposed metabolic pathway for this conversion involves the acetyl-CoA pathway, following the conversion of LA to pyruvate and subsequently to acetyl-CoA by the enzymes LDH and pyruvate dehydrogenase (PDH), respectively. When *E. hallii* and *A. caccae* strains were provided with a complex substrate derived from starch biodegradation containing both lactate and acetate, they converted the full amount of LA and approximately half of the acetate to butyrate, as indicated by the molar ratio of substrates to butyrate (Duncan et al., 2004).

3.4.2.2. Caproic acid. The bioproduction of caproic acid (CA) involves a well-known chain elongation process that extends from acetate (two-carbon molecule) to butyrate (four-carbon molecule), and subsequently to caproate (six-carbon molecule) through the reverse β-oxidation pathway. While the conversion from acetate to butyrate is well understood, the key enzymes responsible for synthesizing caproyl-CoA and CA remain largely unidentified (Fig. 3, **Pathway D**). It is assumed that the enzymes involved in butyrate synthesis via reverse β-oxidation also play a role in the formation of CA, although this is not always supported by physiological and genomic studies (Lu et al., 2021).

Microbial CA production requires synthesis of acetyl-CoA and butyryl-CoA prior to CA formation. In the case of LA being the carbon source, the former is, presumably, established via LA oxidation to pyruvate and subsequently to acetate, generating acetyl-CoA. Additionally, LA oxidation would provide the necessary acetyl-CoA for the acetate to elongate its carbon length to form butyrate, according to the pathway described above. Subsequently, another acetyl-CoA molecule derived from LA would enter the cycle of reverse β-oxidation to form the key intermediate caproyl-CoA via four consecutive enzymatic steps. Finally, condensation of either caproyl-CoA and acetate or caproyl-CoA and butyrate yields CA (Lu et al., 2021; Zhu et al., 2015).

So far, a couple of native microbial systems have been studied for their CA production potential with LA as the sole carbon source. Among the studied strains, *Megasphaera hexanoica* demonstrated the highest efficiency and productivity with a yield of 0.9 g CA/g substrate (Kang et al., 2022), followed by *Ruminococcaceae bacterium* CPB6 with 0.3 g/g (Zhu et al., 2017), and *Megasphaera elsdenii* J1 with 0.1 g/g (h) (Marounek et al., 1989). In more detail, *M. hexanoica* produced 8.9 g/L CA from 10 g/L LA and compared to fructose, that is the conventional substrate for CA production by *M. hexanoica*, LA resulted in 4-fold less biomass. However, it generated 3-fold more CA, ultimately leading to similar final CA titers, demonstrating the higher specific productivity of LA compared to fructose. Conversely, *R. bacterium* CPB6 growing on LA displayed minimal differences in cell growth profiles compared to glucose, but exhibited earlier initiation of CA production, resulting in higher final titers and productivity.

3.5. 1,4-Butanediol

3.5.1. 4-Hydroxybutyric acid and the TCA cycle

Non-pathogenic pseudomonads, especially *P. putida* strains, have emerged as valuable model organisms in bioremediation, biodegradation, and bio-upcycling, owing to their exceptional metabolic versatility and adaptability to diverse physicochemical and nutritional conditions. These Gram-negative, γ-Proteobacteria are resilient to environmental stresses and produce various bioactive compounds. Notably, *P. putida* can accumulate intracellular polyester granules, i.e., PHAs, in response to carbon excess, offering potential as a substitute for conventional plastics.

Particularly, *P. putida* KT2440 is a well-characterized strain that excels as a synthetic biology chassis due to its genetic modifiability, rapid growth rate, and low nutrient demand. Moreover, it exhibits remarkable metabolic versatility towards a variety of carbon sources, including alcohols and aldehydes, and extensive genome-scale modelling studies have enabled the understanding of its intracellular metabolic mechanisms that proceed via a broad spectrum of native oxygenases, oxidoreductases, hydrolases, transferases and

dehydrogenases (Nelson et al., 2002; Nikel et al., 2014; Nikel and de Lorenzo, 2018).

The working mechanism for BDO degradation (Fig. 3**)** involves a two-step conversion of BDO to 4HB via 4HB-aldehyde, with the sequential catalytic action of an aldehyde dehydrogenase and an alcohol dehydrogenase. At the point of 4HB, two putative pathways are branching off. According to the direct oxidation pathway (Fig. 3**, Pathway E**), 4HB is first oxidized to succinate semialdehyde and eventually to succinate, which then enters the TCA cycle. WT *P. putida* KT2440 can grow on BDO as the sole carbon source, albeit with slow rates. Although proteomics data have confirmed the presence of relevant oxidoreductases that could catalyze BDO direct oxidation, it appears that in WT *P. putida* the bottleneck of this pathway is the oxidation of 4HB to succinate, indicated by the accumulation of 4HB in BDO-fed cultures (Li et al., 2020).

According to the alternative β-oxidation pathway (Fig. 3**, Pathway F**), 4HB is CoA-activated via CoA ligases or transferases and undergoes β-oxidation that would result in acetyl-CoA and glycolyl-CoA (Li et al., 2020). The former directly enters the TCA cycle, while glycolyl-CoA may be converted to glycolate and subsequently to glyoxylate. Glyoxylate, then, would either follow the glyoxylate shunt, leading to the production of malate or isocitrate that could enter the TCA cycle, or would be directed to the gcl pathway (Section 3.3.1.1). The gcl pathway results in the formation of glycerate, which is eventually phosphorylated to either of two glycolytic intermediates, glycerate 3-phosphate or glycerate-2-phosphate (Clark and Cronan, 2005).

ALE, atmospheric pressure room temperature plasma induced mutation, and genetic engineering—either for gene knockouts or insertions— have been employed towards the enhancement of *P. putida* KT2440 growth on BDO. Genome sequencing, transcriptomics, and proteomics have shed light on the molecular mechanisms underlying BDO degradation and utilization. ALE studies managed to obtain two evolved strains with 4-fold improved growth rates on BDO and lower 4HB accumulation. Based on knockout analyses and reverse-engineering, additionally supported by associated proteomics data, it was suggested that the evolved strains mainly proceed through the direct oxidation pathway towards SA, although the alternative β-oxidation hypothesis is possibly also operative (Li et al., 2020).

Atmospheric and room-temperature plasma combined with ALE resulted in the mutant *P. putida* NB10 that exhibited a 5-fold higher growth performance on BDO compared to the parental strain, and better tolerance against aldehydes that are putative metabolic intermediates of BDO degradation. Transcriptomics on *P. putida* NB10 revealed that TCA-related genes were downregulated compared to the KT2440 strain, while transcription of genes in the gcl pathway was upregulated, and the mutated *gcl* cluster promotor was shown to confer 17–74 times higher transcription. Based on the above, the authors suggested that BDO metabolism in NB10 strain, certainly proceeds via the alternative β-oxidation/gcl pathway (Qian et al., 2023).

P. putida KT2440 is one of the few microorganisms that possess both the metabolic pathways for 4HB biosynthesis and PHAs production, making it an excellent candidate for the biosynthesis of the valuable homopolymer P4HB. When two *P. putida* KT2440 evolved strains were grown under nitrogen limitation with BDO and octanoic acid as co-substrates (4:1 ratio), P4HB yields were about 60 %. When BDO was the sole carbon source though, both strains performed poorly, if at all (Li et al., 2020). *P. putida* NB10 on the other hand, accumulated 50 % more P4HB compared to the parental KT2440 strain when grown solely on BDO, while transcription of key genes associated with P4HB synthesis was upregulated (Qian et al., 2023). P4HB homopolymer synthesis is, presumably, enhanced via an interruption of the TCA cycle and redirection of the carbon flux towards the 4HB shunt, that would result in CoA-activation of 4HB and eventual synthesis of P4HB by PhaC (Utsunomia et al., 2020). This hypothesis is further supported by an unrelated study on an engineered *E. coli* strain, where deletion of succinate semialdehyde dehydrogenase genes eliminated succinate formation and led to increased 4HB synthesis (Li et al., 2010). Similarly, in *P. putida* and *Pseudomonas entomophila*, inhibition of β-oxidation via gene deletion has been shown to redirect the metabolic flux from fatty acid degradation to PHA biosynthesis, hence, significantly increasing substrate conversion efficiency and PHA synthesis (Chen and Jiang, 2017).

Besides Pseudomonads, *G. oxydans* DSM50049 can also utilize BDO as a carbon source (Ismail et al., 2024). Its genome reveals an incomplete TCA cycle, lacking genes for succinate dehydrogenase and succinyl CoA synthetase, leading to a unique strategy of incomplete oxidation. This allows *G. oxydans* to thrive in nutrient-rich environments despite low energy efficiency and growth yields (Prust et al., 2005). BDO catabolism in *G. oxydans* proceeds through the direct oxidation pathway, as in *P. putida* KT2440. Depending on the culture pH, *G. oxydans* produces either 4HB or a mix of 4HB and SA, with complete substrate consumption in both cases. At neutral pH, only 4HB is produced with an 88 % yield, while at pH 5.0, both products are in equal molar ratios, indicating pH sensitivity of 4HB dehydrogenase and succinate semialdehyde dehydrogenase.

3.5.2. Malic acid

MLA is naturally synthesized in all organisms during cellular metabolism, but its accumulation is only associated with stress conditions or mutant strains. Due to its high commercial value, diverse applicability, and the relatively expensive industrial production routes, microbial production of MLA has attracted research interest. Apart from being cost efficient, microbially produced MLA is also advantageous due to its optically pure L-form as opposed to racemic mixtures produced by chemical processes (Khandelwal et al., 2023). Since its first identification as a yeast fermentation product in the early 20th century (Dakin, 1924), various native fungal species have been used as natural MLA producers, and genetic and metabolic engineering approaches have been employed for the optimization of the process. So far, three different native cellular pathways are known to lead to MLA synthesis (Fig. 3), and these have also been the focus of engineering attempts. The oxidative TCA cycle starts with the synthesis of citric acid followed by several oxidative reactions to synthesize MLA, while the reductive TCA pathway leads to MLA via a two-step enzymatic conversion of pyruvate. MLA is also synthesized through the gcl pathway which acts as an anaplerotic intracellular mechanism.

In the frame of plastic waste streams valorization, a recent study screening native *Ustilaginaceae* strains capable of producing MLA identified *Ustilago trichophora* TZ1 as the first fungal strain that could grow on BDO as the sole carbon source (Phan et al., 2024). Interestingly, this strain would produce MLA and SA while grown on glycerol (Zambanini et al., 2016), but when BDO was used as carbon source, the polyols mannitol and erythritol were additionally produced (Phan et al., 2023). ALE combined with culture optimizations, enhanced growth of *U. trichophora* TZ1 on BDO, with MLA yields reaching 33 % (Phan et al., 2023). The concomitant production of sugar alcohols has not been studied further, but the pathway that could be envisaged proceeds via the 4HB intermediate, the TCA cycle, pyruvate generation, and gluconeogenesis that results in the production of Glu-6-P. The latter is the precursor for the biosynthesis of both mannitol and erythritol, that are produced via established intracellular pathways (Nakagawa et al., 2020; Wisselink et al., 2002).

3.5.3. Rhamnolipids synthesis

Rhamnolipid synthesis relies on two widely known pathways, i.e., fatty acid de novo synthesis and the rhamnose pathway, providing the required precursors 3-(3-hydroxyalkanoyloxy) alkanoic acid and activated deoxy-thymidine-diphospho-L-rhamnose (dTDP-L-rhamnose), respectively (Fig. 3**, Pathway G**). Unlike molecules synthesized through a single pathway, rhamnolipids synthesis requires two central carbon metabolism intermediates: acetyl-CoA for 3-(3-hydroxyalkanoyloxy) alkanoic acid and Glu-6-P—the first intermediate of glucose

metabolism—for dTDP-L-rhamnose. In the rhamnose pathway, Glu-6-P is initially converted to Glu-1-P by an enzyme with phosphoglucomutase activity. Glu-1-P is then transformed into rhamnose by the concerted action of four enzymes, a G1P thymidylyltransferase (RmlA), a dTDP-D-glucose 4,6-dehydratase (RmlB), a dTDP-6-deoxy-D-xylo-4-hexulose 3,5-epimerase (RmlC), and a dTDP-6-deoxy-L-lyxo-4-hexulose reductase (RmlD) (Giraud and Naismith, 2000; Maier and Soberón-Chávez, 2000).

Pseudomonas aeruginosa possesses the essential genes for rhamnolipid synthesis, which involves three dedicated enzymatic reactions. Initially, RhlA, a 3-hydroxyacyl-ACP-O-3 hydroxyacyltransferase, catalyzes the dimerization of 3-hydroxyacyl-ACP, descending from the fatty acid de novo synthesis, forming 3-(3-hydroxyalkanoyloxy) alkanoic acid. Subsequently, RhlB, a rhamnosyltransferase I, condenses 3-(3-hydroxyalkanoyloxy) alkanoic acid with dTDP-L-rhamnose to produce mono-rhamnolipids. The final step involves RhlC, a rhamnosyltransferase II, which adds another rhamnose moiety to the mono-rhamnolipid, resulting in a di-rhamnolipid. The genes *rhlA* and *rhlB* are organized in a single operon, whereas *rhlC* is located elsewhere in the *P. aeruginosa* genome, forming an operon with a gene of unknown function (Tiso et al., 2016; Wittgens et al., 2017).

As mentioned previously, *P. putida* KT2440 was submitted to ALE to be able to metabolize BDO (Li et al., 2020). Afterwards, the evolved strain was engineered with the *rhlAB* operon from *P. aeruginosa* to facilitate mono-rhamnolipid production and it was, indeed, shown to produce 0.13 g/L mono-rhamnolipids, with a yield of 0.09 g/g of substrate (Utomo et al., 2020). Although the metabolic processes underlying BDO upcycling to mono-rhamnolipids were not studied in detail, one could picture a scenario where BDO is intracellularly catabolized via the discussed pathways, eventually reaching the level of G6P and, additionally, fueling de novo fatty acid synthesis.

3.6. Succinic acid

3.6.1. BDO formation

Intracellularly, SA is first activated by succinyl-CoA synthetase (SucCD), and is, subsequently, converted to succinate semialdehyde by a CoA-dependent succinate semialdehyde dehydrogenase (SucD). 4HB dehydrogenase (4HBd) catalyzes 4HB formation, that can be activated by 4HB-CoA transferase (Cat2). From that point, two consecutive reductive steps, catalyzed by 4HB-CoA reductase and aldehyde dehydrogenase, can lead to the formation of 4HB-aldehyde and BDO, respectively (Fig. 3) (Burk et al., 2015; Yim et al., 2011).

E. coli naturally catalyzes the conversions of SA to succinyl-CoA and 4HB-aldehyde to BDO. An engineered *E. coli* system, with heterologous gene expression accounting for the missing steps, was shown to convert SA all the way to BDO (Yim et al., 2011). Specifically, the enzyme SucD from *Porphyromonas gingivalis* was found to be critical for 4HB production, while co-expression of a 4HB dehydrogenase from the same microorganism further enhanced 4HB yield. By constructing a synthetic operon that sequentially incorporates *sucCD* from *E. coli*, and *sucD* and 4HBd from *P. gingivalis*, a significantly higher 4HB:SA ratio was achieved. Additionally, the expression of the aldehyde/alcohol dehydrogenase adhE2, responsible for the conversion of 4HB-aldehyde to BDO, from WT *C. acetobutylicum,* alongside the expression of the *cat2* gene from *P. gingivalis,* were optimized for use in *E. coli,* to facilitate BDO production.

3.6.2. PHAs synthesis

Various WT bacterial strains exhibit the capacity to utilize SA and synthesize PHAs, although the exact molecular mechanism is not definitive. Based on the available knowledge, it is likely that this conversion proceeds via the conversion of SA to acetyl-CoA through the TCA cycle, followed by the subsequent synthesis of PHAs through the established bacterial pathways (Pradhan et al., 2020). For instance, when supplied with SA as the sole carbon source, *R. palustris* SP5212 was able to accumulate PHAs, with P3HB accounting for approximately 3 % CDW (Mukhopadhyay et al., 2005). Bacterial strains *C. glutamicum* DSM 20137 and *Bacillus megaterium* DSM 509, on the other hand, synthesized pure P3HB, representing 10 % and 45 % CDW, respectively. *P. putida* mt-2 accumulated mcl-PHAs at about 15 % CDW, with the C_{10} monomer (3-hydroxydecanoate) comprising 60 % of the total PHAs produced (Shahid et al., 2013).

3.7. Adipic acid

Microbial assimilation of AA by *Acinetobacter baylyi* is encoded in two separate operons and depends on the concerted action of dedicated transporters and enzymes (Fig. 2**, Pathway G**). One operon encodes the transport proteins DcaK and DcaP, the CoA transferase subunits DcaIJ, and the acyl-CoA dehydrogenase DcaA, whose concerted action results in the production of 2,3-didehydro-adipyl-CoA. The latter is further degraded to acetyl-CoA and succinyl-CoA via β-oxidation, which depends on the *dcaECHF* operon that includes an enoyl-CoA hydratase (DcaE), a hydroxyacyl-CoA dehydrogenase (DcaH), and an acyl-CoA thiolase (DcaF) (Ackermann et al., 2021).

3.7.1. PHAs synthesis

Building upon the inherent capacity of *P. putida* KT2440 to synthesize PHAs from diverse carbon substrates (Liu et al., 2022a), metabolic engineering efforts targeted the expression of the *dcaAKIJP* operon, complemented by the organism's innate genetic repertoire for the downstream metabolic pathway, i.e., β-oxidation. Unexpectedly, the engineered strain could not grow on AA as the sole carbon source, but subsequent ALE supported growth as well as PHAs production with a yield of about 25 % CDW, leading to the hypothesis that the native *P. putida* genes for β-oxidation were not induced previously. The PHAs produced were composed of C_6, C_8, C_{10}, and C_{12} monomers, with the C_{10} being the more predominant, accounting for 56 % of the total (Ackermann et al., 2021).

Sullivan and coworkers (Sullivan et al., 2022) studied the valorization of mixed plastics starting with metal-catalyzed autooxidation of different combinations of polystyrene, high-density polyethylene, and PET mixtures, that yielded oxygenated small organic molecules. Their microbial upcycling approach was focused on the production of βKA and PHAs, demonstrating a tunable bioconversion microbial chassis. The authors based their metabolic design on two previously engineered *P. putida* strains from (Werner et al., 2021) (Section 3.2.3) and (Ackermann et al., 2021) (**current Section**). In summary, the new *P. putida* AW162 strain was capable of: (i) TPA assimilation and conversion to PCA (engineered pathway), (ii) PCA 3,4-cleavage pathway (native pathway) leading to the TCA cycle (Section 3.2.3 & Fig. 2**, Pathway C**), (iii) AA assimilation due to the incorporation of the *A. baylyi dca* gene cluster (engineered pathway), along with the deletion of native *paaX* and *psrA*, which repress phenylacetate catabolism and β-oxidation, respectively, and (iv) PHAs production (native pathway). Indeed, *P. putida* AW162 could produce mcl-PHAs, primarily comprised of C_{10} and C_{12}, when grown on effluent from mixed postconsumer high-density polyethylene bottles and expanded polystyrene cups. *P. putida* AW307 was tuned towards βKA accumulation instead, and thus its native PCA 3,4-cleavage pathway was interrupted by the *pcaIJ* gene deletion. *P. putida* AW307 grew on a model mixture and an effluent of the depolymerized mixed plastics—both containing benzoate, terephthalate, C_4-C_{18} dicarboxylates, and acetate—and βKA was produced at a 76 % molar yield (calculated on benzoate and terephthalate) (Sullivan et al., 2022).

3.7.2. 1,6-diaminohexane synthesis

The microbial conversion of AA to DAH is another upcycling system that has been constructed, based on the action of select CARs and transaminases (TA). According to the simplest pathway, AA is first reduced to adipic semialdehyde, which is, subsequently, converted into

either adipaldehyde or 6-aminocaproic acid. Both these intermediates are then metabolically transformed into 6-aminohexanoic acid, which is further transaminated to DAH (Fig. 2**, Pathway H**).

An *E. coli* BL21 strain was selected for the construction of a whole-cell artificial pathway for DAH biosynthesis, due to its inherent tolerance to DAH and its intermediate, 6-aminocaproic acid. In the first step, the strain was genetically engineered to heterologously express genes encoding a CAR from *Mycobacteroides abscessus* (MAB CAR), a TA from *Chromobacterium violaceum* (CVTA) and a phosphopantetheinyl transferase (SFP) from *B. subtilis* (Quadri et al., 1998). The necessity of enzymes with these functionalities for the conversion of AA to DAH was validated, and various CAR and TA enzymes from diverse microbial sources were evaluated, both individually and in combinations. The selection and arrangement of different CARs and TAs in the constructed vectors influenced the efficiency of reduction and transamination for the intermediate conversions. The most efficient cascade module for DAH synthesis was found to be the CAR – CAR – TA – TA (CCTT) branch, that was comprised of a CAR from *Mycolicibacterium smegmatis* MC2 I55 (MSM CAR), a MAB CAR, a TA from *Silicibacter pomeroyi* (SPTA), and a TA from *E. coli* (PatA); the latter was proven to be essential for 6-aminohexanoic acid transamination to DAH. Furthermore, given that CARs are NADPH-dependent enzymes, optimization of NADPH supply to the system was crucial. Indeed, the deletion of the *sthA* gene, encoding a transhydrogenase isoenzyme responsible for the mutual transformation between NADH and NADP in *E. coli*, resulted in a significant enhancement of DAH yield. In the end, the engineered *E. coli* strain achieved a production of 239 mg/L of DAH in shake flask fermentation, more than 500-fold increase relative to the initial strain (Wang et al., 2023).

3.8. 6-hydroxyhexanoic acid

3.8.1. Adipic acid production

The metabolic pathway of cyclohexanol utilization by *Acinetobacter* has been elucidated already for 50 years and is known to depend on at least five enzymes that work consecutively to produce AA (Iwaki et al., 1999). In this pathway, HHA serves as the third metabolic intermediate that is converted to 6-oxohexanoic acid by HHA dehydrogenase (*chnD*), and eventually to AA by the action of 6-oxohexanoate dehydrogenase (*chnE*) (Fig. 2). Two recent independent studies managed to engineer *E. coli* JM109 to express the gene products of *chnE* and *chnD* and, therefore, yield about 2–4 g/L AA when HHA was supplied in batch fermentations. By regulating the addition of HHA during fed-batch fermentations, AA production increased approximately 3.6-fold, reaching about 16 g/L (Oh et al., 2022, 2023).

4. Significance and applications of added-value products

4.1. Aromatics

Aromatic compounds, particularly phenolic acids and derivatives, possess a variety of biological and industrial applications. These compounds exhibit significant antioxidant, anti-inflammatory, antimicrobial, and anticancer properties, along with diverse uses in pharmaceuticals, food preservation, and material science.

Protocatechuic acid (PCA; IUPAC: 3,4-dihydroxybenzoic acid) is a potent antioxidant with anti-inflammatory, antihyperglycemic, anticancer, and antimicrobial properties. It mitigates oxidative stress by scavenging free radicals, reduces reactive oxygen species, and boosts endogenous antioxidant enzymes, protecting against degenerative diseases. PCA also regulates inflammatory mediators, improves glucose homeostasis, and promotes apoptosis in cancer cells. Its diverse therapeutic applications include antiulcer, antiaging, antifibrotic, cardioprotective, and neuroprotective effects, with potential in preventing colon cancer, managing type 2 diabetes, and protecting against toxicity from both natural and synthetic agents (Kakkar and Bais, 2014; Kelidari et al., 2024). Its antimicrobial effects against various bacteria and fungi suggest applications in health protection and food preservation (Semaming et al., 2015).

Gallic acid (GA; IUPAC: 3,4,5-trihydroxybenzoic acid) is known for its antioxidant, anti-inflammatory, and neuroprotective properties, especially in the treatment of neurodegenerative diseases like Alzheimer's and Parkinson's. It acts through modulation of oxidative stress and inflammation, with applications in managing psychiatric disorders and neuroinflammation. GA also has anticancer potential due to its prooxidant activity, inducing apoptosis in cancer cells (Bhuia et al., 2023; Kahkeshani et al., 2019). Beyond health applications, it is widely used in food preservation, cosmetics, and leather tanning (Badhani et al., 2015).

Catechol (IUPAC: benzene-1,2-diol) is a versatile compound found in fruits, vegetables, and as a metabolic product in humans (Schweigert et al., 2001). It serves as an intermediate in various industrial processes, including the production of antioxidants, polymers, and in the cosmetic and pharmaceutical industries, in photographic development and as a flavoring agent (National Center for Biotechnology Information, 2024a). Catechol's unique adhesive properties, inspired by mussel proteins, are also being explored for synthetic coatings and biomedical materials (Zhang et al., 2022).

Pyrogallol (PG; IUPAC: benzene-1,2,3-triol) is a trihydroxybenzene with strong reducing and antioxidant properties. Historically used in photographic development, PG has applications in dyeing, environmental monitoring, medicinal chemistry, and materials science (National Center for Biotechnology Information, 2024b). It also plays a role in the preparation of metal colloids and as an analytical reagent for oxygen measurement. Its natural occurrence in hardwoods like oak and eucalyptus highlights its longstanding relevance in both traditional and modern uses.

Vanillic acid (VA; IUPAC: 4-hydroxy-3-methoxybenzoic acid) is a phenolic compound found in medicinal plants and used as a flavoring agent (National Center for Biotechnology Information, 2024c). VA demonstrates anticancer, anti-obesogenic, antidiabetic, and antimicrobial effects. It induces apoptosis, inhibits cancer cell cycle progression, and mitigates oxidative stress and inflammation (Kaur et al., 2022). VA also holds potential in treating obesity and metabolic disorders, as well as offering cardioprotective and hepatoprotective benefits (Ingole et al., 2021).

Vanillin (IUPAC: 4-hydroxy-3-methoxybenzaldehyde), the primary compound in vanilla extract, is widely used as a flavoring agent but also exhibits antioxidant, anti-inflammatory, anticancer, and antidiabetic properties. While often considered merely a food additive, research indicates that vanillin has significant therapeutic potential, warranting further exploration for clinical applications due to its bioavailability bioavailability (Olatunde et al., 2022).

2-Pyrone-4,6-dicarboxylic Acid (PDC; IUPAC: 2-oxo-2H-pyran-4,6-dicarboxylic acid) is a pseudoaromatic compound obtained through microbial conversion of PCA (Kang et al., 2020). Its structure enables polymerization with diols to form biodegradable polyesters with enhanced mechanical properties. PDC-based polyesters, polyamides, and polyurethanes exhibit excellent biodegradability, thermal stability, and elasticity, making them valuable in producing eco-friendly materials (Otsuka et al., 2023; Zhou et al., 2023c).

L-tyrosine (IUPAC: (2*S*)-2-amino-3-(4-hydroxyphenyl)propanoic acid) is a non-essential amino acid with diverse applications, synthesized in vivo from *L*-phenylalanine. It serves as a precursor for catecholamines such as dopamine, norepinephrine, and epinephrine, as well as thyroid hormones and melanin, emphasizing its critical role in neurological and metabolic functions. In the brain, dietary tyrosine directly influences neurotransmitter levels, which are vital for stress response and cognitive performance. Beyond its biological significance, L-tyrosine is utilized as a flavoring agent, nutritional supplement, and ingredient in hair and skin conditioning products in the cosmetics industry. Its applications in treating phenylketonuria, biochemical depression, and Parkinson's disease highlight its therapeutic potential,

although certain claims remain inconclusive (National Center for Biotechnology Information, 2025a).

Phenylalanine (IUPAC: (2*S*)-2-amino-3-phenylpropanoic acid) is an essential aromatic amino acid fundamental to protein biosynthesis and a precursor to tyrosine. It plays a pivotal role in the production of catecholamines, including dopamine and norepinephrine, which are integral to the nervous system (National Center for Biotechnology Information, 2025b). *L*-phenylalanine is also a key component in artificial sweeteners like aspartame, underscoring its industrial importance (Doble and Kruthiventi, 2007). Beyond food applications, its therapeutic uses extend to managing vitiligo, chronic pain, and certain mood disorders (National Center for Biotechnology Information, 2025b).

p-Coumaric acid (IUPAC: (E)-3-(4-hydroxyphenyl)prop-2-enoic acid) is a naturally occurring phenolic compound found in a variety of vegetables and fruits. Known for its antioxidative properties, it mitigates oxidative stress, reducing the risk of cardiovascular diseases (Ponnian et al., 2024). p-Coumaric acid also has applications in cosmetics as a skin-conditioning agent, while its potential in food preservation leverages its antimicrobial effects (National Center for Biotechnology Information, 2025c). Additionally, its role as a precursor in synthesizing bio-based and biodegradable materials supports the development of sustainable industrial solutions (Singh et al., 2020; Zhang et al., 2025).

4.2. Saturated monocarboxylic acids

Saturated monocarboxylic acids are widely used in various industries and have significant biological effects. These compounds, ranging from small alpha-hydroxy acids to fatty acids, play crucial roles in therapeutic applications, skincare, flavoring, and industrial processes.

Glycolic acid (IUPAC: 2-hydroxyacetic acid) is the smallest alpha-hydroxy acid and is extensively used in dermatology, particularly for chemical peels. It addresses skin concerns like wrinkles, acne scarring, and hyperpigmentation by facilitating exfoliation and revealing fresher skin. As a keratolytic agent, it also aids in treating corns, warts, and fungal infections (Chemical Entities of Biological Interest (ChEBI), 2021). Beyond skincare, glycolic acid is used in food processing, textile and leather dyeing, metal processing, adhesives manufacturing, and ink production, improving flow properties and gloss (National Center for Biotechnology Information, 2024d).

2,4-dixydroxybutyric acid (DHB; IUPAC: 2,4-dihydroxybutanoic acid) is a hydroxy-substituted short-chain fatty acid derived from butyric acid (National Center for Biotechnology Information, 2025d). Its industrial relevance stems from its role as a versatile platform molecule for synthesizing value-added products. It serves as an intermediate in producing 1,3-propanediol and 1,2,4-butanetriol—key compounds in the manufacturing of plastics, solvents, and propellants. Under acidic conditions, 2,4-dihydroxybutyric acid spontaneously forms 2-hydroxy-γ-butyrolactone, which can be further processed into γ-butyrolactone and 1,4-butanediol, both critical in polymer production. Additionally, it contributes to the synthesis of the methionine analog 2-hydroxy-4-(methylthio)butyrate, widely utilized in animal nutrition (Walther et al., 2017).

Butyric acid (IUPAC: butanoic acid) is a short-chain fatty acid with significant therapeutic potential. It exhibits anti-inflammatory and anticancer properties by modulating transcription factors involved in immune response. Butyrate, its active form, is beneficial for managing gastrointestinal disorders such as irritable bowel syndrome and Crohn's disease by enhancing intestinal barrier function. Butyrate also influences the gut-brain axis, affecting metabolism and systemic functions, and is useful in treating skin conditions like atopic dermatitis and psoriasis (Liu et al., 2018) (Coppola et al., 2022).

Caproic acid (CA; IUPAC: hexanoic acid) is a six-carbon chain fatty acid synthesized endogenously and found in plants. It serves as a precursor in producing esters used in perfumery, pharmaceuticals, and the polymer industry. Caproic acid is also a flavoring agent with a distinctive cheesy odor and is utilized in making metal hexanoates for use as drying agents in paints and varnishes (National Center for Biotechnology Information, 2024e).

4-Hydroxybutyric acid (4HB; IUPAC: 4-hydroxybutanoic acid), also known as γ-hydroxybutyric acid, is derived from butyric acid and acts as a neurotransmitter. It is used in medical applications, such as a general anesthetic and to treat narcolepsy-related conditions. 4HB influences neurotransmitter activities by crossing the blood-brain barrier and interacting with specific receptors, leading to central nervous system depression (Chemical Entities of Biological Interest (ChEBI), 2024; National Center for Biotechnology Information, 2024f).

4.3. Saturated dicarboxylic acids

Saturated dicarboxylic acids, including adipic acid and succinic acid, are key intermediates in industrial processes and have a wide range of applications across multiple sectors, such as polymers, food, pharmaceuticals, and environmental management.

Adipic acid (AA; IUPAC: hexanedioic acid) is a key aliphatic α,ω-dicarboxylic acid and a primary precursor for nylon-6,6 production, which accounts for around 90 % of its use. It is also used in manufacturing polyester polyols for polyurethane systems (National Center for Biotechnology Information, 2024g). In addition to its role in polymers, AA is employed in producing plasticizers, lubricants, and food additives (E355), such as gelling agents, acidulants, and leavening agents. It is further utilized in pesticides, dyes, textile treatments, fungicides, and pharmaceuticals (Goldberg and Rokem, 2009). However, its production can release N_2O, a potent greenhouse gas, prompting efforts to reduce emissions from production facilities (Shimizu et al., 2000).

Succinic acid (SA; IUPAC: butanedioic acid) is a valuable four-carbon dicarboxylic acid with applications in food, cosmetics, and chemistry. As an intermediate in the TCA cycle, SA contributes to cellular energy production and serves as a precursor for many compounds (National Center for Biotechnology Information, 2024h). In the food industry, it functions as a flavor enhancer and acidity regulator (E363). It is also used in detergents, cosmetics, dyes, and pharmaceuticals, particularly in treatments for metabolic diseases and diabetes (Lee et al., 2019). Additionally, SA has antibiotic properties and can support neural recovery and immune function. It is a precursor for chemicals like BDO, γ-butyrolactone, and tetrahydrofuran, as well as bio-based polymers like PBS and PBSA. Moreover, SA and its derivatives are employed in the leather and metallurgy industries for water resistance, strength enhancement, and ore flotation (Raj et al., 2024).

4.4. Unsaturated dicarboxylic acids

Unsaturated dicarboxylic acids, including muconic acid, β-ketoadipic acid, and malic acid, are essential compounds with significant roles in industrial and biological applications. These acids contribute to various processes in polymer chemistry, bioplastics, food, and pharmaceuticals, while also offering sustainable alternatives to traditional materials.

Muconic acid (MA; IUPAC: (2E,4E)-hexa-2,4-dienedioic acid) is a conjugated dicarboxylic acid derived mainly from the oxidative cleavage of benzene derivatives. It serves as a critical precursor for producing high-demand chemicals like AA and TPA, essential in nylon, polyurethanes, and polyesters (Khalil et al., 2020). MA exists in three isomeric forms—*cis,cis*-MA, *cis,trans*-MA, and *trans,trans*-MA—each with distinct chemical properties for diverse applications. In addition to polymer chemistry, MA is used in bioplastics, functional resins, agrochemicals, and as an intermediate in food additives, medicines, cosmetics, and textiles (Choi et al., 2020; Wang et al., 2020a).

β-ketoadipate (βKA; IUPAC: 3-oxohexanedioic acid) is a six-carbon diacid that serves as an alternative to AA in nylon-6,6 analogue production. Featuring a β-ketone group, βKA results in materials with improved thermal stability and reduced water permeability. Biologically synthesized from sugars, βKA offers a sustainable alternative to fossil-

based AA, requiring significantly less energy and generating fewer greenhouse gases. The same bioprocess also yields products with superior performance characteristics, making it an environmentally friendly choice for bio-based polymer production (Rorrer et al., 2022).

Malic acid (MLA; IUPAC: 2-hydroxybutanedioic acid) is an alpha-hydroxy acid naturally found in fruits and wines, with multiple roles in food and biological systems. It serves as a food acidity regulator and enhances flavors in beverages, jams, and candies. In skincare, MLA helps exfoliate dead skin cells and stimulates saliva production for individuals with dry mouth. As a key metabolite in the Krebs cycle, it plays a critical role in energy production (National Center for Biotechnology Information, 2024i). Additionally, MLA is used in metal cleaning, textile finishing, water treatment, and fabric dyeing. Its biopolymer, poly(β-L-MLA), is biocompatible, biodegradable, and water-soluble, making it ideal for drug delivery systems and advanced biomaterials (Lee et al., 2019).

4.5. Saturated and functionalized organic compounds

Saturated and functionalized organic compounds, such as BDO and DAH, play crucial roles in various industries, from pharmaceuticals and polymers to sustainable material development. Their versatility as intermediate compounds and their use in producing high-performance materials make them essential to modern manufacturing processes.

1,4-butanediol (BDO; IUPAC: butane-1,4-diol) is a straight-chain glycol with hydroxyl groups at both ends, renowned for its versatility as an intermediate compound. BDO is utilized across several industries, including pharmaceuticals, food, cosmetics, and plasticizers. It serves as a humectant, solvent, food additive, and pharmaceutical intermediate. BDO is also used in the production of polyurethane elastomers, contributing to automotive parts, footwear, and recreational equipment. Furthermore, it is integral to the synthesis of tetrahydrofuran and γ-butyrolactone, essential in electronics, pharmaceuticals, and agrochemicals (National Center for Biotechnology Information, 2024j). One of BDO's key applications is in the creation of biodegradable polymers such as PBS, PBSA, and PBAT, which are vital for sustainable material development.

1,6-diaminohexane (DAH; IUPAC: hexane-1,6-diamine) is a versatile organic compound, particularly important in polymer synthesis. Its two functional amine groups make it ideal for creating robust and resilient polymers. DAH plays a pivotal role in the production of nylon-6,6, where it reacts with AA in condensation polymerization. This process is critical for manufacturing nylon, which is used extensively in textiles and engineering plastics (Palmer, 2003). Additionally, DAH can undergo phosgenation to generate hexamethylene diisocyanate, a precursor for polyurethane manufacturing (Hu et al., 2017). DAH is also utilized as a cross-linking agent in resin systems, including epoxy resins, adhesives, and paper manufacturing (Lainioti et al., 2021).

4.6. Biopolymers

The biopolymers polyhydroxyalkanoates (PHAs) and bacterial nanocellulose (BNC) are biodegradable, biocompatible, and non-toxic materials with a broad range of applications. These sustainable alternatives to conventional plastics are gaining attention across industries like healthcare, agriculture, packaging, and beyond.

In healthcare, PHAs are widely used in drug delivery systems, tissue engineering, and medical devices such as sutures, surgical needles, and bone tissue replacements. Specific PHAs, like poly(3-hydroxybutyrate-*co*-3-hydroxyvalerate), poly(3-hydroxybutyrate-co-3-hydroxyhexanoate), and poly(3-hydroxybutyrate-co-4-hydroxybutyrate), are employed for skin regeneration, bone tissue engineering, and heart valve replacements, respectively (Pandey et al., 2022). In the packaging industry, PHAs serve as a sustainable alternative to petroleum-based plastics, being used in products such as plastic bags, food packaging, and disposable items like utensils and straws (Ladhari et al., 2023). Furthermore, PHAs are utilized in agriculture for improving soil structure and water retention, as well as in water treatment processes for denitrification. Additionally, PHAs have potential as biofuels, offering an eco-friendly alternative to traditional fuels (Pandey et al., 2022). The mcl-PHAs P3HB and P4HB are particularly notable for their unique properties and diverse applications, including use in biodegradable polymers and medical devices.

Poly(3-hydroxybutyrate) (P3HB) is widely used in bone tissue engineering, especially in internal bone fixation devices and composite implants, where it supports osteoblast adherence and bone formation. It is also employed in absorbable sutures and wound dressings due to its biocompatibility, tensile strength, and minimal tissue reactivity (Israni and Shivakumar, 2019). Mcl-PHAs like P3HB are also ideal for low mechanical integrity products such as hot melt adhesives, coatings, and as carriers for slow-release bioactives (Muthuraj et al., 2021).

Poly(4-hydroxybutyrate) (P4HB) is a biodegradable thermoplastic polyester known for its strength, elasticity, and biocompatibility. It is widely used in resorbable medical devices, including sutures and surgical meshes, and has been FDA-approved for various medical applications. P4HB's ability to degrade slowly in vivo minimizes complications and enhances long-term mechanical support (Mitra et al., 2021a). Additionally, it is the only type of PHAs that has received FDA approval for medical use, with applications in tissue engineering, drug delivery systems, and even congenital cardiovascular defect repairs (Martin and Williams, 2003; Utsunomia et al., 2020). Despite its high production costs, P4HB represents a significant advancement in medical materials, offering promising applications in tissue engineering and drug delivery (Martin and Williams, 2003; Mitra et al., 2021b).

BNC is a nanomaterial derived from bacterial cellulose, which has exceptional properties, including high porosity, low cytotoxicity, and biocompatibility. BNC emerges as a ribbon-shaped nanomaterial with dimensions typically ranging from 20 to 100 nm in diameter and several μm in length (Kaur et al., 2021). BNC is widely used in biomedical applications as a scaffold for tissue engineering and regenerative medicine. Its three-dimensional network offers substantial mechanical strength, making it ideal for these purposes. Additionally, BNC serves in the food and cosmetics industries as a thickening, stabilizing, and gelling agent (de Amorim et al., 2020). It is also employed in drug delivery systems, enhancing drug stability and facilitating controlled release (Bacakova et al., 2019). BNC has further applications in ion-exchange membranes and fuel cells, contributing to environmentally friendly technologies due to its thermal-oxidative stability (Kaur et al., 2021).

4.7. Lycopene

Lycopene (IUPAC: [6E,8E,10E,12E,14E,16E,18E,20E,22E,24E,26E]-2,6,10,14,19,23,27,31-octamethyldotriaconta-2,6,8,10,12,14,16,18,20,22,24,26,30-tridecaene) is a carotenoid pigment closely related to β-carotene and is responsible for the red colour of various fruits and vegetables, such as tomatoes, pink grapefruits, apricots, and guavas (Mangels et al., 1993). Known for its antioxidant and anti-inflammatory properties, lycopene helps protect cells from oxidative damage caused by environmental toxins and chronic diseases (Javanmardi and Kubota, 2006). A diet rich in lycopene may lower the risk of certain cancers, including prostate and breast cancer (Mazidi et al., 2020), reduce pain, and offer benefits for ocular, neurological, and skeletal health. In addition, lycopene may improve cholesterol levels, potentially reducing the risk of heart disease and premature mortality, as well as enhance the skin's defense against UV-induced damage (Cooperstone et al., 2017; Mozos et al., 2018).

4.8. Rhamnolipids

Rhamnolipids, biosurfactants primarily produced by *Pseudomonas* and *Burkholderia* species, are known for their high surface activity, emulsification, and biodegradability. Their low toxicity and effectiveness in reducing surface and interfacial tension make them valuable in

agriculture, enhanced oil recovery, environmental remediation, food preservation, and pharmaceuticals. In agriculture, rhamnolipids combat plant pathogens and improve soil quality, while in oil recovery, they enhance extraction efficiency. They also aid in hydrocarbon and heavy metal bioremediation, prevent fungal growth in food storage, and show promise in cancer therapy and drug delivery (Thakur et al., 2021; Tiso et al., 2017b). Growing industrial interest is reflected in numerous patents, and in 2024, the first commercial rhamnolipid production plant opened in Slovakia, marking a key step in sustainable biosurfactant manufacturing (Evonik, 2024).

5. Concluding remarks

The growing incentive for circular bioplastic economy value chains is reflected by the rising number of scientific studies, global academic and industrial synergies, and expanding funding opportunities, especially the past five years. Polyester upcycling is a promising innovation that adheres to circular economy principles by mitigating global plastic pollution, reducing natural resources depletion, and promoting sustainable industrial practices. Hydrolytic degradation of polymers into oligomers and their constituent building blocks can be followed by microbial assimilation and eventual production of compounds of interest, essentially transforming waste into commercially valuable products.

Among the polyesters examined, PET has received the lion's share of depolymerization and upcycling research, owing to its prevalence in single-use plastics, particularly beverage bottles, food packaging, and disposable containers. In parallel, biodegradable plastics have gained increasing attention for their potential role in circular economy. PLA exemplifies this trend, offering a distinct advantage in that its hydrolysis yields a single monomeric product through de-esterification. Research on sustainable management and upcycling of other polyesters is gaining momentum, as it has become clear that landfilling biodegradable materials alone does not prevent their long-term environmental accumulation. Effective waste management strategies, including industrial composting, controlled (bio)degradation, and upcycling, are essential to facilitate their reintegration into natural biogeochemical cycles or circular value chains.

Successful microbial upcycling designs must meet two conditions, i.e., efficient carbon assimilation from polyester monomers, and functional biosynthetic pathways yielding valuable bioproducts. Thus, bioprospecting and synthetic biology are used in tandem, with the aim of discovering microorganisms naturally capable of performing either and, subsequently, engineering or modifying the other process. Among the several WT microorganisms that have been found capable of either process, *P. putida* is in the limelight, not only due to its central carbon metabolism that supports rerouting of carbon fluxes towards desired inherent pathways via transcription regulation, but also because of its relatively easy genetic manipulation leading to the introduction of novel synthetic pathways. However, many biochemical pathways for plastic degradation and assimilation are found in non-model microorganisms, highlighting the need to explore their metabolic diversity for future advancements in the field (Wilkes et al., 2023).

The array of products obtained thus far in a laboratory scale, span a wide range of applications, from repolymerization processes to pharmaceutical and material industries: (i) commodity chemicals valuable for diverse industrial applications, such as catechol, PG, and rhamnolipids; (ii) bioactive compounds utilized in pharmaceutical and cosmetic industries, such as PCA, GA, L-tyrosine, phenylalanine, glycolic acid, butyric acid, 4HB, and MLA; (iii) precursors utilized in polymer production, such as MA, PDC, βKA, DHB, and DAH; (iv) specialty chemicals abundantly used in food industry, such as VA, vanillin, and lycopene; (v) biodegradable and highly biocompatible biopolymers gaining momentum in the field of material science, such as BNC and PHAs; and (vi) others that are versatile enough to pervade diverse industrial fields, such as AA, CA, p-coumaric acid, SA, and BDO.

As the global plastic waste crisis intensifies, innovative and daring strategies are deemed essential to effectively process and reintegrate plastics into the economy. Biological upcycling offers an alternative approach to managing plastic waste by converting it into valuable products, all the while minimizing humanity's dependence on finite fossil fuel resources. Nonetheless, several hurdles and challenges remain to be overcome. The efficiency and specificity of microbial upcycling processes need further optimization to enhance yield and product diversity. Additionally, scaling these biotechnological solutions to industrial levels requires addressing issues related to process stability and economic viability. Future research should focus on engineering robust microbial strains and optimizing metabolic pathways to improve the conversion rates of plastic monomers into desired products. Looking ahead, integrating these biological upcycling systems with existing waste management infrastructure could revolutionize recycling practices, making them more sustainable and eco-friendlier, while collaborative efforts between researchers, industry stakeholders, and policymakers will be crucial in driving the adoption and implementation of these technologies.

Declaration of competing interest

The authors declare that they have no known competing financial interests or personal relationships that could have appeared to influence the work reported in this paper.

Acknowledgments

This work has been financially supported by the European Union under Horizon Europe (TwInn4MicroUp Project, Grant Agreement No 101159570) and the H.F.R.I call "Basic research Financing (Horizontal support of all Sciences)" under the National Recovery and Resilience Plan "Greece 2.0" funded by the European Union – NextGenerationEU (EnZyReMix Project, Project No 15024).

References

Ackermann, Y.S., Li, W.J., Op de Hipt, L., Niehoff, P.J., Casey, W., Polen, T., Köbbing, S., Ballerstedt, H., Wynands, B., O'Connor, K., Blank, L.M., Wierckx, N., 2021. Engineering adipic acid metabolism in Pseudomonas putida. Metab. Eng. 67, 29–40. https://doi.org/10.1016/J.YMBEN.2021.05.001.

Al Mamun, A., Prasetya, T.A.E., Dewi, I.R., Ahmad, M., 2023. Microplastics in human food chains: food becoming a threat to health safety. Sci. Total Environ. 858, 159834. https://doi.org/10.1016/J.SCITOTENV.2022.159834.

Aliotta, L., Seggiani, M., Lazzeri, A., Gigante, V., Cinelli, P., 2022. A brief review of poly (butylene succinate) (PBS) and its main copolymers: synthesis, blends, composites, biodegradability, and applications. Polymers (Basel) 14, 844. https://doi.org/10.3390/POLYM14040844.

Alkim, C., Cam, Y., Trichez, D., Auriol, C., Spina, L., Vax, A., Bartolo, F., Besse, P., François, J.M., Walther, T., 2015. Optimization of ethylene glycol production from (d)-xylose via a synthetic pathway implemented in Escherichia coli. Microb. Cell Factories 14, 127. https://doi.org/10.1186/s12934-015-0312-7.

Alteri, C.J., Smith, S.N., Mobley, H.L.T., 2009. Fitness of Escherichia coli during urinary tract infection requires gluconeogenesis and the TCA cycle. PLoS Pathog. 5. https://doi.org/10.1371/journal.ppat.1000448.

Bacakova, L., Pajorova, J., Bacakova, M., Skogberg, A., Kallio, P., Kolarova, K., Svorcik, V., 2019. Versatile application of nanocellulose: from industry to skin tissue engineering and wound healing. Nanomaterials 9, 164. https://doi.org/10.3390/NANO9020164.

Badhani, B., Sharma, N., Kakkar, R., 2015. Gallic acid: a versatile antioxidant with promising therapeutic and industrial applications. RSC Adv. 5, 27540–27557. https://doi.org/10.1039/C5RA01911G.

Bao, T., Qian, Y., Xin, Y., Collins, J.J., Lu, T., 2023. Engineering microbial division of labor for plastic upcycling. Nat. Commun. 14, 1–13. https://doi.org/10.1038/s41467-023-40777-x.

Barja, F., 2021. Bacterial nanocellulose production and biomedical applications. J. Biomed. Res. 35, 310. https://doi.org/10.7555/JBR.35.20210036.

Barletta, M., Aversa, C., Ayyoob, M., Gisario, A., Hamad, K., Mehrpouya, M., Vahabi, H., 2022. Poly(butylene succinate) (PBS): materials, processing, and industrial applications. Prog. Polym. Sci. 132, 101579. https://doi.org/10.1016/J.PROGPOLYMSCI.2022.101579.

Basu, P., Sandhu, N., Bhatt, A., Singh, A., Balhana, R., Gobe, I., Crowhurst, N.A., Mendum, T.A., Gao, L., Ward, J.L., Beale, M.H., McFadden, J., Beste, D.J.V., 2018. The anaplerotic node is essential for the intracellular survival of Mycobacterium tuberculosis. J. Biol. Chem. 293, 5695–5704. https://doi.org/10.1074/jbc.RA118.001839.

Benedict, C.V., Cameron, J.A., Huang, S.J., 1983. Polycaprolactone degradation by mixed and pure cultures of bacteria and a yeast. J. Appl. Polym. Sci. 28, 335–342. https://doi.org/10.1002/APP.1983.070280129.

Bentley, R., Haslam, E., 1990. The shikimate pathway - a metabolic tree with many branches. Crit. Rev. Biochem. Mol. Biol. 25, 307–384. https://doi.org/10.3109/10409239009090615.

Bhuia, M.S., Rahaman, M.M., Islam, T., Bappi, M.H., Sikder, M.I., Hossain, K.N., Akter, F., Al Shamsh Prottay, A., Rokonuzzman, M., Gürer, E.S., Calina, D., Islam, M. T., Sharifi-Rad, J., 2023. Neurobiological effects of gallic acid: current perspectives. Chin. Med. 18, 1–19. https://doi.org/10.1186/S13020-023-00735-7.

Buchholz, P.C.F., Feuerriegel, G., Zhang, H., Perez-Garcia, P., Nover, L.L., Chow, J., Streit, W.R., Pleiss, J., 2022. Plastics degradation by hydrolytic enzymes: the plastics-active enzymes database—PAZy. Proteins Struct. Funct. Bioinforma. 90, 1443–1456. https://doi.org/10.1002/PROT.26325.

Burk, M.J., Burgard, A.P., Osterhout, R.E., Sun, J., 2015. Microorganisms for the production of 1,4-Butanediol. Google patents. US9175297B2.

Cam, Y., Alkim, C., Trichez, D., Trebosc, V., Vax, A., Bartolo, F., Besse, P., François, J.M., Walther, T., 2016. Engineering of a synthetic metabolic pathway for the assimilation of (d)-xylose into value-added chemicals. ACS Synth. Biol. 5, 607–618. https://doi.org/10.1021/acssynbio.5b00103.

Carniel, A., Santos, A.G., Chinelatto, L.S., Castro, A.M., Coelho, M.A.Z., 2023. Biotransformation of ethylene glycol to glycolic acid by Yarrowia lipolytica: a route for poly(ethylene terephthalate) (PET) upcycling. Biotechnol. J. 18, 2200521. https://doi.org/10.1002/BIOT.202200521.

Chacón, M., Wongsirichot, P., Winterburn, J., Dixon, N., 2024. Genetic and process engineering for polyhydroxyalkanoate production from pre- and post-consumer food waste. Curr. Opin. Biotechnol. 85, 103024. https://doi.org/10.1016/j.copbio.2023.103024.

Chakraborty, P., Muthukumarappan, K., Gibbons, W.R., 2012. PHA productivity and yield of Ralstonia eutropha when intermittently or continuously fed a mixture of short chain fatty acids. J. Biomed. Biotechnol. https://doi.org/10.1155/2012/506153.

Chemical Entities of Biological Interest (ChEBI), 2021. CHEBI:17497 - Glycolic Acid [WWW Document]. URL. https://www.ebi.ac.uk/chebi/searchId.do?chebiId=CHEBI:17497 (accessed 12.16.24).

Chemical Entities of Biological Interest (ChEBI), 2024. CHEBI:30830–4-Hydroxybutyric Acid [WWW Document]. URL. https://www.ebi.ac.uk/chebi/searchId.do?chebiId=30830.

Chen, G.Q., Jiang, X.R., 2017. Engineering bacteria for enhanced polyhydroxyalkanoates (PHA) biosynthesis. Synth. Syst. Biotechnol. 2, 192–197. https://doi.org/10.1016/J.SYNBIO.2017.09.001.

Choi, K.Y., Kim, D., Sul, W.J., Chae, J.-C., Zylstra, G.J., Kim, Y.M., Kim, E., 2005. Molecular and biochemical analysis of phthalate and terephthalate degradation by Rhodococcus sp. strain DK17. FEMS Microbiol. Lett. 252, 207–213. https://doi.org/10.1016/j.femsle.2005.08.045.

Choi, S., Lee, H.N., Park, E., Lee, S.J., Kim, E.S., 2020. Recent advances in microbial production of cis,cis-muconic acid. Biomolecules 10, 1–14. https://doi.org/10.3390/BIOM10091238.

Clark, D.P., Cronan, J.E., 2005. Two-carbon compounds and fatty acids as carbon sources. EcoSal Plus 1. https://doi.org/10.1128/ECOSALPLUS.3.4.4/ASSET/D4B5BFCC-D0D0-4EC9-BFFC-8ED764486037/ASSETS/GRAPHIC/3.4.4_FIG_008.GIF.

Cooperstone, J.L., Tober, K.L., Riedl, K.M., Teegarden, M.D., Cichon, M.J., Francis, D.M., Schwartz, S.J., Oberyszyn, T.M., 2017. Tomatoes protect against development of UV-induced keratinocyte carcinoma via metabolomic alterations. Sci. Rep. 7, 5106. https://doi.org/10.1038/S41598-017-05568-7.

Coppola, S., Avagliano, C., Sacchi, A., Laneri, S., Calignano, A., Voto, L., Luzzetti, A., Canani, R.B., 2022. Potential clinical applications of the postbiotic butyrate in human skin diseases. Molecules 27, 1849. https://doi.org/10.3390/MOLECULES27061849.

Dakin, H.D., 1924. The formation of l-malic acid as a product of alcoholic fermentation by yeast. J. Biol. Chem. 61, 139–145. https://doi.org/10.1016/S0021-9258(18)85164-X.

Darby, R.T., Kaplan, A.M., 1968. Fungal susceptibility of polyurethanes. Appl. Microbiol. 16, 900–905. https://doi.org/10.1128/AM.16.6.900-905.1968.

Davis, J.T., Moore, R.N., Imperiali, B., Pratt, A.J., Kobayashi, K., Masamune, S., Sinskey, A.J., Walsh, C.T., Fukui, T., Tomita, K., 1987. Biosynthetic thiolase from zoogloea ramigera. I. Preliminary characterization and analysis of proton transfer reaction. J. Biol. Chem. 262, 82–89. https://doi.org/10.1016/S0021-9258(19)75891-8.

de Amorim, J.D.P., de Souza, K.C., Duarte, C.R., da Silva Duarte, I., de Assis Sales Ribeiro, F., Silva, G.S., de Farias, P.M.A., Stingl, A., Costa, A.F.S., Vinhas, G.M., Sarubbo, L.A., 2020. Plant and bacterial nanocellulose: production, properties and applications in medicine, food, cosmetics, electronics and engineering. A review. Environ. Chem. Lett. 18, 851–869. https://doi.org/10.1007/S10311-020-00989-9.

de França, J.O.C., da Silva Valadares, D., Paiva, M.F., Dias, S.C.L., Dias, J.A., 2022. Polymers based on PLA from synthesis using D,L-lactic acid (or racemic lactide) and some biomedical applications: a short review. Polymers (Basel) 14, 2317. https://doi.org/10.3390/POLYM14122317.

Debuissy, T., Pollet, E., Avérous, L., 2017. Synthesis and characterization of biobased poly(butylene succinate-ran-butylene adipate). Analysis of the composition-dependent physicochemical properties. Eur. Polym. J. 87, 84–98. https://doi.org/10.1016/J.EURPOLYMJ.2016.12.012.

Diao, J., Hu, Y., Tian, Y., Carr, R., Moon, T.S., 2023. Upcycling of poly(ethylene terephthalate) to produce high-value bio-products. Cell Rep. 42, 111908. https://doi.org/10.1016/J.CELREP.2022.111908.

Doble, M., Kruthiventi, A.K., 2007. Chapter 9 - Industrial examples. In: Green Chemistry and Engineering. Academic Press. https://doi.org/10.1016/B978-012372532-5/50010-9.

Duncan, S.H., Louis, P., Flint, H.J., 2004. Lactate-utilizing bacteria, isolated from human feces, that produce butyrate as a major fermentation product. Appl. Environ. Microbiol. 70, 5810. https://doi.org/10.1128/AEM.70.10.5810-5817.2004.

Elhacham, E., Ben-Uri, L., Grozovski, J., Bar-On, Y.M., Milo, R., 2020. Global human-made mass exceeds all living biomass. Nature 588, 442–444. https://doi.org/10.1038/s41586-020-3010-5.

Esmail, A., Rebocho, A.T., Marques, A.C., Silvestre, S., Gonçalves, A., Fortunato, E., Torres, C.A.V., Reis, M.A.M., Freitas, F., 2022. Bioconversion of terephthalic acid and ethylene glycol into bacterial cellulose by Komagataeibacter xylinus DSM 2004 and DSM 46604. Front. Bioeng. Biotechnol. 10, 853322. https://doi.org/10.3389/FBIOE.2022.853322/BIBTEX.

European Commission Eurostat, 2025. Packaging Waste Statistics [WWW Document]. Eurostat. https://doi.org/10.2908/ENV_WASPAC.

Evonik, 2024. Evonik manufactures first product from world's first industrial-scale rhamnolipid biosurfactant plant [WWW Document]. https://personal-care.evonik.com/en/evonik-manufactures-first-product-from-worlds-first-industrial-scale-rhamnolipid-biosurfactant-plant-233324.html.

Fields, R.D., Rodriguez, F., Finn, R.K., 1974. Microbial degradation of polyesters: polycaprolactone degraded by P. pullulans†. J. Appl. Polym. Sci. 18, 3571–3579. https://doi.org/10.1002/APP.1974.070181207.

Franden, M.A., Jayakody, L.N., Li, W.J., Wagner, N.J., Cleveland, N.S., Michener, W.E., Hauer, B., Blank, L.M., Wierckx, N., Klebensberger, J., Beckham, G.T., 2018. Engineering Pseudomonas putida KT2440 for efficient ethylene glycol utilization. Metab. Eng. 48, 197–207. https://doi.org/10.1016/J.YMBEN.2018.06.003.

Frazão, C.J.R., Topham, C.M., Malbert, Y., François, J.M., Walther, T., 2018. Rational engineering of a malate dehydrogenase for microbial production of 2,4-dihydroxybutyric acid via homoserine pathway. Biochem. J. 475, 3887–3901. https://doi.org/10.1042/BCJ20180765.

Frazão, C.J.R., Wagner, N., Rabe, K., Walther, T., 2023. Construction of a synthetic metabolic pathway for biosynthesis of 2,4-dihydroxybutyric acid from ethylene glycol. Nat. Commun. 14, 1–14. https://doi.org/10.1038/s41467-023-37558-x.

Fredi, G., Dorigato, A., 2021. Recycling of bioplastic waste: a review. Adv. Ind. Eng. Polym. Res. 4, 159–177. https://doi.org/10.1016/J.AIEPR.2021.06.006.

Fujiwara, R., Sanuki, R., Ajiro, H., Fukui, T., Yoshida, S., 2021. Direct fermentative conversion of poly(ethylene terephthalate) into poly(hydroxyalkanoate) by Ideonella sakaiensis. Sci. Rep. 11, 1–7. https://doi.org/10.1038/s41598-021-99528-x.

Gambarini, V., Pantos, O., Kingsbury, J.M., Weaver, L., Handley, K.M., Lear, G., 2021. Phylogenetic distribution of plastic-degrading microorganisms. mSystems 6. https://doi.org/10.1128/mSystems.01112-20.

Gambarini, V., Pantos, O., Kingsbury, J.M., Weaver, L., Handley, K.M., Lear, G., 2022. PlasticDB: a database of microorganisms and proteins linked to plastic biodegradation. Database 2022. https://doi.org/10.1093/DATABASE/BAAC008.

Gan, Z., Zhang, H., 2019. PMBD: a comprehensive plastics microbial biodegradation database. Database 2019. https://doi.org/10.1093/DATABASE/BAZ119.

Gao, X., Ma, Z., Yang, L., Ma, J., 2014. Enhanced bioconversion of ethylene glycol to glycolic acid by a newly isolated Burkholderia sp. EG13. Appl. Biochem. Biotechnol. 174, 1572–1580. https://doi.org/10.1007/s12010-014-1114-9.

Gao, R., Pan, H., Kai, L., Han, K., Lian, J., 2022. Microbial degradation and valorization of poly(ethylene terephthalate) (PET) monomers. World J. Microbiol. Biotechnol. 38, 1–14. https://doi.org/10.1007/S11274-022-03270-Z.

Gaspar, V.M., Moreira, A.F., de Melo-Diogo, D., Costa, E.C., Queiroz, J.A., Sousa, F., Pichon, C., Correia, I.J., 2016. Multifunctional nanocarriers for codelivery of nucleic acids and chemotherapeutics to cancer cells. In: Nanobiomaterials in Medical Imaging: Applications of Nanobiomaterials. William Andrew Publishing, pp. 163–207. https://doi.org/10.1016/B978-0-323-41736-5.00006-6.

Giraud, M.F., Naismith, J.H., 2000. The rhamnose pathway. Curr. Opin. Struct. Biol. 10, 687–696. https://doi.org/10.1016/S0959-440X(00)00145-7.

Goldberg, I., Rokem, J.S., 2009. Organic and Fatty Acid Production, Microbial. Encyclopedia of Microbiology, Third edition, pp. 421–442. https://doi.org/10.1016/B978-012373944-5.00156-5.

Grant View Reearch, 2025. Polybutylene Succinate Market Size, Share & Trends Analysis Report By Type (Bio-based, Petro-based), By Application (Mulch Films, Packaging, Medicine), By Region, And Segment Forecasts, 2022–2030 [WWW Document]. Grant View Reearch n.d.. URL. https://www.grandviewresearch.com/industry-analysis/polybutylene-succinate-market-report (accessed 3.30.25).

Grigorakis, K., Ferousi, C., Topakas, E., 2025. Protein engineering for industrial biocatalysis: principles, approaches, and lessons from engineered PETases. Catalysts 15. https://doi.org/10.3390/catal15020147.

Hanson, R.W., Owen, O.E., 2004. Gluconeogenesis. In: Encyclopedia of Biological Chemistry, 197–203. https://doi.org/10.1016/B0-12-443710-9/00268-4.

Harwood, C.S., Parales, R.E., 1996. The β-ketoadipate pathway and the biology of self-identity. Ann. Rev. Microbiol. 50, 553–590. https://doi.org/10.1146/ANNUREV.MICRO.50.1.553/CITE/REFWORKS.

Henke, N.A., Heider, S.A.E., Peters-Wendisch, P., Wendisch, V.F., 2016. Production of the marine carotenoid astaxanthin by metabolically engineered Corynebacterium glutamicum. Mar. Drugs 14, 124. https://doi.org/10.3390/MD14070124.

Hoffmann, N., Steinbüchel, A., Rehm, B.H.A., 2000. The Pseudomonas aeruginosa phaG gene product is involved in the synthesis of polyhydroxyalkanoic acid consisting of medium-chain-length constituents from non-related carbon sources. FEMS Microbiol. Lett. 184, 253–259. https://doi.org/10.1111/j.1574-6968.2000.tb09023.x.

Hu, J., Chen, Z., He, Y., Huang, H., Zhang, X., 2017. Synthesis and structure investigation of hexamethylene diisocyanate (HDI)-based polyisocyanates. Res. Chem. Intermed. 43, 2799–2816. https://doi.org/10.1007/s11164-016-2795-1.

Huschner, F., Grousseau, E., Brigham, C.J., Plassmeier, J., Popovic, M., Rha, C., Sinskey, A.J., 2015. Development of a feeding strategy for high cell and PHA density fed-batch fermentation of Ralstonia eutropha H16 from organic acids and their salts. Process Biochem. 50, 165–172. https://doi.org/10.1016/J.PROCBIO.2014.12.004.

Ingole, A., Kadam, M.P., Dalu, A.P., Kute, S.M., Mange, P.R., Theng, V.D., Lahane, O.R., Nikas, A.P., Kawal, Y.V., Nagrik, S.U., Patil, P.A., 2021. A review of the pharmacological characteristics of vanillic acid. J. Drug Deliv. Ther. 11, 200–204. https://doi.org/10.22270/JDDT.V11I2-S.4823.

Ismail, M., Abouhmad, A., Warlin, N., Pyo, S.H., Örn, O.E., Al-Rudainy, B., Tullberg, C., Zhang, B., Hatti-Kaul, R., 2024. Closing the loop for poly(butylene-adipate-co-terephthalate) recycling: depolymerization, monomers separation, and upcycling. Green Chem. 26, 3863–3873. https://doi.org/10.1039/D3GC04728H.

Israni, N., Shivakumar, S., 2019. Polyhydroxybutyrate. In: Materials for Biomedical Engineering. Elsevier, pp. 405–444. https://doi.org/10.1016/B978-0-12-816872-1.00014-5.

Iwaki, H., Hasegawa, Y., Teraoka, M., Tokuyama, T., Bergeron, H., Lau, P.C.K., 1999. Identification of a transcriptional activator (ChnR) and a 6- oxohexanoate dehydrogenase (ChnE) in the cyclohexanol catabolic pathway in Acinetobacter sp. strain NCIMB 9871 and localization of the genes that encode them. Appl. Environ. Microbiol. 65, 5158–5162. https://doi.org/10.1128/AEM.65.11.5158-5162.1999/ASSET/E4BF3CDF-0FAA-44CB-800E-AC34960BF869/ASSETS/GRAPHIC/AM1190338004.JPEG.

Javanmardi, J., Kubota, C., 2006. Variation of lycopene, antioxidant activity, total soluble solids and weight loss of tomato during postharvest storage. Postharvest Biol. Technol. 41, 151–155. https://doi.org/10.1016/J.POSTHARVBIO.2006.03.008.

Jian, J., Xiangbin, Z., Xianbo, H., 2020. An overview on synthesis, properties and applications of poly(butylene-adipate-co-terephthalate)–PBAT. Adv. Ind. Eng. Polym. Res. 3, 19–26. https://doi.org/10.1016/J.AIEPR.2020.01.001.

Jicsinszky, L., Bucciol, F., Chaji, S., Cravotto, G., 2023. Mechanochemical degradation of biopolymers. Molecules 28, 8031. https://doi.org/10.3390/MOLECULES28248031.

Jiménez, N., Curiel, J.A., Reverón, I., de Las Rivas, B., Muñoz, R., 2013. Uncovering the Lactobacillus plantarum WCFS1 gallate decarboxylase involved in tannin degradation. Appl. Environ. Microbiol. 79, 4253. https://doi.org/10.1128/AEM.00840-13.

Johnson, C.W., Salvachúa, D., Khanna, P., Smith, H., Peterson, D.J., Beckham, G.T., 2016. Enhancing muconic acid production from glucose and lignin-derived aromatic compounds via increased protocatechuate decarboxylase activity. Metab. Eng. Commun. 3, 111–119. https://doi.org/10.1016/J.METENO.2016.04.002.

Joo, J.C., Khusnutdinova, A.N., Flick, R., Kim, T., Bornscheuer, U.T., Yakunin, A.F., Mahadevan, R., 2017. Alkene hydrogenation activity of enoate reductases for an environmentally benign biosynthesis of adipic acid. Chem. Sci. 8, 1406–1413. https://doi.org/10.1039/C6SC02842J.

Jung, Y.K., Kim, T.Y., Park, S.J., Lee, S.Y., 2010. Metabolic engineering of Escherichia coli for the production of polylactic acid and its copolymers. Biotechnol. Bioeng. 105, 161–171. https://doi.org/10.1002/BIT.22548.

Kahkeshani, N., Farzaei, F., Fotouhi, M., Alavi, S.S., Bahramsoltani, R., Naseri, R., Momtaz, S., Abbasabadi, Z., Rahimi, R., Farzaei, M.H., Bishayee, A., 2019. Pharmacological effects of gallic acid in health and diseases: a mechanistic review. Iran. J. Basic Med. Sci. 22, 225. https://doi.org/10.22038/IJBMS.2019.32806.7897.

Kakkar, S., Bais, S., 2014. A review on protocatechuic acid and its pharmacological potential. Int. Sch. Res. Notices 2014, 952943. https://doi.org/10.1155/2014/952943.

Kang, M.J., Kim, H.T., Lee, M.W., Kim, K.A., Khang, T.U., Song, H.M., Park, S.J., Joo, J. C., Cha, H.G., 2020. A chemo-microbial hybrid process for the production of 2-pyrone-4,6-dicarboxylic acid as a promising bioplastic monomer from PET waste. Green Chem. 22, 3461–3469. https://doi.org/10.1039/D0GC00007H.

Kang, S., Kim, H., Jeon, B.S., Choi, O., Sang, B.I., 2022. Chain elongation process for caproate production using lactate as electron donor in Megasphaera hexanoica. Bioresour. Technol. 346, 126660. https://doi.org/10.1016/J.BIORTECH.2021.126660.

Kaplun, A., Binshtein, E., Vyazmensky, M., Steinmetz, A., Barak, Z., Chipman, D.M., Tittmann, K., Shaanan, B., 2008. Glyoxylate carboligase lacks the canonical active site glutamate of thiamine-dependent enzymes. Nat. Chem. Biol. 4, 113–118. https://doi.org/10.1038/nchembio.62.

Kataoka, M., Sasaki, M., Hidalgo, A.R.G.D., Nakano, M., Shimizu, S., 2001. Glycolic acid production using ethylene glycol-oxidizing microorganisms. Biosci. Biotechnol. Biochem. 65, 2265–2270. https://doi.org/10.1271/BBB.65.2265.

Kaur, P., Sharma, N., Munagala, M., Rajkhowa, R., Aallardyce, B., Shastri, Y., Agrawal, R., 2021. Nanocellulose: resources, physio-chemical properties, current uses and future applications. Front. Nanotechnol. 3, 747329. https://doi.org/10.3389/FNANO.2021.747329/BIBTEX.

Kaur, J., Gulati, M., Singh, S.K., Kuppusamy, G., Kapoor, B., Mishra, V., Gupta, S., Arshad, M.F., Porwal, O., Jha, N.K., Chaitanya, M.V.N.L., Chellappan, D.K., Gupta, G., Gupta, P.K., Dua, K., Khursheed, R., Awasthi, A., Corrie, L., 2022. Discovering multifaceted role of vanillic acid beyond flavours: nutraceutical and therapeutic potential. Trends Food Sci. Technol. 122, 187–200. https://doi.org/10.1016/J.TIFS.2022.02.023.

Kelidari, M., Abedi, F., Hayes, A.W., Jomehzadeh, V., Karimi, G., 2024. The protective effects of protocatechuic acid against natural and chemical toxicants: cellular and molecular mechanisms. Naunyn Schmiedeberg's Arch. Pharmacol. 1–20. https://doi.org/10.1007/s00210-024-03072-0.

Kenny, S.T., Runic, J.N., Kaminsky, W., Woods, T., Babu, R.P., Keely, C.M., Blau, W., O'Connor, K.E., 2008. Up-cycling of PET (polyethylene terephthalate) to the biodegradable plastic PHA (polyhydroxyalkanoate). Environ. Sci. Technol. 42, 7696–7701. https://doi.org/10.1021/ES801010E/ASSET/IMAGES/LARGE/ES-2008-01010E_0002.JPEG.

Kenny, S.T., Runic, J.N., Kaminsky, W., Woods, T., Babu, R.P., O'Connor, K.E., 2012. Development of a bioprocess to convert PET derived terephthalic acid and biodiesel derived glycerol to medium chain length polyhydroxyalkanoate. Appl. Microbiol. Biotechnol. 95, 623–633. https://doi.org/10.1007/S00253-012-4058-4.

Khalil, I., Quintens, G., Junkers, T., Dusselier, M., 2020. Muconic acid isomers as platform chemicals and monomers in the biobased economy. Green Chem. 22, 1517–1541. https://doi.org/10.1039/C9GC04161C.

Khandelwal, R., Srivastava, P., Bisaria, V.S., 2023. Recent advances in the production of malic acid by native fungi and engineered microbes. World J. Microbiol. Biotechnol. 39, 1–16. https://doi.org/10.1007/S11274-023-03666-5/TABLES/3.

Khanna, S., Srivastava, A.K., 2005. Statistical media optimization studies for growth and PHB production by Ralstonia eutropha. Process Biochem. 40, 2173–2182. https://doi.org/10.1016/J.PROCBIO.2004.08.011.

Khouri, N.G., Bahú, J.O., Blanco-Llamero, C., Severino, P., Concha, V.O.C., Souto, E.B., 2024. Polylactic acid (PLA): properties, synthesis, and biomedical applications – a review of the literature. J. Mol. Struct. 1309, 138243. https://doi.org/10.1016/J.MOLSTRUC.2024.138243.

Kim, H.T., Kim, J.K., Cha, H.G., Kang, M.J., Lee, H.S., Khang, T.U., Yun, E.J., Lee, D.H., Song, B.K., Park, S.J., Joo, J.C., Kim, K.H., 2019. Biological valorization of poly (ethylene terephthalate) monomers for upcycling waste PET. ACS Sustain. Chem. Eng. 7, 19396–19406. https://doi.org/10.1021/ACSSUSCHEMENG.9B03908.

Kleerebezem, R., Lettinga, G., 2000. High-rate anaerobic treatment of purified terephthalic acid wastewater. Water Sci. Technol. 42, 259–268. https://doi.org/10.2166/WST.2000.0522.

Kornberg, H.L., Morris, J.G., 1963. βHydroxyaspartate pathway: a new route for biosyntheses from glyoxylate. Nature 197, 456–457. https://doi.org/10.1038/197456a0.

Ladhari, S., Vu, N.N., Boisvert, C., Saidi, A., Nguyen-Tri, P., 2023. Recent development of polyhydroxyalkanoates (PHA)-based materials for antibacterial applications: a review. ACS Appl. Bio Mater. 6, 1398–1430. https://doi.org/10.1021/ACSABM.3C00078.

Lainioti, G.C., Savva, P., Druvari, D., Avramidis, P., Panagiotaras, D., Karellou, E.I.E., Kallitsis, J.K., 2021. Cross-linking of antimicrobial polymers with hexamethylene diamine to prevent biofouling in marine applications. Prog. Org. Coat. 157, 106336. https://doi.org/10.1016/J.PORGCOAT.2021.106336.

Lancen, L., 2023. The History of Plastic Recycling: The Inventor Behind the Process and its Impact on our Environment [WWW Document]. Climate of our Future. URL. https://www.climateofourfuture.org/the-history-of-plastic-recycling-the-inventor-behind-the-process-and-its-impact-on-our-environment/ (accessed 12.27.24).

Lee, S.Y., 1996. Plastic bacteria? Progress and prospects for polyhydroxyalkanoate production in bacteria. Trends Biotechnol. 14, 431–438. https://doi.org/10.1016/0167-7799(96)10061-5.

Lee, J.A., Ahn, J.H., Lee, S.Y., 2019. Organic acids: succinic and malic acids. Compr. Biotechnol. 172–187. https://doi.org/10.1016/B978-0-444-64046-8.00159-2.

Li, Z.J., Shi, Z.Y., Jian, J., Guo, Y.Y., Wu, Q., Chen, G.Q., 2010. Production of poly(3-hydroxybutyrate-co-4-hydroxybutyrate) from unrelated carbon sources by metabolically engineered Escherichia coli. Metab. Eng. 12, 352–359. https://doi.org/10.1016/J.YMBEN.2010.03.003.

Li, Q., Chen, Q., Li, M.J., Wang, F.S., Qi, Q.S., 2011. Pathway engineering results the altered polyhydroxyalkanoates composition in recombinant Escherichia coli. New Biotechnol. 28, 92–95. https://doi.org/10.1016/J.NBT.2010.08.007.

Li, W.J., Jayakody, L.N., Franden, M.A., Wehrmann, M., Daun, T., Hauer, B., Blank, L.M., Beckham, G.T., Klebensberger, J., Wierckx, N., 2019. Laboratory evolution reveals the metabolic and regulatory basis of ethylene glycol metabolism by Pseudomonas putida KT2440. Environ. Microbiol. 21, 3669–3682. https://doi.org/10.1111/1462-2920.14703.

Li, W.J., Narancic, T., Kenny, S.T., Niehoff, P.J., O'Connor, K., Blank, L.M., Wierckx, N., 2020. Unraveling 1,4-Butanediol metabolism in Pseudomonas putida KT2440. Front. Microbiol. 11, 520662. https://doi.org/10.3389/FMICB.2020.00382/BIBTEX.

Liu, H., Wang, J., He, T., Becker, S., Zhang, G., Li, D., Ma, X., 2018. Butyrate: a double-edged sword for health? Adv. Nutr. 9, 21. https://doi.org/10.1093/ADVANCES/NMX009.

Liu, P., Zhang, T., Zheng, Y., Li, Q., Su, T., Qi, Q., 2021. Potential one-step strategy for PET degradation and PHB biosynthesis through co-cultivation of two engineered microorganisms. Eng. Microbiol. 1, 100003. https://doi.org/10.1016/J.ENGMIC.2021.100003.

Liu, H., Chen, Y., Zhang, Y., Zhao, W., Guo, H., Wang, Siqi, Xia, W., Wang, Shufang, Liu, R., Yang, C., 2022a. Enhanced production of polyhydroxyalkanoates in Pseudomonas putida KT2440 by a combination of genome streamlining and promoter engineering. Int. J. Biol. Macromol. 209, 117–124. https://doi.org/10.1016/J.IJBIOMAC.2022.04.004.

Liu, P., Zheng, Y., Yuan, Y., Zhang, T., Li, Q., Liang, Q., Su, T., Qi, Q., 2022b. Valorization of polyethylene terephthalate to muconic acid by engineering Pseudomonas putida. Int. J. Mol. Sci. 23, 10997. https://doi.org/10.3390/IJMS231910997/S1.

Liu, Y., Shi, J., Jin, H., Guo, L., 2023. Chemical recycling methods for managing waste plastics: a review. Environ. Chem. Lett. 22, 149–169. https://doi.org/10.1007/S10311-023-01664-5.

Lu, S., Jin, H., Wang, Y., Tao, Y., 2021. Genome-wide transcriptomic analysis of n-caproic acid production in Ruminococcaceae bacterium CPB6 with lactate supplementation. J. Microbiol. Biotechnol. 31, 1533–1544. https://doi.org/10.4014/JMB.2107.07009.

Lu, H., Diaz, D.J., Czarnecki, N.J., Zhu, C., Kim, W., Shroff, R., Acosta, D.J., Alexander, B. R., Cole, H.O., Zhang, Y., Lynd, N.A., Ellington, A.D., Alper, H.S., 2022. Machine

learning-aided engineering of hydrolases for PET depolymerization. Nature 604, 662–667. https://doi.org/10.1038/s41586-022-04599-z.
Maier, R.M., Soberón-Chávez, G., 2000. Pseudomonas aeruginosa rhamnolipids: biosynthesis and potential applications. Appl. Microbiol. Biotechnol. 54, 625–633. https://doi.org/10.1007/S002530000443/METRICS.
Mangels, A.R., Holden, J.M., Beecher, G.R., Forman, M.R., Lanza, E., 1993. Carotenoid content of fruits and vegetables: an evaluation of analytic data. J. Am. Diet. Assoc. 93, 284–296. https://doi.org/10.1016/0002-8223(93)91553-3.
Marounek, M., Fliegrova, K., Bartos, S., 1989. Metabolism and some characteristics of ruminal strains of Megasphaera elsdenii. Appl. Environ. Microbiol. 55, 1570–1573. https://doi.org/10.1128/AEM.55.6.1570-1573.1989.
Marrero, J., Rhee, K.Y., Schnappinger, D., Pethe, K., Ehrt, S., 2010. Gluconeogenic carbon flow of tricarboxylic acid cycle intermediates is critical for Mycobacterium tuberculosis to establish and maintain infection. Proc. Natl. Acad. Sci. 107, 9819–9824. https://doi.org/10.1073/pnas.1000715107.
Martin, D.P., Williams, S.F., 2003. Medical applications of poly-4-hydroxybutyrate: a strong flexible absorbable biomaterial. Biochem. Eng. J. 16, 97–105. https://doi.org/10.1016/S1369-703X(03)00040-8.
Martínez-Gómez, K., Flores, N., Castañeda, H.M., Martínez-Batallar, G., Hernández-Chávez, G., Ramírez, O.T., Gosset, G., Encarnación, S., Bolivar, F., 2012. New insights into Escherichia coli metabolism: carbon scavenging, acetate metabolism and carbon recycling responses during growth on glycerol. Microb. Cell Factories 11, 46. https://doi.org/10.1186/1475-2859-11-46.
Mashima, T., Seimiya, H., Tsuruo, T., 2009. De novo fatty-acid synthesis and related pathways as molecular targets for cancer therapy. Br. J. Cancer 100, 1369–1372. https://doi.org/10.1038/sj.bjc.6605007.
Mateos-Timoneda, M.A., 2009. Polymers for bone repair. Bone Repair Biomater. 231–251. https://doi.org/10.1533/9781845696610.2.231.
Mazidi, M., Ferns, G.A., Banach, M., 2020. A high consumption of tomato and lycopene is associated with a lower risk of cancer mortality: results from a multi-ethnic cohort. Public Health Nutr. 23, 1569. https://doi.org/10.1017/S1368980019003227.
Mclauchlin, A.R., Thomas, N.L., 2012. Biodegradable polymer nanocomposites. In: Advances in Polymer Nanocomposites: Types and Applications. Woodhead Publishing. https://doi.org/10.1533/9780857096241.2.398.
Mitra, R., Xiang, H., Han, J., 2021a. Current advances towards 4-hydroxybutyrate containing polyhydroxyalkanoates production for biomedical applications. Molecules 26. https://doi.org/10.3390/MOLECULES26237244.
Mitra, R., Xiang, H., Han, J., 2021b. Current advances towards 4-hydroxybutyrate containing polyhydroxyalkanoates production for biomedical applications. Molecules 26. https://doi.org/10.3390/MOLECULES26237244.
Mohanan, N., Montazer, Z., Sharma, P.K., Levin, D.B., 2020. Microbial and enzymatic degradation of synthetic plastics. Front. Microbiol. 11, 580709. https://doi.org/10.3389/FMICB.2020.580709.
Morunga, A.M., 2024. Plastic Pollution's Devastating Impact on Wildlife [WWW Document]. Greenpeace. URL. https://www.greenpeace.org/aotearoa/story/plastic-pollutions-devastating-impact-on-wildlife/ (accessed 12.18.24).
Możejko-Ciesielska, J., Mostek, A., 2019. Time-course proteomic analysis of Pseudomonas putida KT2440 during Mcl-polyhydroxyalkanoate synthesis under nitrogen deficiency. Polymers (Basel) 11. https://doi.org/10.3390/polym11050748.
Mozejko-Ciesielska, J., Szacherska, K., Marciniak, P., 2019. Pseudomonas species as producers of eco-friendly polyhydroxyalkanoates. J. Polym. Environ. 27, 1151–1166. https://doi.org/10.1007/S10924-019-01422-1.
Mozos, I., Stoian, D., Caraba, A., Malainer, C., Horbanczuk, J.O., Atanasov, A.G., 2018. Lycopene and vascular health. Front. Pharmacol. 9, 312695. https://doi.org/10.3389/fphar.2018.00521.
Mückschel, B., Simon, O., Klebensberger, J., Graf, N., Rosche, B., Altenbuchner, J., Pfannstiel, J., Huber, A., Hauer, B., 2012. Ethylene glycol metabolism by Pseudomonas putida. Appl. Environ. Microbiol. 78, 8531–8539. https://doi.org/10.1128/AEM.02062-12.
Mukhopadhyay, M., Patra, A., Paul, A.K., 2005. Production of poly(3-hydroxybutyrate) and poly(3-hydroxybutyrate-co-3- hydroxyvalerate) by Rhodopseudomonas palustris SP5212. World J. Microbiol. Biotechnol. 21, 765–769. https://doi.org/10.1007/S11274-004-5565-Y/METRICS.
Muthuraj, R., Valerio, O., Mekonnen, T.H., 2021. Recent developments in short- and medium-chain- length Polyhydroxyalkanoates: production, properties, and applications. Int. J. Biol. Macromol. 187, 422–440. https://doi.org/10.1016/j.ijbiomac.2021.07.143.
Nakagawa, Y., Kasumi, T., Ogihara, J., Tamura, M., Arai, T., Tomishige, K., 2020. Erythritol: another C4 platform chemical in biomass refinery. ACS Omega 5, 2520–2530. https://doi.org/10.1021/ACSOMEGA.9B04046/ASSET/IMAGES/LARGE/AO9B04046_0006.JPEG.
National Center for Biotechnology Information, 2024a. PubChem Compound Summary for CID 289, Catechol [WWW Document]. National Center for Biotechnology Information. URL. https://pubchem.ncbi.nlm.nih.gov/compound/289 (accessed 12.16.24).
National Center for Biotechnology Information, 2024b. PubChem Compound Summary for CID 1057, Pyrogallol [WWW Document]. National Center for Biotechnology Information. URL. https://pubchem.ncbi.nlm.nih.gov/compound/Pyrogallol (accessed 12.16.24).
National Center for Biotechnology Information, 2024c. PubChem Compound Summary for CID 8468, Vanillic Acid [WWW Document]. National Center for Biotechnology Information. URL. https://pubchem.ncbi.nlm.nih.gov/compound/Vanillic-Acid (accessed 12.16.24).
National Center for Biotechnology Information, 2024d. PubChem Compound Summary for CID 757, Glycolic Acid [WWW Document]. National Center for Biotechnology Information. URL. https://pubchem.ncbi.nlm.nih.gov/compound/Glycolic-Acid (accessed 12.13.24).
National Center for Biotechnology Information, 2024e. PubChem Compound Summary for CID 8892, Caproic Acid [WWW Document]. National Center for Biotechnology Information. URL. https://pubchem.ncbi.nlm.nih.gov/compound/Caproic-Acid (accessed 12.16.24).
National Center for Biotechnology Information, 2024f. PubChem Compound Summary for CID 10413, 4-Hydroxybutanoic Acid [WWW Document]. National Center for Biotechnology Information. URL. https://pubchem.ncbi.nlm.nih.gov/compound/4-Hydroxybutanoic-acid (accessed 12.16.24).
National Center for Biotechnology Information, 2024g. PubChem Compound Summary for CID 196, Adipic Acid. [WWW Document]. National Center for Biotechnology Information. URL. https://pubchem.ncbi.nlm.nih.gov/compound/Adipic-Acid (accessed 12.16.24).
National Center for Biotechnology Information, 2024h. PubChem Compound Summary for CID 1110, Succinic Acid [WWW Document]. National Center for Biotechnology Information. URL. https://pubchem.ncbi.nlm.nih.gov/compound/Succinic-Acid (accessed 12.16.24).
National Center for Biotechnology Information, 2024i. PubChem Compound Summary for CID 525, Malic Acid [WWW Document]. National Center for Biotechnology Information. URL. https://pubchem.ncbi.nlm.nih.gov/compound/Malic-Acid (accessed 12.16.24).
National Center for Biotechnology Information, 2024j. PubChem Annotation Record for 1,4-Butanediol [WWW Document]. National Center for Biotechnology Information, Hazardous Substances Data Bank (HSDB). URL. https://pubchem.ncbi.nlm.nih.gov/source/hsdb/1112 (accessed 12.16.24).
National Center for Biotechnology Information, 2025a. PubChem Compound Summary for CID 6057, Tyrosine [WWW Document]. National Center for Biotechnology Information. URL. https://pubchem.ncbi.nlm.nih.gov/compound/Tyrosine (accessed 4.4.25).
National Center for Biotechnology Information, 2025b. PubChem Compound Summary for CID 6140, Phenylalanine [WWW Document]. National Center for Biotechnology Information. URL. https://pubchem.ncbi.nlm.nih.gov/compound/Phenylalanine (accessed 4.4.25).
National Center for Biotechnology Information, 2025c. PubChem Compound Summary for CID 637542, p-Coumaric Acid [WWW Document]. National Center for Biotechnology Information. URL. https://pubchem.ncbi.nlm.nih.gov/compound/637542 (accessed 4.4.25).
National Center for Biotechnology Information, 2025d. PubChem Compound Summary for CID 192742, 2,4-Dihydroxybutanoic Acid [WWW Document]. National Center for Biotechnology Information. URL. https://pubchem.ncbi.nlm.nih.gov/compound/2_4-Dihydroxybutanoic-acid (accessed 4.4.25).
Nelson, K.E., Weinel, C., Paulsen, I.T., Dodson, R.J., Hilbert, H., Martins dos Santos, V.A. P., Fouts, D.E., Gill, S.R., Pop, M., Holmes, M., Brinkac, L., Beanan, M., DeBoy, R.T., Daugherty, S., Kolonay, J., Madupu, R., Nelson, W., White, O., Peterson, J., Khouri, H., Hance, I., Chris Lee, P., Holtzapple, E., Scanlan, D., Tran, K., Moazzez, A., Utterback, T., Rizzo, M., Lee, K., Kosack, D., Moestl, D., Wedler, H., Lauber, J., Stjepandic, D., Hoheisel, J., Straetz, M., Heim, S., Kiewitz, C., Eisen, J., Timmis, K.N., Düsterhöft, A., Tümmler, B., Fraser, C.M., 2002. Complete genome sequence and comparative analysis of the metabolically versatile Pseudomonas putida KT2440. Environ. Microbiol. 4, 799–808. https://doi.org/10.1046/J.1462-2920.2002.00366.X.
Niaounakis, M., 2015. Chapter 1 - Introduction. In: Biopolymers: Processing and Products. William Andrew Publishing, pp. 1–77. https://doi.org/10.1016/B978-0-323-26698-7.00001-5.
Nihart, A.J., Garcia, M.A., El Hayek, E., Liu, R., Olewine, M., Kingston, J.D., Castillo, E.F., Gullapalli, R.R., Howard, T., Bleske, B., Scott, J., Gonzalez-Estrella, J., Gross, J.M., Spilde, M., Adolphi, N.L., Gallego, D.F., Jarrell, H.S., Dvorscak, G., Zuluaga-Ruiz, M. E., West, A.B., Campen, M.J., 2025. Bioaccumulation of microplastics in decedent human brains. Nat. Med. https://doi.org/10.1038/s41591-024-03453-1.
Nikel, P.I., de Lorenzo, V., 2018. Pseudomonas putida as a functional chassis for industrial biocatalysis: from native biochemistry to trans-metabolism. Metab. Eng. 50, 142–155. https://doi.org/10.1016/J.YMBEN.2018.05.005.
Nikel, P.I., Martínez-García, E., De Lorenzo, V., 2014. Biotechnological domestication of pseudomonads using synthetic biology. Nat. Rev. Microbiol. 12, 368–379. https://doi.org/10.1038/nrmicro3253.
Nojiri, H., Fukuda, M., Tsuda, M., Kamagata, Y., 2014. Biodegradative Bacteria: How Bacteria Degrade, Survive, Adapt, and Evolve. Biodegradative Bacteria: How Bacteria Degrade, Survive, Adapt, and Evolve, 1–358. https://doi.org/10.1007/978-4-431-54520-0/COVER.
Oh, Y.R., Jang, Y.A., Song, J.K., Eom, G.T., 2022. Efficient enzymatic depolymerization of polycaprolactone into 6-hydroxyhexanoic acid by optimizing reaction conditions and microbial conversion of 6-hydroxyhexanoic acid into adipic acid for eco-friendly upcycling of polycaprolactone. Biochem. Eng. J. 185, 108504. https://doi.org/10.1016/J.BEJ.2022.108504.
Oh, Y.-R., Jang, Y.-A., Song, J.K., Eom, G.T., 2023. Valorization of waste polycaprolactone via microbial upcycling of 6- hydroxyhexanoic acid into adipic acid by metabolically engineered Escherichia coli. https://doi.org/10.21203/RS.3.RS-3434395/V1.
Olatunde, A., Mohammed, A., Ibrahim, M.A., Tajuddeen, N., Shuaibu, M.N., 2022. Vanillin: a food additive with multiple biological activities. Eur. J. Med. Chem. Rep. 5, 100055. https://doi.org/10.1016/J.EJMCR.2022.100055.
Otsuka, Y., Araki, T., Suzuki, Y., Nakamura, M., Kamimura, N., Masai, E., 2023. High-level production of 2-pyrone-4,6-dicarboxylic acid from vanillic acid as a lignin-related aromatic compound by metabolically engineered fermentation to realize

industrial valorization processes of lignin. Bioresour. Technol. 377, 128956. https://doi.org/10.1016/J.BIORTECH.2023.128956.
Ouyang, S.-P., Luo, R.C., Chen, S.-S., Liu, Q., Chung, A., Wu, Q., Chen, G.-Q., 2007. Production of polyhydroxyalkanoates with high 3-hydroxydodecanoate monomer content by fadB and fadA knockout mutant of Pseudomonas putida KT2442. Biomacromolecules 8, 2504–2511. https://doi.org/10.1021/bm0702307.
Pagola, S., 2023. Outstanding advantages, current drawbacks, and significant recent developments in mechanochemistry: a perspective view. Crystals (Basel) 13. https://doi.org/10.3390/cryst13010124.
Palmer, R.J., 2003. Polyamides, Plastics. Encyclopedia of Polymer Science and Technology. https://doi.org/10.1002/0471440264.PST251.
Panda, S., Zhou, J.F.J., Feigis, M., Harrison, E., Ma, X., Fung Kin Yuen, V., Mahadevan, R., Zhou, K., 2023. Engineering Escherichia coli to produce aromatic chemicals from ethylene glycol. Metab. Eng. 79, 38–48. https://doi.org/10.1016/J.YMBEN.2023.06.012.
Pandey, A., Adama, N., Adjallé, K., Blais, J.F., 2022. Sustainable applications of polyhydroxyalkanoates in various fields: a critical review. Int. J. Biol. Macromol. 221, 1184–1201. https://doi.org/10.1016/J.IJBIOMAC.2022.09.098.
Pandit, A.V., Harrison, E., Mahadevan, R., 2021. Engineering Escherichia coli for the utilization of ethylene glycol. Microb. Cell Factories 20, 1–17. https://doi.org/10.1186/s12934-021-01509-2.
Phan, A.N.T., Prigolovkin, L., Blank, L.M., 2023. LC-UV/RI-MS2 as the analytical platform for bioconversion of sustainable carbon sources: A showcase of 1,4-butanediol plastic monomer degradation using Ustilago trichophora. bioRxiv 2023.08.16.553358. https://doi.org/10.1101/2023.08.16.553358.
Phan, A.N.T., Prigolovkin, L., Blank, L.M., 2024. Unlocking the potentials of Ustilago trichophora for up-cycling polyurethane-derived monomer 1,4-butanediol. Microb. Biotechnol. 17. https://doi.org/10.1111/1751-7915.14384.
Plastics Europe, 2023. Plastics – The Fast Facts 2023 [WWW Document]. Plastics Europe. URL. https://plasticseurope.org/knowledge-hub/plastics-the-fast-facts-2023/ (accessed 12.20.24).
Ploux, O., Masamune, S., Walsch, C.T., 1988. The NADPH-linked acetoacetyl-CoA reductase from Zoogloea ramigera. Eur. J. Biochem. 174, 177–182. https://doi.org/10.1111/j.1432-1033.1988.tb14079.x.
Ponnian, S.M.P., Stanely, S.P., Roy, A.J., 2024. Cardioprotective effects of p-coumaric acid on tachycardia, inflammation, ion pump dysfunction, and electrolyte imbalance in isoproterenol-induced experimental myocardial infarction. J. Biochem. Mol. Toxicol. 38, e23668. https://doi.org/10.1002/JBT.23668.
Pradhan, S., Dikshit, P.K., Moholkar, V.S., 2020. Production, Characterization, and Applications of Biodegradable Polymer: Polyhydroxyalkanoates. Materials Horizons: From Nature to Nanomaterials, 51–94. https://doi.org/10.1007/978-981-15-1251-3_4/TABLES/4.
Pratiwi, O.A., Achmadi, U.F., Kurniawan, R., 2024. Microplastic pollution in landfill soil: emerging threats the environmental and public health. Environ. Anal. Health Toxicol. 39. https://doi.org/10.5620/eaht.2024009 e2024009–0.
Prust, C., Hoffmeister, M., Liesegang, H., Wiezer, A., Fricke, W.F., Ehrenreich, A., Gottschalk, G., Deppenmeier, U., 2005. Complete genome sequence of the acetic acid bacterium Gluconobacter oxydans. Nat. Biotechnol. 23, 195–200. https://doi.org/10.1038/nbt1062.
Qi, X., Ma, Y., Chang, H., Li, B., Ding, M., Yuan, Y., 2021. Evaluation of PET degradation using artificial microbial consortia. Front. Microbiol. 12, 778828. https://doi.org/10.3389/FMICB.2021.778828.
Qian, X., Xin, K., Zhang, L., Zhou, J., Xu, A., Dong, W., Jiang, M., 2023. Integration of ARTP mutation and adaptive laboratory evolution to reveal 1,4-butanediol degradation in Pseudomonas putida KT2440. Microbiol. Spectr. 11. https://doi.org/10.1128/SPECTRUM.04988-22/SUPPL_FILE/SPECTRUM.04988-22-S0001.PDF.
Quadri, L.E.N., Weinreb, P.H., Lei, M., Nakano, M.M., Zuber, P., Walsh, C.T., 1998. Characterization of Sfp, a Bacillus subtilis phosphopantetheinyl transferase for peptidyl carrier protein domains in peptide synthetases. Biochemistry 37, 1585–1595. https://doi.org/10.1021/BI9719861.
Raj, M., Devi, T., Kumar, V., Mishra, P., Upadhyay, S.K., Yadav, M., Kr Sharma, A., Sehrawat, N., Kumar, S., Singh, M., 2024. Succinic acid: applications and microbial production using organic wastes as low cost substrates. In: Microbial Organic Acids Production: Utilizing Waste Feedstocks, 51–67. https://doi.org/10.1515/PSR-2022-0160/ASSET/GRAPHIC/J_PSR-2022-0160_FIG_002.JPG.
Rorrer, N.A., Notonier, S.F., Knott, B.C., Black, B.A., Singh, A., Nicholson, S.R., Kinchin, C.P., Schmidt, G.P., Carpenter, A.C., Ramirez, K.J., Johnson, C.W., Salvachúa, D., Crowley, M.F., Beckham, G.T., 2022. Production of β-ketoadipic acid from glucose in Pseudomonas putida KT2440 for use in performance-advantaged nylons. Cell. Rep. Phys. Sci. 3, 100840. https://doi.org/10.1016/J.XCRP.2022.100840.
Ross, P., Mayer, R., Benziman, M., 1991. Cellulose biosynthesis and function in bacteria. Microbiol. Rev. 55, 35–58. https://doi.org/10.1128/MR.55.1.35-58.1991.
Sadler, J.C., Wallace, S., 2021. Microbial synthesis of vanillin from waste poly(ethylene terephthalate). Green Chem. 23, 4665–4672. https://doi.org/10.1039/D1GC00931A.
Saint-Amans, S., Girbal, L., Andrade, J., Ahrens, K., Soucaille, P., 2001. Regulation of carbon and electron flow in Clostridium butyricum VPI 3266 grown on glucose-glycerol mixtures. J. Bacteriol. 183, 1748–1754. https://doi.org/10.1128/JB.183.5.1748-1754.2001/ASSET/86973BBA-AA3E-4708-A6A6-982A19A55148/ASSETS/GRAPHIC/JB0510628001.JPEG.
Salvador, M., Abdulmutalib, U., Gonzalez, J., Kim, J., Smith, A.A., Faulon, J.L., Wei, R., Zimmermann, W., Jimenez, J.I., 2019. Microbial genes for a circular and sustainable bio-PET economy. Genes 10, 373. https://doi.org/10.3390/GENES10050373.
Sasajima, K.-I., Sinskey, A.J., 1979. Oxidation of l-glucose by a pseudomonad. Biochim. Biophys. Acta (BBA) - Enzymol. 571, 120–126. https://doi.org/10.1016/0005-2744(79)90232-8.
Sasoh, M., Masai, E., Ishibashi, S., Hara, H., Kamimura, N., Miyauchi, K., Fukuda, M., 2006. Characterization of the terephthalate degradation genes of Comamonas sp. strain E6. Appl. Environ. Microbiol. 72, 1825. https://doi.org/10.1128/AEM.72.3.1825-1832.2006.
Sathya, A.B., Sivasubramanian, V., Santhiagu, A., Sebastian, C., Sivashankar, R., 2018. Production of polyhydroxyalkanoates from renewable sources using bacteria. J. Polym. Environ. 26, 3995–4012. https://doi.org/10.1007/S10924-018-1259-7/TABLES/4.
Sauer, U., Eikmanns, B.J., 2005. The PEP—pyruvate—oxaloacetate node as the switch point for carbon flux distribution in bacteria: we dedicate this paper to Rudolf K. Thauer, Director of the Max-Planck-Institute for Terrestrial Microbiology in Marburg, Germany, on the occasion of his 65th birthday. FEMS Microbiol. Rev. 29, 765–794. https://doi.org/10.1016/j.femsre.2004.11.002.
Schada von Borzyskowski, L., Severi, F., Krüger, K., Hermann, L., Gilardet, A., Sippel, F., Pommerenke, B., Claus, P., Cortina, N.S., Glatter, T., Zauner, S., Zarzycki, J., Fuchs, B.M., Bremer, E., Maier, U.G., Amann, R.I., Erb, T.J., 2019. Marine proteobacteria metabolize glycolate via the β-hydroxyaspartate cycle. Nature 575, 500–504. https://doi.org/10.1038/s41586-019-1748-4.
Schada von Borzyskowski, L., Schulz-Mirbach, H., Troncoso Castellanos, M., Severi, F., Gómez-Coronado, P.A., Paczia, N., Glatter, T., Bar-Even, A., Lindner, S.N., Erb, T.J., 2023. Implementation of the β-hydroxyaspartate cycle increases growth performance of Pseudomonas putida on the PET monomer ethylene glycol. Metab. Eng. 76, 97–109. https://doi.org/10.1016/J.YMBEN.2023.01.011.
Scheffen, M., Marchal, D.G., Beneyton, T., Schuller, S.K., Klose, M., Diehl, C., Lehmann, J., Pfister, P., Carrillo, M., He, H., Aslan, S., Cortina, N.S., Claus, P., Bollschweiler, D., Baret, J.C., Schuller, J.M., Zarzycki, J., Bar-Even, A., Erb, T.J., 2021. A new-to-nature carboxylation module to improve natural and synthetic CO2 fixation. Nat. Catal. 4, 105–115. https://doi.org/10.1038/s41929-020-00557-y.
Schubert, P., Steinbuchel, A., Schlegel, H.G., 1988. Cloning of the Alcaligenes eutrophus genes for synthesis of poly-beta-hydroxybutyric acid (PHB) and synthesis of PHB in Escherichia coli. J. Bacteriol. 170, 5837–5847.
Schweigert, N., Zehnder, A.J.B., Eggen, R.I.L., 2001. Chemical properties of catechols and their molecular modes of toxic action in cells, from microorganisms to mammals. Environ. Microbiol. 3, 81–91. https://doi.org/10.1046/J.1462-2920.2001.00176.X.
Schyns, Z.O.G., Shaver, Michael P., 2021. Mechanical recycling of packaging plastics: a review. Macromol. Rapid Commun. 42, 2000415. https://doi.org/10.1002/MARC.202000415.
Sehgal, R., Gupta, R., 2020. Polyhydroxyalkanoate and its efficient production: an eco-friendly approach towards development. 3 Biotech 10, 1–14. https://doi.org/10.1007/S13205-020-02550-5/FIGURES/3.
Semaming, Y., Pannengpetch, P., Chattipakorn, S.C., Chattipakorn, N., 2015. Pharmacological properties of protocatechuic acid and its potential roles as complementary medicine. Evid. Based Complement. Alternat. Med. 2015. https://doi.org/10.1155/2015/593902.
Shahid, S., Mosrati, R., Ledauphin, J.Ò., Amiel, C., Fontaine, P., Gaillard, J.L., Corroler, D., 2013. Impact of carbon source and variable nitrogen conditions on bacterial biosynthesis of polyhydroxyalkanoates: evidence of an atypical metabolism in Bacillus megaterium DSM 509. J. Biosci. Bioeng. 116, 302–308. https://doi.org/10.1016/J.JBIOSC.2013.02.017.
Shigematsu, T., Yumihara, K., Ueda, Y., Morimura, S., Kida, K., 2003. Purification and gene cloning of the oxygenase component of the terephthalate 1,2-dioxygenase system from Delftia tsuruhatensis strain T7. FEMS Microbiol. Lett. 220, 255–260. https://doi.org/10.1016/S0378-1097(03)00124-1.
Shimao, M., Saimoto, H., Kato, N., Sakazawa, C., 1983. Properties and roles of bacterial symbionts of polyvinyl alcohol-utilizing mixed cultures. Appl. Environ. Microbiol. 46, 605. https://doi.org/10.1128/AEM.46.3.605-610.1983.
Shimizu, A., Tanaka, K., Fujimori, M., 2000. Abatement technologies for N2O emissions in the adipic acid industry. Chemosphere Global Change Sci. 2, 425–434. https://doi.org/10.1016/S1465-9972(00)00024-6.
Singh, N., Walker, T.R., 2024. Plastic recycling: a panacea or environmental pollution problem. npj Mater. Sustain. 2, 1–7. https://doi.org/10.1038/s44296-024-00024-w.
Singh, M., Takada, K., Kaneko, T., 2020. Biobased liquid crystalline poly(coumarate)s composites and their potential applications. Compos. Commun. 22, 100531. https://doi.org/10.1016/J.COCO.2020.100531.
Singh, R., Kumar, N., Mehrotra, T., Bisaria, K., Sinha, S., 2021. Environmental hazards and biodegradation of plastic waste: challenges and future prospects. In: Bioremediation for Environmental Sustainability: Toxicity, Mechanisms of Contaminants Degradation, Detoxification and Challenges. Elsevier. https://doi.org/10.1016/B978-0-12-820524-2.00009-2.
Sourkouni, G., Jeremić, S., Kalogirou, C., Höfft, O., Nenadovic, M., Jankovic, V., Rajasekaran, D., Pandis, P., Padamati, R., Nikodinovic-Runic, J., Argirusis, C., 2023. Study of PLA pre-treatment, enzymatic and model-compost degradation, and valorization of degradation products to bacterial nanocellulose. World J. Microbiol. Biotechnol. 39, 1–13. https://doi.org/10.1007/S11274-023-03605-4/FIGURES/8.
State of Green, 2024. Amager Bakke: Waste-to-Energy Meets Carbon Capture [WWW Document]. URL. https://stateofgreen.com/en/solutions/amager-bakke-waste-to-energy-meets-carbon-capture/ (accessed 3.31.25).
Statista, 2023. Market volume of polyethylene terephthalate worldwide from 2015 to 2022, with a forecast for 2023 to 2030 [WWW Document]. URL. https://www.statista.com/statistics/1245264/polyethylene-terephthalate-market-volume-worldwide/?utm_source=chatgpt.com (accessed 3.30.25).

Statista, 2024. Annual production of plastics worldwide from 1950 to 2023 [WWW Document]. URL. https://www.statista.com/statistics/282732/global-production-of-plastics-since-1950/ (accessed 12.18.24).
Sullivan, K.P., Werner, A.Z., Ramirez, K.J., Ellis, L.D., Bussard, J.R., Black, B.A., Brandner, D.G., Bratti, F., Buss, B.L., Dong, X., Haugen, S.J., Ingraham, M.A., Konev, M.O., Michener, W.E., Miscall, J., Pardo, I., Woodworth, S.P., Guss, A.M., Román-Leshkov, Y., Stahl, S.S., Beckham, G.T., 2022. Mixed plastics waste valorization through tandem chemical oxidation and biological funneling. Science 1979, 378. https://doi.org/10.1126/SCIENCE.ABO4626.
Suzuki, M., Tachibana, Y., Kasuya, K. Ichi, 2020. Biodegradability of poly(3-hydroxyalkanoate) and poly(ε-caprolactone) via biological carbon cycles in marine environments. Polym. J. 53, 47–66. https://doi.org/10.1038/s41428-020-00396-5.
Szekrenyi, A., Soler, A., Garrabou, X., Guérard-Hélaine, C., Parella, T., Joglar, J., Lemaire, M., Bujons, J., Clapés, P., 2014. Engineering the donor selectivity of D-fructose-6-phosphate aldolase for biocatalytic asymmetric cross-aldol additions of glycolaldehyde. Chemistry 20, 12572–12583. https://doi.org/10.1002/chem.201403281.
Thakur, P., Saini, N.K., Thakur, V.K., Gupta, V.K., Saini, R.V., Saini, A.K., 2021. Rhamnolipid the glycolipid biosurfactant: emerging trends and promising strategies in the field of biotechnology and biomedicine. Microb. Cell Factories 20, 1–15. https://doi.org/10.1186/S12934-020-01497-9/FIGURES/5.
Tiso, T., Sabelhaus, P., Behrens, B., Wittgens, A., Rosenau, F., Hayen, H., Blank, L.M., 2016. Creating metabolic demand as an engineering strategy in Pseudomonas putida – Rhamnolipid synthesis as an example. Metab. Eng. Commun. 3, 234–244. https://doi.org/10.1016/J.METENO.2016.08.002.
Tiso, T., Zauter, R., Tulke, H., Leuchtle, B., Li, W.-J., Behrens, B., Wittgens, A., Rosenau, F., Hayen, H., Blank, L.M., 2017a. Designer rhamnolipids by reduction of congener diversity: production and characterization microbial cell factories. Microb. Cell Factories 16, 225. https://doi.org/10.1186/s12934-017-0838-y.
Tiso, Till, Thies, Stephan, Müller, Michaela, Tsvetanova, Lora, Carraresi, Laura, Bröring, Stefanie, Jaeger, K.-E., Blank, Lars Mathias, Tiso, T., Blank, L.M., Thies, S., Müller, M., Tsvetanova, L., Carraresi, L., Bröring, S., Jaeger, K.E., 2017b. Rhamnolipids: Production, performance, and application. In: Lee, S. (Ed.), Consequences of Microbial Interactions with Hydrocarbons, Oils, and Lipids: Production of Fuels and Chemicals. Handbook of Hydrocarbon and Lipid Microbiology. Springer, Cham, pp. 1–37. https://doi.org/10.1007/978-3-319-31421-1_388-1.
Tiso, T., Narancic, T., Wei, R., Pollet, E., Beagan, N., Schröder, K., Honak, A., Jiang, M., Kenny, S.T., Wierckx, N., Perrin, R., Avérous, L., Zimmermann, W., O'Connor, K., Blank, L.M., 2021. Towards bio-upcycling of polyethylene terephthalate. Metab. Eng. 66, 167–178. https://doi.org/10.1016/J.YMBEN.2021.03.011.
Tokiwa, Y., Suzuki, T., 1977. Hydrolysis of polyesters by lipases. Nature 270, 76–78. https://doi.org/10.1038/270076a0.
Tournier, V., Topham, C.M., Gilles, A., David, B., Folgoas, C., Moya-Leclair, E., Kamionka, E., Desrousseaux, M.L., Texier, H., Gavalda, S., Cot, M., Guémard, E., Dalibey, M., Nomme, J., Cioci, G., Barbe, S., Chateau, M., André, I., Duquesne, S., Marty, A., 2020. An engineered PET depolymerase to break down and recycle plastic bottles. Nature 580, 216–219. https://doi.org/10.1038/s41586-020-2149-4.
Trifunović, D., Schuchmann, K., Müller, V., 2016. Ethylene glycol metabolism in the acetogen Acetobacterium woodii. J. Bacteriol. 198, 1058–1065. https://doi.org/10.1128/JB.00942-15/ASSET/80C14B7F-9EE4-4131-A2E9-F6C7C549B006/ASSETS/GRAPHIC/ZJB9990939770007.JPEG.
Tsuge, T., Tanaka, K., Ishizaki, A., 2001. Development of a novel method for feeding a mixture of l-lactic acid and acetic acid in fed-batch culture of Ralstonia eutropha for poly-d-3-hydroxybutyrate production. J. Biosci. Bioeng. 91, 545–550. https://doi.org/10.1016/S1389-1723(01)80171-7.
Utomo, R.N.C., Li, W.J., Tiso, T., Eberlein, C., Doeker, M., Heipieper, H.J., Jupke, A., Wierckx, N., Blank, L.M., 2020. Defined microbial mixed culture for utilization of polyurethane monomers. ACS Sustain. Chem. Eng. 8, 17466–17474. https://doi.org/10.1021/acssuschemeng.0c06019.
Utsunomia, C., Ren, Q., Zinn, M., 2020. Poly(4-hydroxybutyrate): current state and perspectives. Front. Bioeng. Biotechnol. 8, 525813. https://doi.org/10.3389/FBIOE.2020.00257.
Valenzuela-Ortega, M., Suitor, J.T., White, M.F.M., Hinchcliffe, T., Wallace, S., 2023. Microbial upcycling of waste PET to Adipic acid. ACS Cent. Sci. 9, 2057–2063. https://doi.org/10.1021/ACSCENTSCI.3C00414.
Van Duuren, Wittmann, C., 2014. First and second generation production of bio-adipic acid. In: Bioprocessing of renewable resources to commodity bioproducts. Wiley Blackwell, pp. 519–540. https://doi.org/10.1002/9781118845394.ch19.
Vital, M., Howe, A.C., Tiedje, J.M., 2014. Revealing the bacterial butyrate synthesis pathways by analyzing (meta)genomic data. mBio 5. https://doi.org/10.1128/MBIO.00889-14.
Vollmer, I., Jenks, M.J.F., Roelands, M.C.P., White, R.J., van Harmelen, T., de Wild, P., van der Laan, G.P., Meirer, F., Keurentjes, J.T.F., Weckhuysen, B.M., 2020. Beyond mechanical recycling: giving new life to plastic waste. Angew. Chem. Int. Ed. 59, 15402–15423. https://doi.org/10.1002/ANIE.201915651.
Wagner, N., Bade, F., Straube, E., Rabe, K., Frazão, C.J.R., Walther, T., 2023. In vivo implementation of a synthetic metabolic pathway for the carbon-conserving conversion of glycolaldehyde to acetyl-CoA. Front. Bioeng. Biotechnol. 11, 1125544. https://doi.org/10.3389/FBIOE.2023.1125544.
Walther, T., Topham, C.M., Irague, R., Auriol, C., Baylac, A., Cordier, H., Dressaire, C., Lozano-Huguet, L., Tarrat, N., Martineau, N., Stodel, M., Malbert, Y., Maestracci, M., Huet, R., André, I., Remaud-Siméon, M., François, J.M., 2017. Construction of a synthetic metabolic pathway for biosynthesis of the non-natural methionine precursor 2,4-dihydroxybutyric acid. Nat. Commun. 8, 1–12. https://doi.org/10.1038/ncomms15828.
Wang, Jia, Shen, X., Wang, Jian, Yang, Y., Yuan, Q., Yan, Y., 2018. Exploring the promiscuity of phenol hydroxylase from Pseudomonas stutzeri OX1 for the biosynthesis of phenolic compounds. ACS Synth. Biol. 7, 1238–1243. https://doi.org/10.1021/ACSSYNBIO.8B00067/ASSET/IMAGES/LARGE/SB-2018-00067S_0004.JPEG.
Wang, G., Øzmerih, S., Guerreiro, R., Meireles, A.C., Carolas, A., Milne, N., Jensen, M.K., Ferreira, B.S., Borodina, I., 2020a. Improvement of cis, cis-Muconic acid production in Saccharomyces cerevisiae through biosensor-aided genome engineering. ACS Synth. Biol. 9, 634–646. https://doi.org/10.1021/ACSSYNBIO.9B00477.
Wang, Z., Sun, J., Yang, Q., Yang, J., Drasar, P.B., Khripach, V.A., Mcphee, D.J., 2020b. Metabolic engineering Escherichia coli for the production of lycopene. Molecules 25, 3136. https://doi.org/10.3390/MOLECULES25143136.
Wang, L., Li, G., Li, A., Deng, Y., 2023. Directed synthesis of biobased 1,6-diaminohexane from adipic acid by rational regulation of a functional enzyme cascade in Escherichia coli. ACS Sustain. Chem. Eng. 11, 6011–6020. https://doi.org/10.1021/ACSSUSCHEMENG.3C00275/ASSET/IMAGES/LARGE/SC3C00275_0006.JPEG.
Wang, Z., Hou, X., Shang, G., Deng, G., Luo, K., Peng, M., 2024a. Exploring fatty acid β-oxidation pathways in bacteria: from general mechanisms to DSF signaling and pathogenicity in xanthomonas. Curr. Microbiol. 81, 336. https://doi.org/10.1007/s00284-024-03866-8.
Wang, Y., van Putten, R.J., Tietema, A., Parsons, J.R., Gruter, G.J.M., 2024b. Polyester biodegradability: importance and potential for optimisation. Green Chem. 26, 3698–3716. https://doi.org/10.1039/D3GC04489K.
Wei, G., Yang, X., Gan, T., Zhou, W., Lin, J., Wei, D., 2009. High cell density fermentation of Gluconobacter oxydans DSM 2003 for glycolic acid production. J. Ind. Microbiol. Biotechnol. 36, 1029–1034. https://doi.org/10.1007/S10295-009-0584-1.
Welch, R.P.E., Descalzo, J., Justus, E., 2022. Memorandum: Best Practices around the World – Waste to Energy in Sweden. City of Beverly Hills.
Werner, A.Z., Clare, R., Mand, T.D., Pardo, I., Ramirez, K.J., Haugen, S.J., Bratti, F., Dexter, G.N., Elmore, J.R., Huenemann, J.D., Peabody, G.L., Johnson, C.W., , Salvachúa, D., Guss, A.M., Beckham, G.T., 2021. Tandem chemical deconstruction and biological upcycling of poly(ethylene terephthalate) to β-ketoadipic acid by Pseudomonas putida KT2440. Metab. Eng. 67, 250–261. https://doi.org/10.1016/J.YMBEN.2021.07.005.
Westlake, A.C., 2019. Thermostable Enzymes Important for Industrial Biotechnology. University of Exeter.
Wilkes, R.A., Waldbauer, J., Caroll, A., Nieto-Domínguez, M., Parker, D.J., Zhang, L., Guss, A.M., Aristilde, L., 2023. Complex regulation in a Comamonas platform for diverse aromatic carbon metabolism. Nat. Chem. Biol. 19, 651. https://doi.org/10.1038/S41589-022-01237-7.
Wisselink, H.W., Weusthuis, R.A., Eggink, G., Hugenholtz, J., Grobben, G.J., 2002. Mannitol production by lactic acid bacteria: a review. Int. Dairy J. 12, 151–161. https://doi.org/10.1016/S0958-6946(01)00153-4.
Wittgens, A., Kovacic, F., Müller, M.M., Gerlitzki, M., Santiago-Schübel, B., Hofmann, D., Tiso, T., Blank, L.M., Henkel, M., Hausmann, R., Syldatk, C., Wilhelm, S., Rosenau, F., 2017. Novel insights into biosynthesis and uptake of rhamnolipids and their precursors. Appl. Microbiol. Biotechnol. 101, 2865. https://doi.org/10.1007/S00253-016-8041-3.
Wu, C.S., 2012. Characterization and biodegradability of polyester bioplastic-based green renewable composites from agricultural residues. Polym. Degrad. Stab. 97, 64–71. https://doi.org/10.1016/J.POLYMDEGRADSTAB. 2011.10.012.
Xu, X., Liu, J., Lu, Y., Lan, H., Tian, L., Zhang, Z., Xie, C., Jiang, L., 2021. Pathway engineering of Saccharomyces cerevisiae for efficient lycopene production. Bioprocess Biosyst. Eng. 44, 1033–1047. https://doi.org/10.1007/S00449-020-02503-5.
Yamada, M., Matsumoto, K., Uramoto, S., Motohashi, R., Abe, H., Taguchi, S., 2011. Lactate fraction dependent mechanical properties of semitransparent poly(lactate-co-3-hydroxybutyrate)s produced by control of lactyl-CoA monomer fluxes in recombinant Escherichia coli. J. Biotechnol. 154, 255–260. https://doi.org/10.1016/J.JBIOTEC.2011.05.011.
Yang, T.H., Kim, T.W., Kang, H.O., Lee, S.H., Lee, E.J., Lim, S.C., Oh, S.O., Song, A.J., Park, S.J., Lee, S.Y., 2010. Biosynthesis of polylactic acid and its copolymers using evolved propionate CoA transferase and PHA synthase. Biotechnol. Bioeng. 105, 150–160. https://doi.org/10.1002/BIT.22547.
Yang, X., Yuan, Q., Luo, H., Li, F., Mao, Y., Zhao, X., Du, J., Li, P., Ju, X., Zheng, Y., Chen, Y., Liu, Y., Jiang, H., Yao, Y., Ma, H., Ma, Y., 2019. Systematic design and in vitro validation of novel one-carbon assimilation pathways. Metab. Eng. 56, 142–153. https://doi.org/10.1016/J.YMBEN.2019.09.001.
Yew, W.S., Fedorov, A.A., Fedorov, E.V., Rakus, J.F., Pierce, R.W., Almo, S.C., Gerlt, J.A., 2006. Evolution of enzymatic activities in the enolase superfamily: l-Fuconate dehydratase from Xanthomonas campestris. Biochemistry 45, 14582–14597. https://doi.org/10.1021/bi061687o.
Yim, H., Haselbeck, R., Niu, W., Pujol-Baxley, C., Burgard, A., Boldt, J., Khandurina, J., Trawick, J.D., Osterhout, R.E., Stephen, R., Estadilla, J., Teisan, S., Schreyer, H.B., Andrae, S., Yang, T.H., Lee, S.Y., Burk, M.J., Van Dien, S., 2011. Metabolic engineering of Escherichia coli for direct production of 1,4-butanediol. Nat. Chem. Biol. 7, 445–452. https://doi.org/10.1038/nchembio.580.
You, S.M., Lee, S.S., Ryu, M.H., Song, H.M., Kang, M.S., Jung, Y.J., Song, E.C., Sung, B. H., Park, S.J., Joo, J.C., Kim, H.T., Cha, H.G., 2023. β-Ketoadipic acid production from poly(ethylene terephthalate) waste via chemobiological upcycling. RSC Adv. 13, 14102–14109. https://doi.org/10.1039/D3RA02072J.
Zambanini, T., Kleineberg, W., Sarikaya, E., Buescher, J.M., Meurer, G., Wierckx, N., Blank, L.M., 2016. Enhanced malic acid production from glycerol with high-cell density Ustilago trichophora TZ1 cultivations. Biotechnol. Biofuels 9, 1–10. https://doi.org/10.1186/S13068-016-0553-7/FIGURES/6.

Zaroog, O.S., Borhana, A.A., Perumal, S.S.A., 2019. Biomaterials for Bone Replacements: Past and Present, Reference Module in Materials Science and Materials Engineering. Elsevier. https://doi.org/10.1016/B978-0-12-803581-8.11442-0.

Zhang, H., Themelis, N.J., Bourtsalas, A., 2021. Environmental impact assessment of emissions from non-recycled plastic-to-energy processes. Waste Dispos Sustain. Energy 3, 1–11. https://doi.org/10.1007/s42768-020-00063-8.

Zhang, C., Xue, J., Yang, X., Ke, Y., Ou, R., Wang, Y., Madbouly, S.A., Wang, Q., 2022. From plant phenols to novel bio-based polymers. Prog. Polym. Sci. 125, 101473. https://doi.org/10.1016/J.PROGPOLYMSCI.2021.101473.

Zhang, C., Qi, Z., Ma, Z., Gong, Y., Feng, H., Zang, J., Du, W., Shang, L., 2025. Sustainably sourced p-coumaric acid-derived bio-based epoxy resins: functionalized thermosetting epoxy materials with excellent flame retardancy, ultra-high strength, toughness, and transparency. J. Ind. Eng. Chem. https://doi.org/10.1016/J.JIEC.2025.01.040.

Zheng, S., Xu, X., Gao, T., Song, H., 2024. One-pot microbial cell factory strategy for the production of protocatechuic acid from polyethylene terephthalate waste. ACS Sustain. Chem. Eng. 12, 5632–5639. https://doi.org/10.1021/ACSSUSCHEMENG.4C00363/ASSET/IMAGES/LARGE/SC4C00363_0005.JPEG.

Zhou, W., Bergsma, S., Colpa, D.I., Euverink, G.J.W., Krooneman, J., 2023a. Polyhydroxyalkanoates (PHAs) synthesis and degradation by microbes and applications towards a circular economy. J. Environ. Manag. 341, 118033. https://doi.org/10.1016/J.JENVMAN.2023.118033.

Zhou, J., Hsu, T.G., Wang, J., 2023b. Mechanochemical degradation and recycling of synthetic polymers. Angew. Chem. Int. Ed. 62, e202300768. https://doi.org/10.1002/ANIE.202300768.

Zhou, D., Wu, F., Peng, Y., Qazi, M.A., Li, R., Wang, Y., Wang, Q., 2023c. Multi-step biosynthesis of the biodegradable polyester monomer 2-pyrone-4,6-dicarboxylic acid from glucose. Biotechnol. Biofuels Bioprod. 16, 1–12. https://doi.org/10.1186/S13068-023-02350-Y/TABLES/1.

Zhu, X., Tao, Y., Liang, C., Li, X., Wei, N., Zhang, W., Zhou, Y., Yang, Y., Bo, T., 2015. The synthesis of n-caproate from lactate: a new efficient process for medium-chain carboxylates production. Sci. Rep. 5, 1–9. https://doi.org/10.1038/srep14360.

Zhu, X., Zhou, Y., Wang, Y., Wu, T., Li, X., Li, D., Tao, Y., 2017. Production of high-concentration n-caproic acid from lactate through fermentation using a newly isolated Ruminococcaceae bacterium CPB6. Biotechnol. Biofuels 10, 102. https://doi.org/10.1186/s13068-017-0788-y.